WWW.OEAW.AC.AT

ÖAW ÖSTERREICHISCHE AKADEMIE DER WISSENSCHAFTEN

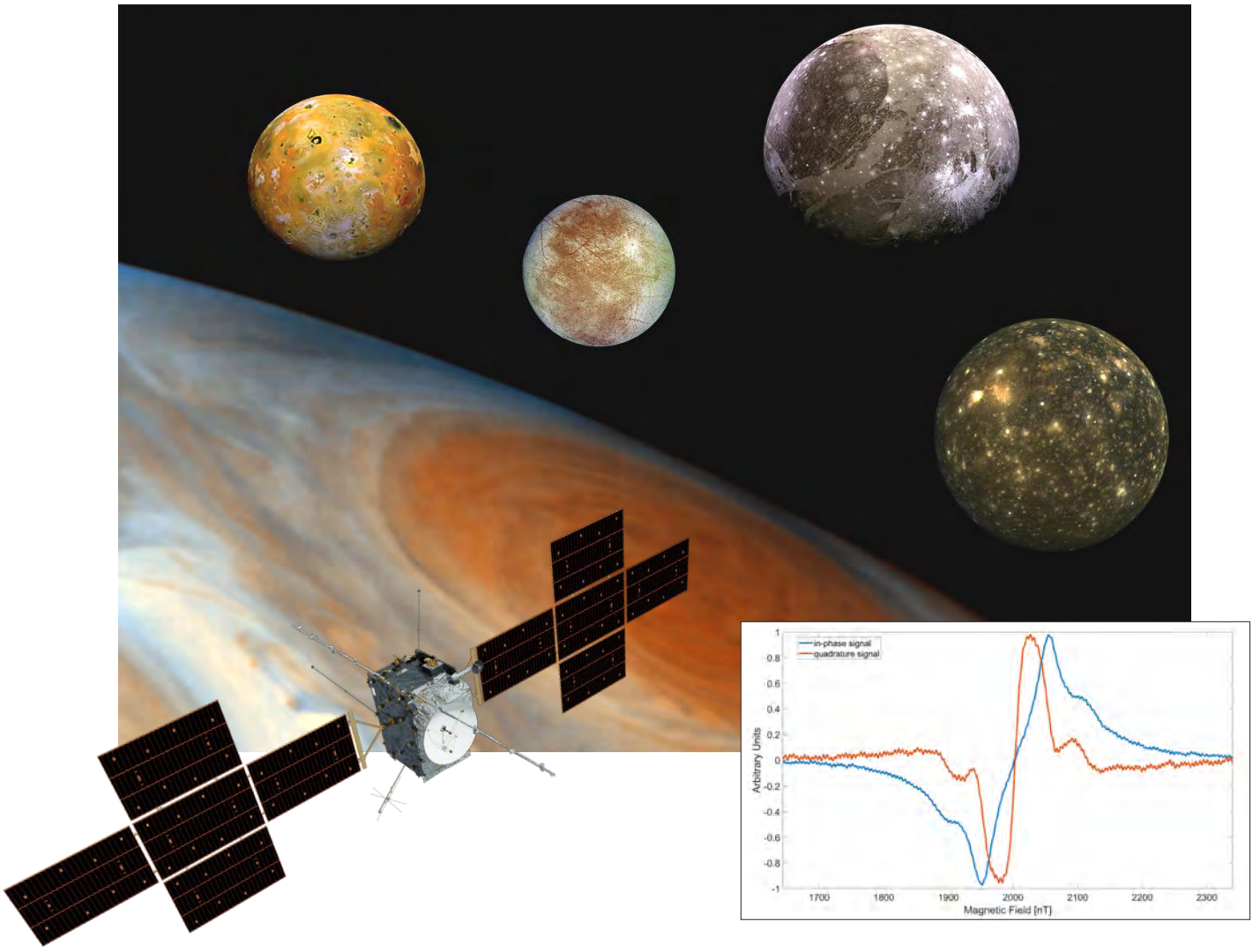

ANNUAL REPORT 2023

IWF INSTITUT FÜR WELTRAUMFORSCHUNG

WWW.OEAW.AC.AT/IWF

COVER IMAGE

ESA's *JUICE* spacecraft (© ESA/ATG medialab) is on the way to Jupiter and its icy moons (© NASA/JPL/DLR). The insert shows the first quantum interference signal of the Graz *MAGSCA* sensor, confirming the perfect functioning of the instrument after launch.

TABLE OF CONTENTS

THE DIRECTOR'S PAGE 2023 5

INTRODUCTION 7

SOLAR WIND & GEOSPACE 9

SOLAR SYSTEM 19

- EARLY EARTH 19
- MERCURY 21
- VENUS & MARS 22
- JUPITER 23
- ICY MOONS & COMETS 24

EXOPLANETS & DISKS 27

SATELLITE LASER RANGING 37

TECHNOLOGIES 39

- NEW DEVELOPMENTS 39
- INFRASTRUCTURE 41

IMPACT BEYOND SCIENCE 43

PUBLICATIONS 49

PERSONNEL 65

IMPRINT

THE DIRECTOR'S PAGE 2023

In 2023, the IWF welcomed Vice President Ulrike Diebold and the IWF Scientific Advisory Board. OeAW President Heinz Fassmann, the previous and present TU Graz Rectors Harald Kainz and Horst Bischof joined us for the launch event for the *JUICE* mission at the IWF in Graz. In September, the IWF hosted the Austrian astrophysics, space science and space technology community for the visit of the ESA Director of Science, Prof. Carole Mundell, and her team, kindly invited by the FFG. We celebrated the 10th anniversary of Graz in Space in 2023 and shaped a Urania lecture series with focus on the *James Webb Space Telescope (JWST).*

JWST has reached its science phase and IWF research groups were involved in early science exoplanet and astrochemistry projects, followed by successful proposals in cycle 2 and 3. *CHEOPS* and *CUTE* are now in the science production phase for exoplanet research. *BepiColombo* had its third close approach to the innermost rocky planet in the solar system. Our *Planetary Ion Camera (PICAM)* monitored the very dense and dynamic solar wind that interacts with Mercury's surface and picked up first ions from Mercury itself. Two of the quantum interference magnetometers jointly developed by IWF and TU Graz were launched in 2023. One is on its way into the outer solar system aboard ESA's Jupiter mission *JUICE*, the other circles the Earth on board *Macau Science Satellite 1*. Both have proven to function well with healthy "magnetic heartbeats". Preparing for the *SMILE* launch in 2025, the IWF digital processing unit and electronics box were built, tested and delivered. The IWF is intensely working on its parts for the ESA F-class mission *Comet Interceptor*, which is planned for a piggy-bag launch with ESA's M4 mission *ARIEL* in 2029. To our delight, out of the originally 10 ESA M7 mission candidates, the IWF is participating in 2 of the 3 down-selected missions: *Plasma Observatory* and *M-Matisse* with science and hardware contributions for the Phase A studies.

In December, our 8 group leaders gathered again for a strategy meeting to discuss how our research and technology work answers the IWF's driving science questions regarding the diversity of planets inside and outside the solar system, the uniqueness of Earth and our responsibility for our home planet. Observations with *CHEOPS, CUTE, JWST* now and with future missions like *PLATO, ARIEL* and the *Habitable Exoplanet Observatory* enable the measurement of exoplanet parameters, their atmospheres and mass losses to characterize and understand the evolution of exoplanets. The diversity of exoplanets is also explored with regard to the astrochemical environments in planet-forming disks in different galactic environments.

IWF Director Prof. Dr. Christiane Helling (© OeAW/IWF/Scherr).

Our participations in solar system missions like *Cluster, THEMIS, MMS, BepiColombo* and in the future in *SMILE* and *Comet Interceptor* forges our fundamental research in understanding the solar system objects in their interaction with the Sun. Our research at the IWF unanimously points to our home planet Earth as unique regarding its formation, its evolution, its atmospheric composition, as well as its magnetic environment so far. This uniqueness was also explored in the arts & science collaboration of the Mobile Pavilion as part of Showing Styria 2023 by putting Earth's atmosphere in its astronomical context.

The IWF's Satellite Laser Ranging station develops techniques to trace space debris, a topic of relevance for future space research and space travel aspirations. The IWF technology groups enable us the link to the future by developing and building the next generation of space instruments in collaboration with IWF scientists. This tight interaction between technology development and fundamental research enables the IWF's participation in 24 present and future missions. The near-future mission launches on our schedule are in 2024 *CSES-2*, in 2025 *FORESAIL-2, SWFO* and *SMILE*, in 2026 *PLATO* followed by *HelioSwarm* in 2028, and in 2029 *VIGIL, Comet Interceptor* and *ARIEL*. All our missions challenge present technological limits in order to enable fundamental research, which in turn enables understanding the world that we live in. All our missions engage international collaborations beyond borders and cultural differences.

The IWF is committed to fundamental space research, to sharing its knowledge with the wider public and with the next possibly space-faring generations.

With the best of wishes,

Christiane Helling

ESA's *JUICE* spacecraft launched from Kourou, French Guiana on 12 April 2023 (© ESA/CNES/Arianespace).

INTRODUCTION

The Space Research Institute (IWF) in Graz focuses on the physics of our solar system and the diversity of exoplanets. With about 100 staff members from 20 nations it is one of the largest institutes of the Austrian Academy of Sciences (Österreichische Akademie der Wissenschaften, OeAW).

The IWF develops and builds space-qualified instruments and analyzes and interprets the data returned by the space missions. Its core engineering expertise is in building magnetometers and on-board computers, as well as in satellite laser ranging, which is performed at a station operated by the IWF at the Lustbühel Observatory. In terms of science, the institute concentrates on the physics of solar and extrasolar planets, planet-forming disks, and space plasmas.

The IWF cooperates closely with international space agencies and with numerous other national and international research institutions. Tight cooperation exists with the European Space Agency (ESA).

In 2023, the IWF was involved in 24 active and future international space missions; among these:

- The *Cluster* mission continues to provide unique data to better understand plasma processes in near-Earth space.
- The four *Magnetospheric MulitScale (MMS)* spacecraft perform multi-point measurements to study the dynamics of the Earth's magnetosphere.
- The first *China Seismo-Electromagnetic Satellite (CSES-1)* is studying the Earth's ionosphere. *CSES-2* will follow in 2024.
- On its way to Mercury, *BepiColombo* had its third planetary flyby in June.
- *CHEOPS (CHaracterizing ExOPlanets Satellite)* continues nominal science operations, characterizing exoplanets around bright stars.
- ESA's *Solar Orbiter* observed many interesting aspects of the Sun's activity.
- The NASA CubeSat *CUTE (Colorado Ultraviolet Transit Experiment)* delivered new details about exoplanet WASP-189b as its first science target.
- ESA's *JUpiter ICy moons Explorer (JUICE)* was launched on 14 April 2023 to investigate Jupiter and its icy moons: Ganymede, Callisto, and Europa.
- *SMILE* (launch: 2025) will study the interaction between the solar wind and Earth's magnetosphere.

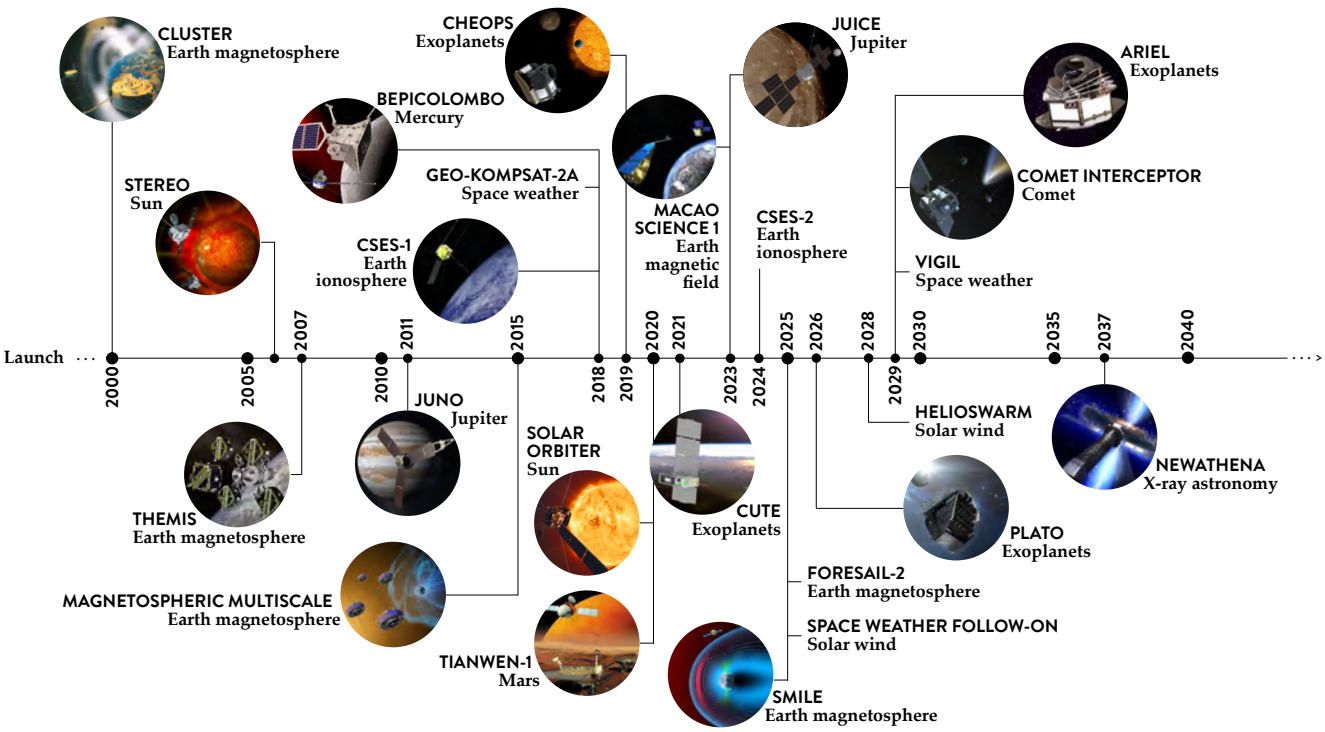

Timeline of IWF's active and future space missions (© *Cluster, BepiColombo, NEWATHENA:* ESA; *STEREO:* NASA/Jay Friedlander, *THEMIS, MMS:* NASA; *JUNO:* NASA/JPL; *CSES-1:* NSSC/CAS; *CHEOPS, Solar Orbiter, JUICE, SMILE, Comet Interceptor:* ESA/ATG medialab; *Tianwen-1:* W. X. Wan, C. Wang, C. L. Li & Y. Wei / CNSA; *CUTE:* LASP/UCB; *Macau Science Satellite 1:* MUST; *PLATO:* OHB System AG; *ARIEL:* Airbus).

- The *FORESAIL-2* (launch: 2025) CubeSat will characterize the variability of ultra-low frequency waves in the inner magnetosphere.
- *PLATO* (launch: 2026) is a space-based observatory to search for planets orbiting alien stars.
- The multi-satellite mission *HelioSwarm* (launch: 2028) will help to better understand the interaction between the solar wind and geospace.
- *Comet Interceptor* (launch: 2029) will characterize in detail, for the first time, a dynamically-new comet or interstellar object.

HIGHLIGHTS IN 2023

- In "Nature Geoscience" P. Barth et al. investigated experimentally the contribution of lightning to the production of biologically useful nitrogen in the early Earth atmosphere, providing new insights into the role of lightning as a source of nutrients for early life forms on Earth and exoplanets.
- T. Käufer et al. used neural networks to predict spectral energy distributions of protoplanetary disks to determine their physical structure and the dust properties. This new and faster innovative approach was presented in "Astronomy & Astrophysics".
- In "Astrophysical Journal Letters" A.G. Sreejith et al. presented the first results of observations carried out with the *CUTE* CubeSat mission. The near-ultraviolet spectra obtained by *CUTE* during the transit of the hot Jupiter WASP-189 b in front of the host star led to detection of Mg and Fe in the planetary upper atmosphere and put constraints on the atmospheric temperature profile. These results demonstrate that also small satellites are capable of providing scientific relevant results in the exoplanetary research field.
- D. Teubenbacher et al. used *MMS*'s *Active Spacecraft Potential Control* data to estimate the electron density and investigate compressive turbulence in the Earth's magnetosheath. Results were published in the "Journal of Geophysical Research: Space Physics".

THE YEAR 2023 IN NUMBERS

Members of the institute published 172 papers in refereed international journals, of which 38 were first author publications. During the same period, articles with authors from the institute were cited 8134 times in the international literature. In addition, 70 talks (16 invited) and 29 posters were presented by IWF members at international conferences. Institute members were involved in the organization of 13 international meetings, e.g. EGU General Assembly, ISSI Team Meetings, EPSC, and a *PLATO* Workshop.

IWF STRUCTURE AND FUNDING

The institute is led by Christiane Helling, who simultaneously holds a university professorship in space science at the Graz University of Technology. Luca Fossati serves as Deputy Director.

The IWF hosts eight research groups:

- Exoplanet Weather and Climate
  (Lead: Christiane Helling)
- Exoplanet Characterization and Evolution
  (Lead: Luca Fossati)
- Planet-Forming Disks and Astrochemistry
  (Lead: Peter Woitke)
- Solar System Planetary Physics
  (Lead: Helmut Lammer)
- Space Plasma Physics
  (Lead: Rumi Nakamura)
- On-Board Computers
  (Lead: Gabriel Giono)
- Space Magnetometers
  (Lead: Werner Magnes)
- Satellite Laser Ranging
  (Lead: Michael Steindorfer)

The IWF is mainly financed by the OeAW and to a lesser extent through competitive grants from the Austrian Research Promotion Agency (FFG), the Austrian Science Fund (FWF), the European Union, ESA, and NASA.

The IWF group leaders Werner Magnes, Michael Steindorfer, Rumi Nakamura, Christiane Helling, Peter Woitke, Helmut Lammer, Gabriel Giono, and Luca Fossati (f.l.t.r., © OeAW/IWF/Scherr).

SOLAR WIND & GEOSPACE

The solar wind is a stream of magnetized plasma produced at the solar atmosphere, which interacts with planets and bodies throughout the solar system. Among the different planetary systems, geospace is a natural plasma laboratory with different types of boundaries and regions that are created as a consequence of the interaction between the solar wind and the Earth's intrinsic magnetic field and plasmas. It allows us to study fundamental plasma physical processes such as acceleration or heating as well as geo/planetary sciences, i.e., how the Sun and solar wind affect the Earth/planetary plasma environment, called, in a more general term, space weather phenomena. The IWF has been participating in a number of missions in geospace and solar wind from the planning and proposal phase, to the development and building of new hardware and finally the operation and calibration of the instruments. Data taken from these missions have been extensively analyzed at the IWF by applying different methods and by theoretical modeling to compare with the observations.

A study using the *BepiColombo* data during its cruise phase towards Mercury revealed the presence of magnetic holes in the solar wind. The occurence rate of these structures remained constant between Earth and Mercury, showing that these holes are created all along the solar wind.

SOLAR ORBITER

Solar Orbiter is an ESA-led space mission with NASA participation to investigate the Sun. Flying a novel trajectory, with partial Sun-spacecraft corotation, the mission plans to investigate in-situ plasma properties of the inner solar heliosphere and to observe the Sun's magnetized atmosphere and polar regions. Gravity assist from Venus and Earth will be used to reach the operational orbit, a highly elliptical orbit with perihelion at 0.28 au.

The IWF built the Digital Processing Unit (DPU) for the *Radio and Plasma Waves (RPW)* instrument and calibrated the *RPW* antennas, using numerical analysis and anechoic chamber measurements. Furthermore, the institute contributed to the fluxgate magnetometer *(MAG)*. *RPW* measures the magnetic and electric fields at high time resolution and determines the characteristics of magnetic and electrostatic waves in the solar wind from almost DC to 20 MHz. Besides the 5 m long antennas and the AC magnetic field sensors, the instrument consists of four analyzers: the thermal noise and high frequency receiver, the time domain sampler, the low frequency receiver, and the bias unit for the antennas. The control of all analyzers and the communication will be performed by the DPU.

In 2023, *Solar Orbiter* made a number of new discoveries about the Sun's corona and dynamics. To name a few, the *Extrem-Ultraviolett Imager (EUI)* discovered tiny jets that could power the solar wind, joint observation with NASA's *Parker Solar Probe* allowed for a first in-situ and remote access to the solar corona, and the *SPICE* instrument captured a transit of Mercury in front of the star.

Solar Orbiter captured these images of tiny jets of material escaping from the Sun's outer atmosphere (© ESA & NASA/*Solar Orbiter/EUI* Team; Lakshmi Pradeep Chitta, MPS).

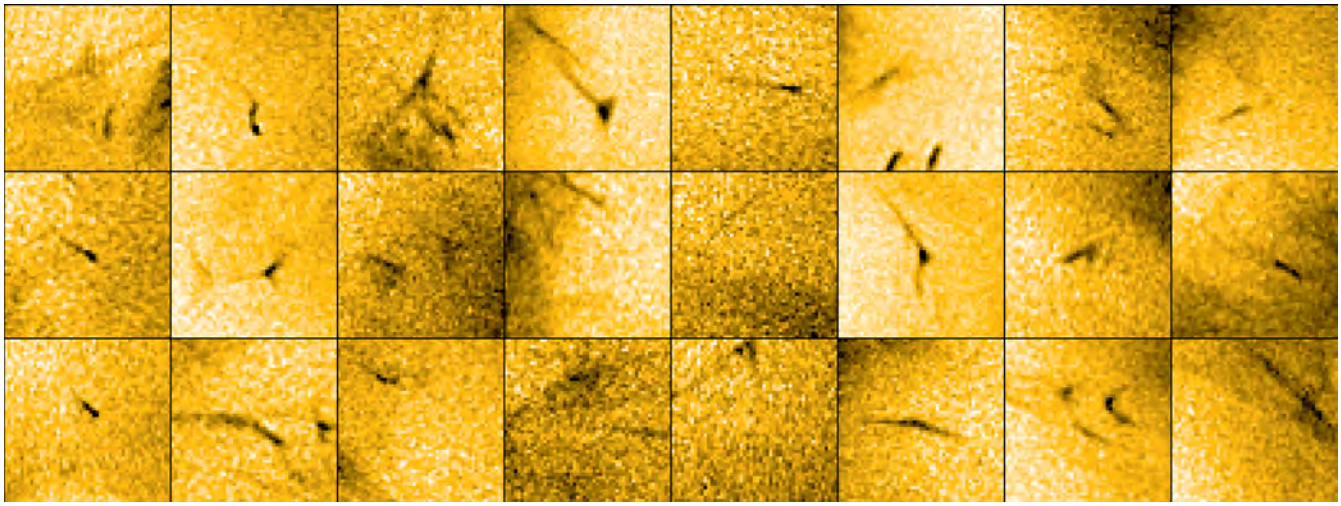

CLUSTER

ESA's *Cluster* mission is designed to study different plasma processes due to the interaction between the solar wind and the Earth's magnetosphere. *Cluster*, launched in July and August 2000, is the first four-spacecraft mission that can differentiate between temporal and spatial changes of the different plasma processes. Request from the scientific community for the *Cluster* mission extension until 2025 has been submitted. The IWF is Principal and/or Co-Investigator (PI/Co-I) on five instruments and has contributed to data archiving activities at the *Cluster Science Archives (CSA)* in addition to the science data analysis.

After 24 years of successful operation, the science phase is planned to end September 2024 when the first satellite of the fleet re-enters the atmosphere with the last one to be expected in 2026.

THEMIS/ARTEMIS

NASA's five-spacecraft mission *THEMIS (Time History of Events and Macroscale Interactions during Substorms)*, was launched in 2007. In 2010, the two outer spacecraft were sent to an orbit around the Moon and renamed *ARTEMIS (Acceleration, Reconnection, Turbulence and Electrodynamics MISsion)*. The inner three probes remained in their near-Earth orbits. An extension until 2028 is under discussion. As Co-I of the magnetometer, the IWF team is using *THEMIS* data to study dynamical processes in the magnetosphere as well as the dayside magnetosphere boundaries.

MMS

NASA's *Magnetospheric Multi-Scale (MMS)* mission, launched in 2015, explores the dynamics of the Earth's magnetosphere and its underlying energy transfer processes. Four identically equipped spacecraft carry out highest temporal and spatial measurements in the Earth's magnetosphere. *MMS* investigates the small-scale basic plasma processes, which transport, accelerate and energize plasmas in thin boundary and current layers. Extension of *MMS* until 2028 is under discussion.

The IWF has taken the lead for the *Active Spacecraft POtential Control (ASPOC)* of the satellites and is participating in the *Electron Drift Instrument (EDI)* and the *Digital FluxGate magnetometer (DFG)*. In addition to the operation of these instruments and the scientific data analysis, the IWF is contributing to inflight calibration activities and also deriving a new data product such as the density determined from the controlled spacecraft potential.

GEO-KOMPSAT-2A

GEO-KOMPSAT-2A (GEOstationary KOrea Multi-Purpose SATellite-2A) is a South Korean meteorological and environmental satellite in geostationary orbit at 128.2° East, which also hosts a space weather environment monitoring system. The Korean Meteorological Administration managed the implementation of the satellite, launched in 2018, and the necessary ground segment. The space weather observations aboard *GEO-KOMPSAT-2A* are performed by the Korean Space Environment Monitor (KSEM), which was developed under the lead of the Kyung Hee University. It consists of a set of particle detectors, a charging monitor and a four-sensor *Service Oriented Spacecraft MAGnetometer (SOSMAG)*.

The *SOSMAG* development was initiated and conducted by ESA as part of the Space Situational Awareness program and built by the *SOSMAG* consortium: IWF, Magson GmbH, Technische Universität Braunschweig, and Imperial College London. The *SOSMAG* instrument is a "ready-to-use" magnetometer avoiding the need of imposing magnetic cleanliness requirements onto the hosting spacecraft. This is achieved using two high quality fluxgate sensors on a one-meter-long boom and two additional magneto-resistive sensors mounted within the spacecraft body. The measurements of the two inner-spacecraft sensors together with the inner boom sensor enable an automated correction of the outer boom sensor measurement for the dynamic stray fields from the spacecraft.

Flight data verification, in-flight calibration and operation support were continued also in 2023, the fifth year of operation. The measured data show that the Sun is developing towards its maximum activity, which is expected in July 2025. This phase is of particular importance for space weather research.

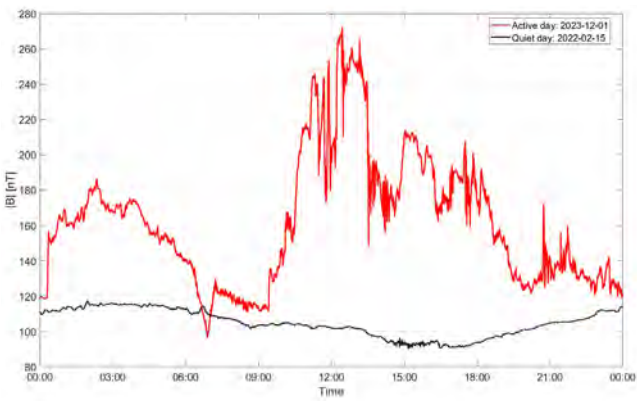

SOSMAG magnetic field data during days with quiet and very active solar wind conditions.

SOSMAG data are publicly available via the Space Weather Service Network of ESA's Space Safety program at swe.ssa.esa.int.

CSES

The *China Seismo-Electromagnetic Satellites (CSES)* are scientific missions dedicated to investigate and monitor varying electromagnetic fields and waves as well as plasma parameters and particle fluxes in near-Earth space, which are induced by natural sources on ground like seismic and volcanic events.

After the successful launch of the first satellite *CSES-1* in February 2018, the second satellite *CSES-2 i*s scheduled for launch in the second half of 2024. It will be in the same Sun-synchronous circular low Earth orbit as *CSES-1*, with a local time of the descending node at 2 pm, but with a phase difference of 180 degrees. The combined observations of both satellites will double the detection probability of natural hazard-related events and will help to separate seismic from non-seismic events.

The *CSES* magnetometers, which are nearly identical on both spacecraft, have been developed in cooperation between the Chinese National Space Science Center (NSSC), the Institute of Experimental Physics of Graz University of Technology (TUG), and the IWF. NSSC is responsible for the dual sensor fluxgate magnetometer, the instrument processor and the power supply unit, while the IWF and TUG participate with the newly developed absolute scalar magnetometer, called *Coupled Dark State Magnetometer (CDSM).*

After the *CDSM* was integrated into the *High Precision Magnetometer (HPM)* with the Chinese hardware in 2022, further functional and calibration tests were performed in 2023. In October, the *HPM* electronics box was installed on the satellite.

The magnetometer sensors of *CSES-1* have completed the fifth year of successful operation in low Earth orbit in February 2023. For the newly developed *CDSM*, this is an important proof of its reliability in space operations.

HPM flight model for *CSES-2* with electronics box (upper left), *CDSM* sensor (lower left), two optical fibers in a protecting cover (middle) and two fluxgate sensors (right; © OeAW/IWF).

MACAU SCIENCE SATELLITE

Macau Science Satellite 1 was initiated by the Institute of Space Technology and Application at the Macau University of Science and Technology and has been implemented with support from the China National Space Administration and the local government of Macau. It consists of two satellites *(1A* and *1B)*, which are placed in a near-equatorial orbit with an inclination of 41 degree to study the geomagnetic field and specifically the South Atlantic Anomaly, from space.

The South Atlantic Anomaly is an area with a significantly weakened geomagnetic field and associated increased radiation impact on Earth. Its center lies over Brazil and its eastern coast. The inner of the two Van Allen radiation belts extends to about 700 kilometers from the Earth at the equator. In the region of the South Atlantic Anomaly, it comes much closer to Earth. Currently, this magnetic anomaly is increasing its spatial extension and the field strength is further decreasing. Together with ESA's *Swarm* mission, launched in 2013, it will be explored and measured in greater detail than ever before.

The scientific payload aboard satellite *1A* consists of a high-energy particle detector, a star tracker, a fluxgate magnetometer, and a scalar magnetometer. The sensor and sensor-related electronics of the scalar magnetometer are contributed by the IWF in cooperation with the Institute of Experimental Physics of Graz University of Technology. The flight instrument is a replica of the instrument for the *CSES-2* satellite. The development of the processor and power supply electronics for the scalar magnetometer as well as its overall integration and testing are carried out by the Harbin Institute of Technology, Shenzhen in cooperation with the National Space Science Center of the Chinese Academy of Sciences.

The highlight of 2023 was the launch on 21 May followed by the successful commissioning of the scalar magnetometer, which supported the start of science phase of the mission end of November.

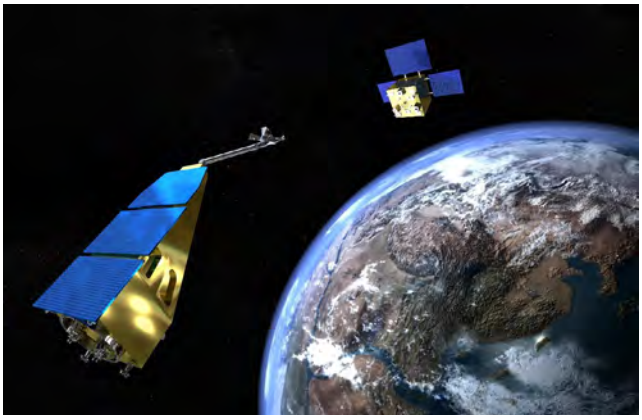

Macau Science Satellites 1A (left) and *1B* (right) orbiting the Earth with an inclination of 41 degrees. The scalar sensor is mounted to the tip of the magnetometer boom of satellite *1A* (© MUST).

FORESAIL-2

FORESAIL is a CubeSat program conducted by Aalto University in the frame of the Finnish Centre of Excellence in Research of Sustainable Space. *FORESAIL-1* was launched in May 2022, but contact was lost after a short time of in-orbit operation. A replacement satellite, *FORESAIL-1-PRIME* is therefore planned to be launched in 2025. The construction and launch of this additional CubeSat delayed the plans for *FORESAIL-2*, which contains an IWF-provided magnetometer. The technology demonstration goal of this mission is to survive the harsh radiation of the Van Allen belts using low-cost components and a fault-tolerant software approach.

The characterization of the variability of ultra-low frequency waves and their role in energizing particles in the inner magnetosphere are the core scientific objectives of *FORESAIL-2*. This shall be achieved by in-situ measurements of the magnetic field as well as relativistic electrons and protons.

In cooperation with the Institute of Electronics of Graz University of Technology, the IWF contributes a miniaturized magnetometer, which will be based on a newly developed microchip for the readout of the triaxial magnetic field sensor.

In 2023, the second prototype microchip was received from XFAB Silicon Foundries and extensively tested. The signal-to-noise ratio of 105.2 dB now achieved in conjunction with a distortion factor of -94.8 dB in the chip's feedback path, makes it a very suitable solution as core component for the flight model of the *FORESAIL-2* magnetometer.

Testing of the second prototype microchip in the magnetometer lab of the IWF (© OeAW/IWF/Magnes).

SPACE WEATHER FOLLOW-ON

The *Space Weather Follow-On (SWFO)* mission is a joint undertaking by NASA and the National Oceanic and Atmospheric Administration (NOAA). The satellite will collect solar wind data and coronal imagery to support NOAA's mission to monitor and forecast space weather events.

The *SWFO* satellite will orbit the Sun at approximately 1.5 million kilometers from Earth in Lagrange point L1. At this point the gravitational and centrifugal forces of Sun and Earth balance each other, which makes it an ideal place for observing the Sun.

The Southwest Research Institute together with two sub-contractors at the University of New Hampshire (UNH), Durham, and the IWF design, develop, integrate, and calibrate the magnetometer instrument *SWFO-MAG*. It includes two three-axis magnetometers and associated electronics to measure the vector of the interplanetary magnetic field. The IWF has the lead for the Sensor Controller Board, which hosts the front-end electronics for the two fluxgate sensors. A microchip, which has originally been developed for the *Magnetospheric Multi-Scale* mission, is the central component of the front-end electronics.

The main activities at the IWF in 2023 included the finalization of the flight model pre-calibration, the shipment of the flight model to UNH and remote support of the magnetometer assembly and test at UNH as well as other test sites in the United States.

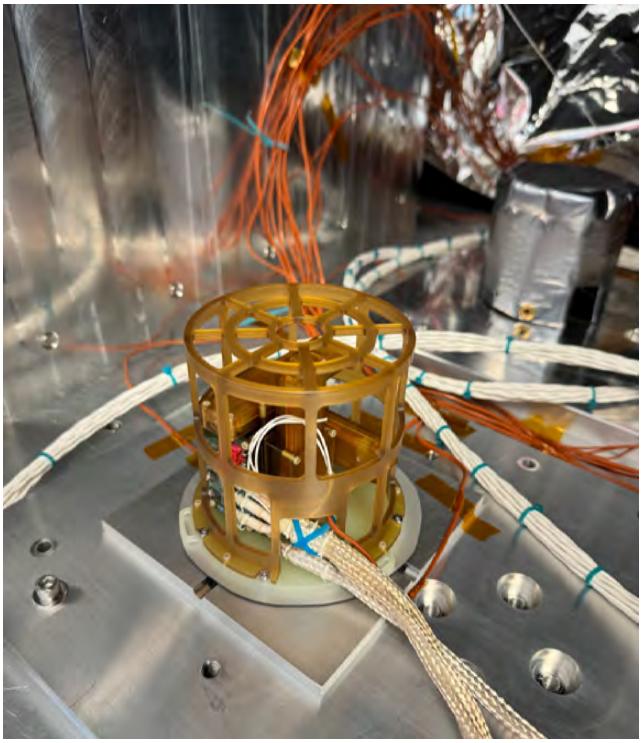

Flight model fluxgate sensor during on-ground thermal-vacuum tests (© UNH).

SMILE

The *Solar wind Magnetosphere Ionosphere Link Explorer (SMILE)* is a joint mission of ESA and the Chinese Academy of Sciences (CAS), scheduled for launch in 2025. It aims to complete our understanding of the Sun-Earth connection by measuring the solar wind and its dynamic interaction with the magnetosphere. The IWF participates in two instruments: the *Soft X-ray Imager (SXI)*, led by the University of Leicester, and the magnetometer *(MAG)*, led by CAS.

The institute, in close cooperation with international partners, contributes the instrument's control and power unit *EBox* for *SXI*. The IWF is coordinating the development and design of the Digital Processing Unit (DPU) and is responsible for the mechanical design and the tests at box level.

In addition to hardware activities, the IWF is participating in the preparation of the science working group activities such as modeling and in-situ measurements.

In 2023, the ProtoFlight Model of the DPUs and the *EBox* were produced and tested. The *EBox* underwent extensive functional testing to check that everything was working as expected. The *EBox* also underwent environmental testings, namely: thermal vacuum cycling at the IWF, vibration testing at Beyond Gravity in Vienna, electromagnetic compatibility (EMC) testing at European Test Services (ETS)/ESTEC in The Netherlands and bakeout at the IWF. Only minor deviations were observed during EMC testing and additional electrical shielding was added to the *EBox*. The *EBox* was delivered to the University of Leicester in December, where it will be integrated to the rest of the *SXI* instrument, namely the X-ray telescope, sensors and front-end electronics.

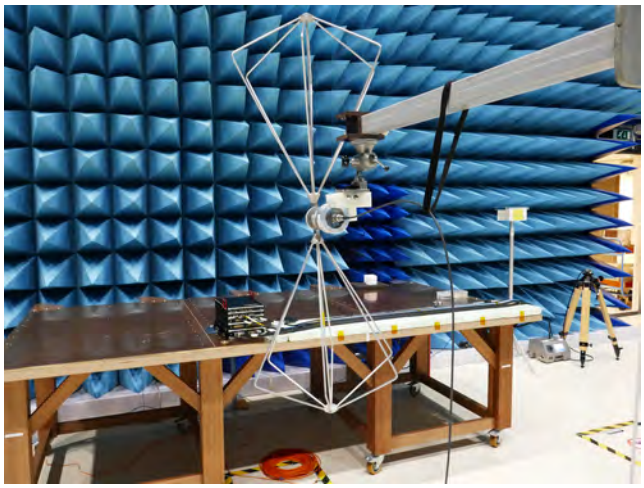

The EMC tests for the Flight Model of the *SMILE SXI EBox* were successfully completed in October at ETS/ESTEC (© OeAW/IWF/Giono).

HELIOSWARM

HelioSwarm is NASA's M(edium)-class Explorers (MIDEX) mission to be launched in 2028 to study the dynamics of the Sun, the Sun-Earth connection, and the constantly changing space environment. *HelioSwarm* consists of nine spacecraft (1 hub and 8 nodes). The *HelioSwarm* constellation makes multipoint measurements of magnetic fields, density and velocity as well as single point measurements of the velocity distribution function.

The mission is led by the University of New Hampshire (UNH). The IWF is a member of the science team contributing to the multipoint analysis.

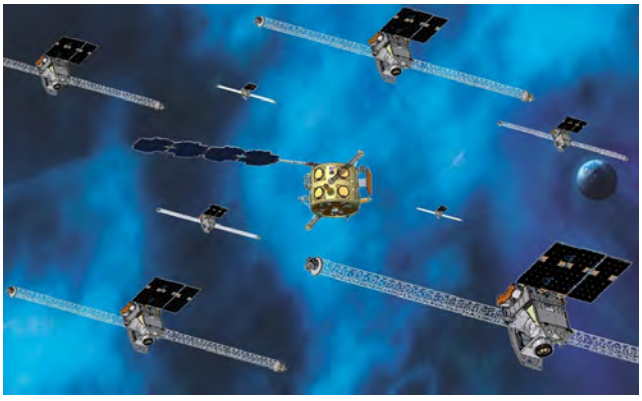

HelioSwarm hub and nodes in turbulent plasma environment (© UNH).

MAGNETIC HOLES IN THE SOLAR WIND

Magnetic holes are decreases in the magnetic field strength, which occur in various regions in the solar system. These holes are created when there is a temperature anisotropy in the plasma: when the temperature perpendicular to the magnetic field is higher than that parallel to it. This happens now and then in the solar wind and interplanetary spacecraft missions, equipped with a magnetometer (and preferably with a plasma instrument) can measure them. In this study the data from *BepiColombo*, on its way from Earth to Mercury, were used to study the occurrence rate and characteristics of these magnetic holes. As the direction of the magnetic field can change across the hole, the dataset was limited to those where the field direction did not change more than 10º, so-called linear magnetic holes.

Looking at the size of the holes, measured in seconds, it seems to vary with distance from the Sun; starting at around 6 seconds close to Mercury to about 15 seconds near Earth. This means that the holes are getting bigger as they move away from the Sun. However, if the seconds are converted to a physical size, by multiplying with the solar wind speed, there does not seem to be a correlation to the local ion gyro radius.

Looking at the occurrence rate of these holes as a function of distance from the Sun, shows that it is basically constant with small variations around a value of 3 holes per day (green line in bottom right panel). There is also good agreement with earlier studies performed e.g. with the *MESSENGER* spacecraft (blue) and other missions (magenta asterisks), with a much larger spread near Earth, which is, most likely, caused by different definitions of linear magnetic holes. The almost constant occurrence rate means that all along the way between Mercury and Earth magnetic holes are generated.

Volwerk et al., A&A, 677, A2, 2023.

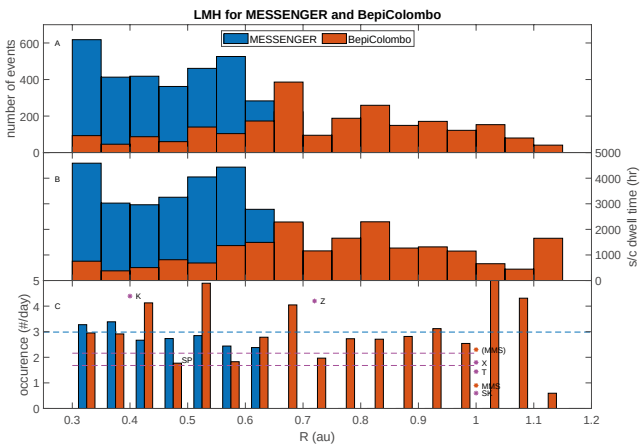

Combination of LMHs observed by *MESSENGER* (blue) and *BepiColombo* (red). Number of events, dwelling time of the spacecraft (s/c), and occurrence rate as a function of the radial distance from the Sun with a binning size of 0.05 au. The horizontal blue dashed line in panel C shows the average rate for *MESSENGER* and *BepiColombo* at about 3 holes per day.

SPECTRAL BREAK OF THE DENSITY POWER SPECTRUM IN SOLAR WIND TURBULENCE

Turbulence is characterized by nonlinear disordered fluctuations spanning several different time and length scales. In a plasma such as the solar wind, the dynamics are further complicated by the presence of a strong magnetic field, which causes anisotropies to develop. By obtaining density data product at high time resolution, using the spacecraft potential data from *MMS* in the solar wind, the transition between the large fluid scale turbulence and the smaller kinetic scales was investigated for magnetic field and density spectra. The smaller kinetic scales are of particular interest since energy conversion, dissipation and the dispersion of waves are possible in these scales, but previous measurements did not resolve these scales properly.

Density spectra show a variety of shapes when compared to the spectral break, which is located at a higher frequency than the magnetic field. An example of a flattening between both scales is shown in the figure below. The flattening has been interpreted as the magnetic field spectra resulting from large-scale Alfvén waves and smaller-scale kinetic Alfvén waves. The density spectra have been interpreted as a mixture of large-scale slow and small-scale kinetic Alfvén waves. The transition between the two regimes in the figure is related to where one process ends (slow wave damping) and another begins (compressibility of kinetic Alfvén wave).

Roberts et al., A&A, 677, L16, 2023.

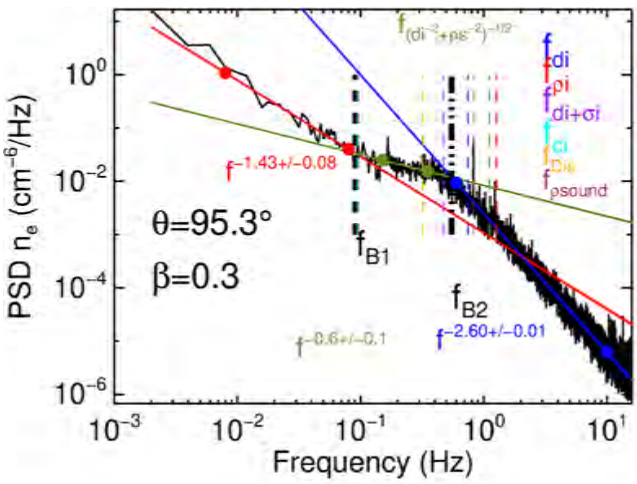

One of the power spectra from the conducted survey. Three clear ranges are seen in contrast to the magnetic field power spectra which shows only two power laws. The break locations, spectral indices and several different plasma characteristic scales are shown.

MHD SHOCKS REVISITED: MAGNETICALLY CONSTRAINING THE UPSTREAM SOLAR WIND CONDITION

Astrophysical objects in space (comets, planets and even entire star systems) present an obstacle to the flowing interplanetary and interstellar plasma. When the plasma flow is supersonic, a collisionless magnetohydrodynamic (MHD) shock emerges ahead of the object, where the plasma velocity suddenly becomes subsonic and the plasma density and temperature increase. The condition for the flow to be supersonic is that the ratio between the plasma flow (u) past the object and the Alfvén velocity (V_A), which is defined as the speed at which a transverse magnetic tension wave propagates along the magnetic field, is large. The dimensionless velocity ratio is called the Alfvénic Mach number, M_A=u/V_A, and is one of the most important parameters to describe the nature of collisionless shocks.

In space science, we often encounter the problem that only the magnetic field data are available when studying interplanetary shocks and planetary bow shocks in the solar system, and not the plasma data due to instrumental and/or telemetry limitations. In a recent work, the mathematical structure of the MHD Rankine-Hugoniot relation was revealed, which describes the relationship between the plasma states on both sides of the shock, under the condition that magnetic field changes across the shock are known. The lesson is that the shock parameters (plasma density jump and Alfvén Mach number) are analytically obtained by inverting the MHD Rankine-Hugoniot equation under the condition that the ratio between plasma pressure and magnetic pressure, the so-called plasma beta, is either a priori set or known. A test case with the Earth bow shock crossing of the *Cluster-1* spacecraft supports the theoretical study, as shown in the figure below.

Schmid and Narita, The Astrophysical Journal, 955, 58, 2023.

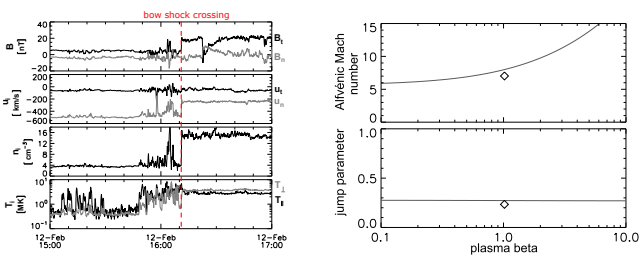

Left: *Cluster-1* Earth bow shock crossing on 12 February 2002. Magnetic field (top panel) and ion bulk velocity (second panel) are given in the shock-normal coordinates (tangential component in black and normal component in gray). The ion number density is plotted in the third panel. The ion temperature (bottom panel) is given with respect to the mean magnetic field direction (parallel component in black and perpendicular component in gray).
Right: Alfvén Mach number (top panel) and density jump (bottom panel) derived from the inverted Rankine-Hugoniot jump relation (black lines) as a function of plasma beta and that from the direct measurement of magnetic field and ions of *Cluster-1* for reference (diamonds).

TACHOCLINE ALFVÉN WAVES MANIFESTED IN STELLAR ACTIVITY

The longitudinal drifts of stellar surface activity regions (star spots), responsible for the varying radiation flux, were studied for a set of ~400 fast-rotating main sequence stars (P_{rot} = 0.5-4 days), observed with Kepler space telescope.

Analogously to the Hovmöller diagrams in meteorology, the Dynamic Diagrams of Stellar Activity Patterns (DDSAPs) were constructed for these stars to visualize rotational variability of their radiation flux as a function of rotation phase and time.

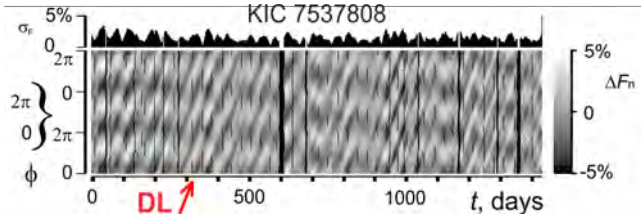

Example of a dynamic diagram of stellar activity pattern: KIC7537808 (T_{eff} = 5430 K; P_{rot} = 2.39 d)

The drifts of quasi-periodic drifting lanes (DLs) in the DDSAPs, clustering versus stellar effective temperatures T_{eff}, were compared for 108 stars with the drifts predicted for different low-frequency waves in stellar photospheres and tachoclines (figure a, b).

The performed analysis reveals that only global kink-type Alfvénic oscillations of the tachocline, which ought to trigger the emergence of the magnetic flux, allow interpreting the measured drift rates, as well as the related Rieger-type periodicity of the stellar activity (figure c) and turnover times in the convective zones, ruling out an alternative hypothesis of the Kelvin and/or Rossby waves. The corresponding tachocline magnetic field strength is of about 50 kG.

Arkhypov et al., A&A, 673, A22, 2023.

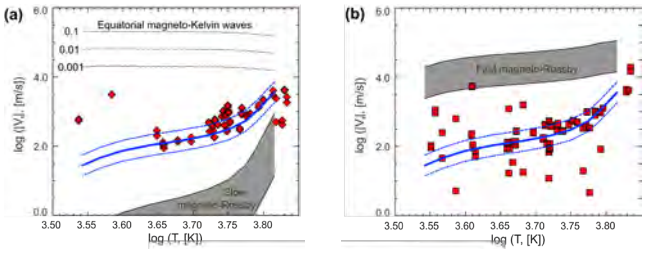

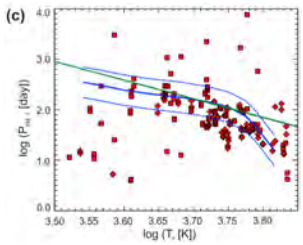

Negative/positive (a/b) DL drifts and corresponding round-star travel periods (c) of the surface activity features vs. stellar T_{eff} compared to tachocline wave phase velocities (a, b) and Rieger-type cycle periods (green line in c). Blue lines depict the range of Alfvén waves for B = 100/50/25 kG (dashed/solid/dashed).

DENSITY DERIVATION IN EARTH'S MAGNETOSHEATH AND MULTI-SCALE FLUCTUATION ANALYSIS

The magnetosheath, distinct from the solar wind, exhibits higher fluctuation amplitudes, potentially linked to shock amplification and increased compressibility. This study focuses on deriving electron plasma density from controlled spacecraft potential and investigates turbulence in Earth's magnetosheath. The derived density offers higher temporal resolution than traditional plasma instruments, enabling fluctuation analyses down to the sub-ion kinetic scale. In situ data from the *Magnetospheric Multiscale (MMS)* Solar Wind Turbulence Campaign (February 2019) are used. During this campaign, the four *MMS* spacecraft were in a logarithmic line constellation facilitating a multi-spacecraft approach and allowing the investigation of turbulent fluctuations over a broad spatial scale range. The methodology involves deriving electron density from spacecraft potential during *Active Spacecraft Potential Control (ASPOC)* operation.

Sub-ion scale intermittency is identified in the magnetosheath, suggesting coherent structures influencing heating and dissipation. Comparison of single and multi-spacecraft statistics reveals higher anisotropies at smaller scales, indicating distinct processes in the strongly compressive magnetosheath compared to the weakly compressive solar wind. The research encourages ongoing multi-spacecraft investigations for a comprehensive understanding of plasma turbulence across various scales.

Teubenbacher et al., J. Geophys. Res., 128, e2022JA031041, 2023.

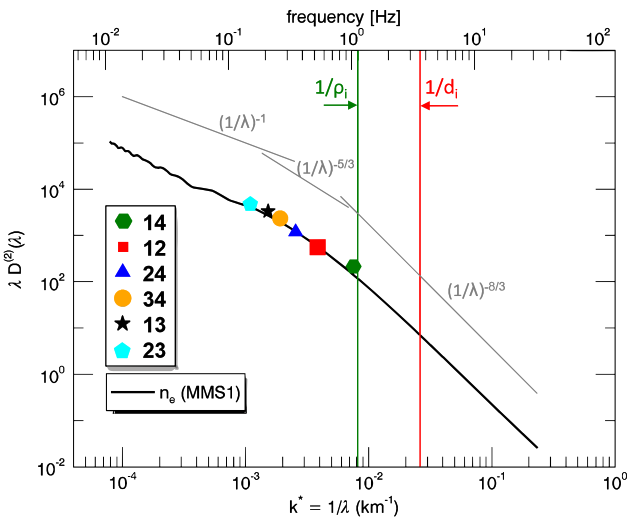

Statistical analysis: Second-order structure function of the electron density as equivalent spectrum. The X-axis is units of the inverse spatial lag λ and is called effective wave number k*. Graphs denote *MMS1* single spacecraft (time-lag) and symbols the multi-spacecraft (spatial-lag) structure functions (six different Magnetospheric Multiscale combinations denoted by numbers in the legend). d_i is the ion inertial length and ϱ_i the ion gyro radius. Three spectral slopes at the scaling exponents of -1, -5/3, and -8/3 are plotted in gray as a reference.

E-SCALE RECONNECTING CURRENT SHEET WITHIN THE LOWER-HYBRID WAVE-ACTIVE REGION OF KH WAVE

When the solar wind is deflected around the Earth's magnetosphere, the viscous interaction between the stagnant magnetospheric plasma and the fast-flowing solar wind can lead to magnetopause surface waves, called Kelvin-Helmholtz (KH) waves. These waves can evolve into vortex structures that are thought to effectively transport solar wind mass and energy into the magnetosphere via various effects.

The properties of the plasma waves around the lower-hybrid (LH) frequency are studied at the compressed boundary layers of the KH waves observed by the *Magnetospheric Multiscale (MMS)* mission on 23 September 2017. These LH waves can create a region of mixed plasma along the KH boundary layer by transporting the high-density magnetosheath plasma into the low-density magnetospheric side. In this mixing region, the magnetic field can be locally twisted and bent, ultimately forming small-scale current sheets. Simulations suggested that magnetic reconnection (a process of explosive energy release via magnetic field topology change) can occur at these electron-scale current sheets. In-situ observations are presented, which show such an electron-scale reconnecting current sheet at the boundary of a lower-hybrid wave-induced mixing region. From the detailed comparison between the observation and the simulation over the entire time of spacecraft crossing both temporal and spatial evolution of reconnection is obtained in spite of its small-scale and fast nature of the electron-scale current sheet. These results on the developed electron-scale currents also suggest the necessity of multi-scale studies to understand the KH instability in space.

Blasl et al., Geophys. Res. Lett., 50, e2023GL104309, 2023.

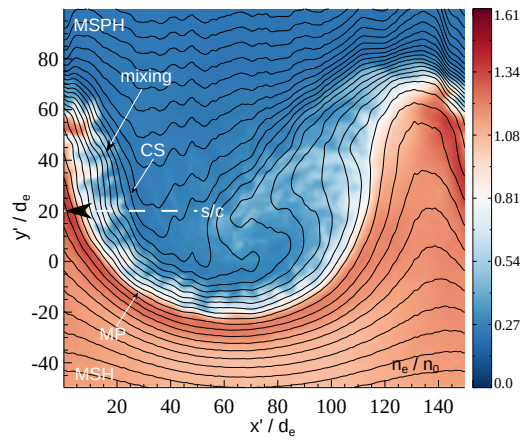

3D run performed to simulate the KH event on 23 September 2017. The color coding shows the electron density and the mixing region is identified by the intermediate density values (white). A virtual spacecraft crossing used for further analysis is indicated by the white dashed arrow. Magnetic field lines are indicated as black lines and shown to be compressed and bent around the mixing region leading to small-scale current sheets.

ELECTRON MHD GRAD–SHAFRANOV RECONSTRUCTION OF THE ELECTRON DIFFUSION REGION

An electron magnetohydrodynamic Grad-Shafranov (EMHD GS) reconstruction is used to study the electron diffusion region (EDR) of magnetic reconnection in the Earth's magnetotail. Two-dimensionality of the magnetoplasma configuration and steady state are the two basic assumptions of the GS reconstruction technique and represent the method's fundamental limitations. The present study demonstrates that the GS reconstruction can provide physically meaningful results even when these two assumptions, which are hardly fulfilled in spacecraft observations, are violated. This conclusion is supported by the reconstruction of magnetic configurations of two EDRs, encountered by the *Magnetospheric Multiscale (MMS)* mission on 11 July 2017 and 8 September 2018. Here, the former event exhibited a violation of two-dimensionality, and the latter event exhibited a violation of steady state. In both cases, despite the deviations from the ideal model configuration, reasonable reconstruction results are obtained by implementing the herein introduced compressible GS reconstruction model.

Korovinskiy et al., Front. Astron. Space Sci., 10, 1069888, 2023.

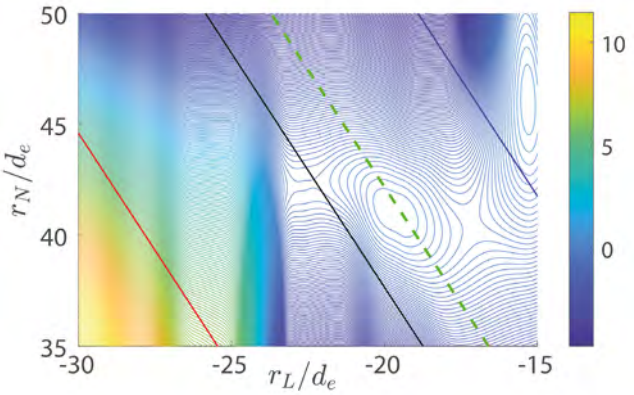

Reconstruction of the event of 8 September 2018, in the co-moving LMN coordinate system. The 2D contour plot shows the magnetic potential reconstructed at the *MMS3* trajectory. The spacecraft trajectories are plotted by black color for *MMS1*, red for *MMS2*, green for *MMS3*, and blue for *MMS4*, where the dashed line plots the reconstruction domain boundary (probes move from the right to the left).

LOADING LOSS-CONE DISTRIBUTIONS IN PARTICLE SIMULATIONS

Particle-in-cell (PIC) simulation is an important tool to study collective behavior of charged particles in space. It calculates the motion of millions of virtual charged particles, in a Monte-Carlo manner. In near-Earth space, plasmas often exhibit "loss-cone"-shaped velocity distributions that are vacant in the parallel directions to the magnetic field lines. Scientists extensively use PIC simulations to study plasma processes in near-Earth space, but it is necessary to set up a loss-cone velocity distribution at startup of simulations.

In this work, Monte-Carlo algorithms have been proposed to generate loss-cone velocity distributions in PIC simulation. Combining uniform, normal, and gamma random variables, numerical procedures for various loss-cone distribution functions have been developed, such as the subtracted Maxwellian, Dory-type loss-cone distribution, and kappa loss-cone (KLC) distribution. Monte-Carlo algorithms have also been developed to generate another kind of loss-cone distributions, based on the pitch angle, using a beta distribution. These new algorithms allow simulation scientists to use loss-cone distributions easier than before.

Zenitani et al., J. Geophys. Res., 128, e2023JA031983, 2023.

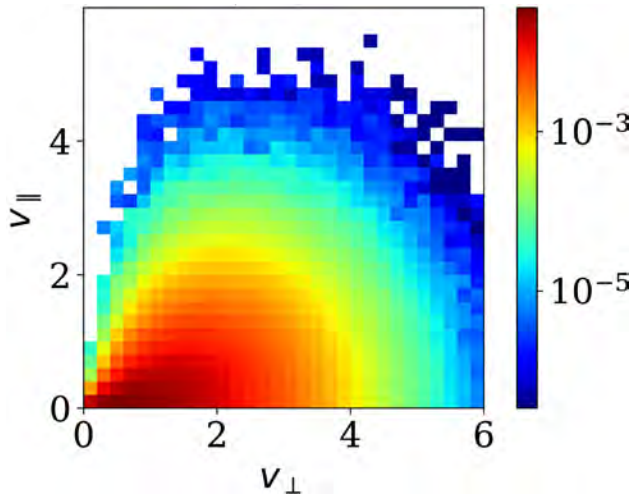

Monte-Carlo results of the new algorithm for the pitch-angle-type loss-cone distribution function with j=1 in particle-in-cell simulation. The color map shows the phase-space density; its vertical (horizontal) axis corresponds to the parallel (perpendicular) plasma velocity with respect to the magnetic field. 10^6 particles are used.

VLF RADIO EMISSION BEAMS RECORDED BY EDF / CSES EXPERIMENT

Electric power density linked to very low frequency (VLF) radio waves has been observed by the E*lectric Field Detector (EFD)* onboard the *China Seismo-Electromagnetic Satellite (CSES)*. The radio signal is emitted by the Northwest Cape (NWC) transmitter, radiating a power of 1 MW at 19.79 kHz. The VLF wave detection has a unique advantage for the remote sensing of the lower ionosphere, which is too high for balloons and too low for in situ satellites. Geometrical key parameters have been considered to analyze the variation of the power density and the hollow beam along the satellite trajectory, above the NWC station and above its conjugate region.

It was shown that the role of the Earth's ionosphere is crucial, because it disturbs the VLF signal propagation along its ray path. The figure below displays the significant beam half opening angle above the NWC station is about 15° with a power density of 0.12 $mVm^{-1}Hz^{-1/2}$ and a distance between the satellite and the NWC transmitter nearly equal to 520 km. Above the conjugate region, the power density is lower than 0.032 $mVm^{-1}Hz^{-1/2}$ with a half-opening angle of about 38°. This indicates that attenuation and scattering effects are dominant above the conjugate region. The beam behavior is subject to significant disturbances in the conjugate region, which shows up as modulations in the signal. Above the NWC transmitter station, the beam can be considered as a hollow cone but with an inconsistency dependence of the half-opening angle on the power density.

Boudjada et al., Adv. Radio Sci., 20, 77-84, 2023.

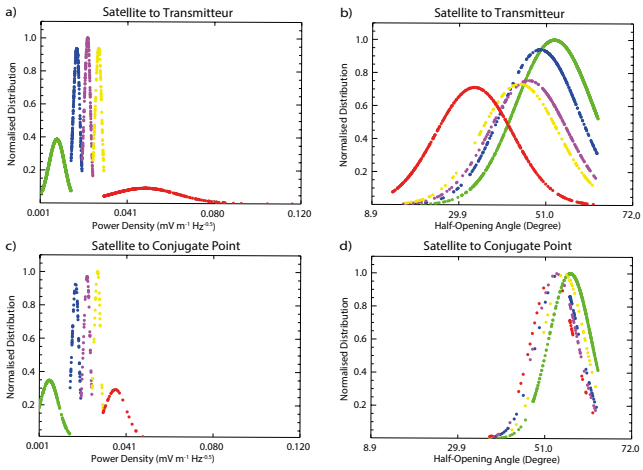

Normalized distributions of power densities (a, c) and of half-opening angles (b, d) when the satellite was above NWC transmitter (a, b) and at its conjugate point (c, d). Green, blue, violet, yellow and red colors correspond, respectively, to [0.1-15], [15-20], [20-25], [25-30] and [30-116] expressed in 10^{-3} mV $m^{-1}Hz^{-1/2}$.

STATISTICAL EVALUATION OF THE ENERGY BUDGET IN THE MAGNETOSHEATH

The terrestrial bow shock and magnetosheath are regions mediating complex couplings between the solar wind and magnetosphere. A substantial part of the electromagnetic and kinetic energies available in the turbulent solar wind is converted into fluctuations, coherent structures and waves at the shock or foreshock regions, then transported and converted further through the magnetosheath. The energy budget of various dayside fluid-, ion- and sub-ion-scale physical processes and their role in solar wind - magnetosphere couplings is purely understood. It is anticipated that, along spacecraft trajectories, the energy transfer rate over fluid scales can be estimated from temporal increments of Alfvénic or compressional fluctuations. Over ion- and sub-ion-scales, the conversion and transport terms for electromagnetic flow and thermal energies can be estimated from a set of moments of the multispecies collisionless Vlasov equation coupled to the Maxwell equations through calculating gradients based on tetrahedron measurements available from *Cluster* and *MMS* missions.

A methodology has been proposed which complements the locally estimated energy terms with the local occurrence of pressure anisotropy instabilities and some relevant kinetic measures describing key features of ion-electron scale physics. To improve our understanding of solar wind – magnetosphere coupling a consistent statistical description has been suggested which comprises a combination of normalized energy terms, kinetic and anisotropic measures, averaged upstream, magnetosheath plasma and field parameters and geomagnetic indices in a properly labeled multi-dimensional parameter space. Data reduction and pattern recognition techniques in the parameter space can be used then for making decisions about the proper coupling parameters.

Vörös et al., Front. Astron. Space Sci., 10, 1163139, 2023.

SOLAR SYSTEM

The IWF is involved in several international space missions and experiments that address solar system phenomena, planetary environments and related data analysis. The interaction of the solar wind with the magnetospheres, upper atmospheres or surfaces of solar system planets and bodies are studied. Moreover, theoretical studies related to comparative planetology, habitability and space plasma physics between solar system planets and exoplanets are also carried out for understanding the early and later evolution of Venus, Earth and Mars.

Two highlights marked the year 2023. ESA's *JUICE* mission to Jupiter and its icy moons was successfully launched in April and the ESA/JAXA *BepiColombo* spacecraft had its third flyby at Mercury in June (see figure below).

EARLY EARTH

The IWF is involved in studies on the build-up and depletion of Earth-like N_2/O_2-dominated atmospheres. Geological, biological, photochemical and aeronomical processes of such atmospheres set the stage for habitable conditions, and how the origin of life likely had a significant impact on volatile inventories and the atmosphere with major implications for global climate and habitability. These studies consider early Earth also as an Earth-like exoplanet where its atmosphere most likely represent a geo-biosignature.

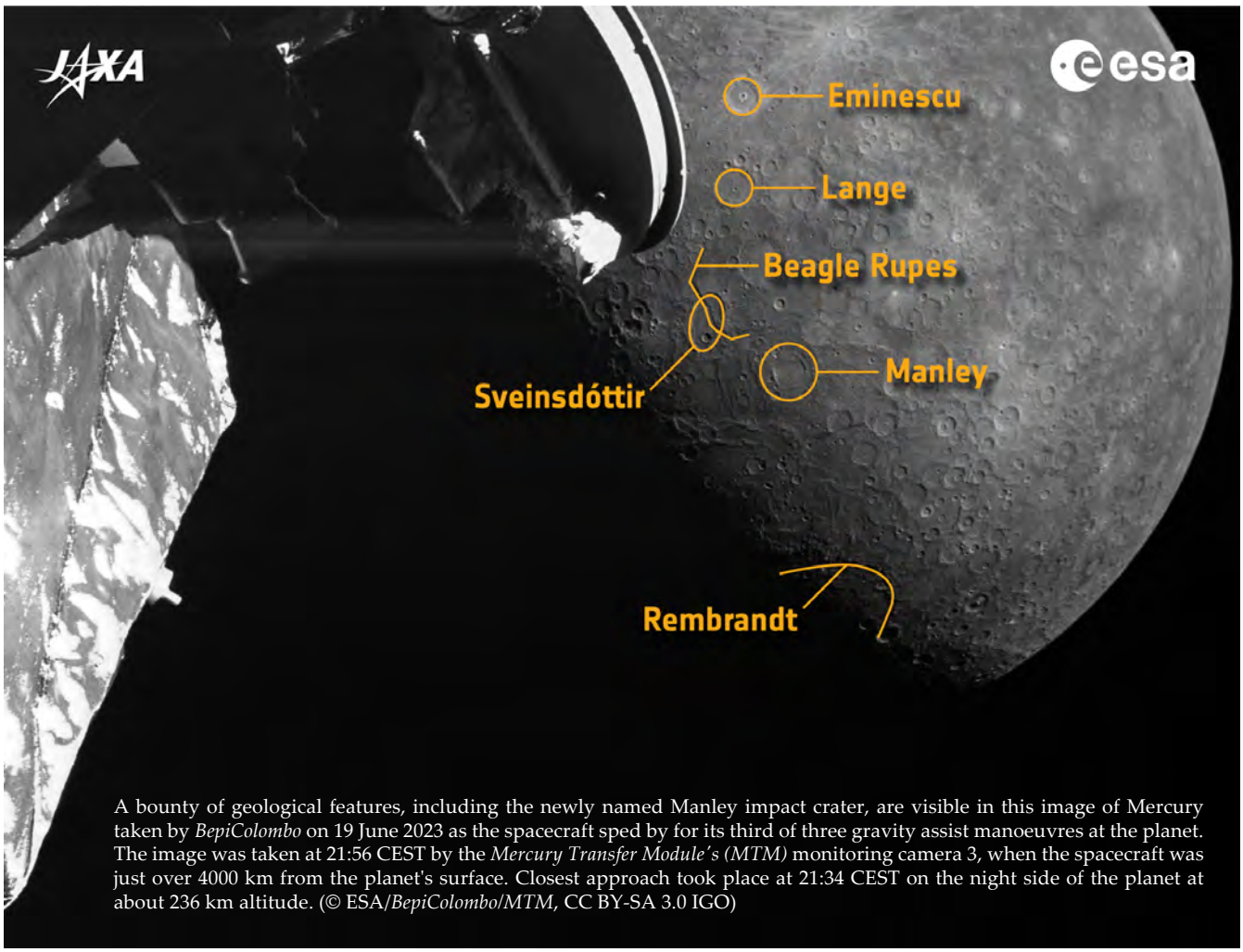

A bounty of geological features, including the newly named Manley impact crater, are visible in this image of Mercury taken by *BepiColombo* on 19 June 2023 as the spacecraft sped by for its third of three gravity assist manoeuvres at the planet. The image was taken at 21:56 CEST by the *Mercury Transfer Module's (MTM)* monitoring camera 3, when the spacecraft was just over 4000 km from the planet's surface. Closest approach took place at 21:34 CEST on the night side of the planet at about 236 km altitude. (© ESA/*BepiColombo/MTM*, CC BY-SA 3.0 IGO)

ION LOSS OVER EARLY EARTH'S POLAR CAPS

The buildup of early Earth's N_2/O_2-dominated atmosphere was strongly influenced by atmospheric escape processes that were due to the X-ray, extreme ultra-violet activity and solar wind density of the younger Sun, which were much higher about 3-4 Gyr ago. At present Earth, polar outflow of heavy ions through the open field lines over the polar cusps of Earth's magnetosphere, is the dominant atmospheric loss process. In an interdisciplinary study, the similar loss process of N^+, O^+ and C^+ ions was investigated during Earth's past with a focus of polar outflow during the Archean eon for an N_2-CO_2 atmosphere. A kinetic Direct Simulation Monte Carlo (DSMC) particle code to simulate the interactions between the solar wind and the Earth's upper atmosphere-magnetosphere environment was applied. Different CO_2 mixing ratios like 10%, 25%, 50%, 75%, and 99% and their effect on the polar outflow ion escape rates of O^+, N^+ and C^+ ions were studied. By using the modeled ion production rates as an estimate for the polar outflow, the results indicate that during the time period of about 3.6 -4.0 Gyr ago, a CO_2 mixing ratio larger than 25% may have been necessary to avoid excessive atmospheric escape from early Earth via polar outflow. As one can see in the figure below, close to about 4 Gyr ago, even 50% CO_2 may have been necessary due to the stronger solar wind of the young Sun. The results agree with previous studies, which suggest also much higher CO_2 mixing ratios for the early Archean.

Grasser et al., Earth Planet. Sci. Lett., 623, 118442, 2023.

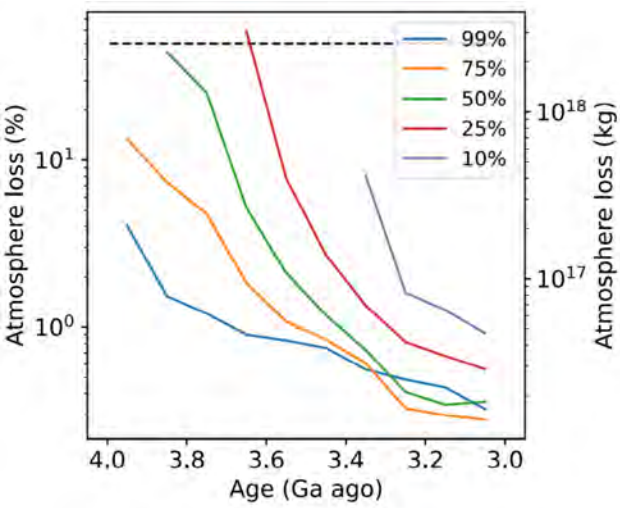

Total atmospheric loss of N^+, O^+ and C^+ ions caused by polar outflow over early Earth's cusp region for different atmospheric CO_2 mixing ratios displayed in % of today's atmosphere shown in the insert as a function of age. For comparison the corresponding atmosphere mass weighted of Earth's present mass of 5.15×10^{18} kg is also shown. The horizontal dashed black line marks a 50% mass loss of today's atmosphere.

ISOTOPIC CONSTRAINTS ON LIGHTNING AS A SOURCE OF FIXED NITROGEN IN EARTH'S EARLY BIOSPHERE

Bioavailable nitrogen is thought to be a requirement for the origin and sustenance of life. Before the onset of biological nitrogen fixation, abiotic pathways to fix atmospheric N_2 must have been prominent to provide bioavailable nitrogen to Earth's earliest ecosystems. Lightning has been shown to produce fixed nitrogen as nitrite and nitrate in both modern atmospheres dominated by N_2 and O_2 and atmospheres dominated by N_2 and CO_2 analogous to the Archaean Earth. However, a better understanding of the isotopic fingerprints of lightning-generated fixed nitrogen is needed to assess the role of this process on early Earth. Results from spark discharge experiments in N_2-CO_2 and N_2-O_2 gas mixtures are presented, which suggest that, compared with modern times, lightning-driven nitrogen fixation may have been similarly efficient in the Archaean atmosphere. Measurements of the isotopic ratio ($\delta^{15}N$) of the discharge-produced nitrite and nitrate in solution show very low values of -6‰ to -15‰ after equilibration with the gas phase with a calculated endmember composition of -17‰. These results are much lower than most $\delta^{15}N$ values documented from the sedimentary rock record, which supports the development of biological nitrogen fixation earlier than 3.2 billion years ago. However, some Paleoarchean records (3.7 billion years ago) may be consistent with lightning-derived nitrogen input, highlighting the potential role of this process for the earliest ecosystems.

Barth et al., Nature Geoscience, 16 (6), 478, 2023.

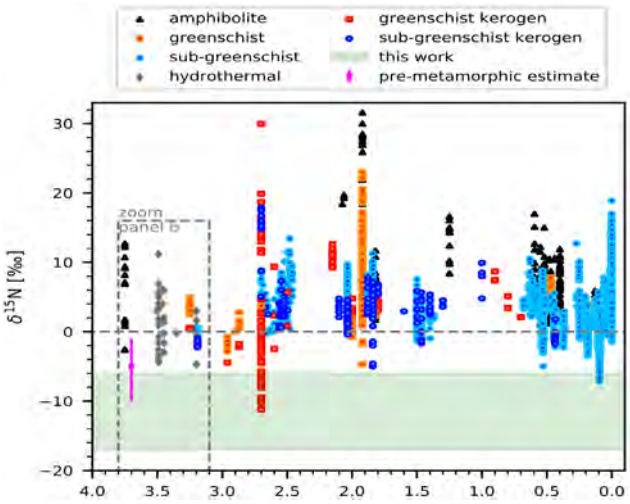

Measurements of $\delta^{15}N$ in sedimentary rocks over geologic time, separated by metamorphic grade (legend on top of figure). The results from the Miller-Urey lightning experiment after letting gas and water equilibrate (green box) may be consistent with the pre-metamorphic estimate of 3.7 Ga old sample (pink x) within errors.

MERCURY

Mercury has garnered significant attention due to the ESA/JAXA *BepiColombo* mission, which focuses on the planet's weak intrinsic magnetic field and its interaction with the solar wind.

BEPICOLOMBO

Launched in 2018, the European-Japanese *BepiColombo* spacecraft is on its 7-year journey to Mercury and will arrive in December 2025.

Due to the Mercury's close proximity to the Sun, it is quite challenging to get the spacecraft into a stable orbit around the planet. To adjust *BepiColombo's* velocity to the orbital velocity of Mercury, nine gravity-assist maneuvers (GAM) are necessary. These GAMs, also referred to as flybys, swingbys, or gravitational slingshots, leverage the gravitational pull of celestial bodies to modify the spacecraft's trajectory and speed with minimum use of thrusters and propellant. So far, *BepiColombo* successfully completed six planetary swing-by maneuvers, one at Earth, two at Venus, and three at Mercury.

On 19 June 2023 *BepiColombo* successfully performed its third Mercury flyby. The closest approach took place at 19:34 UTC at just 235 km above the planet's surface. Similar to the first two Mercury flybys in 2021 and 2022, the spacecraft approached the planet from the nightside. During the flyby most of the science instrument were activated, including the three payloads with an IWF hardware contribution on both the European *Mercury Planetary Orbiter (MPO)* and the Japanese *Mercury Magnetospheric Orbiter (Mio)*.

The IWF-lead ion instrument *PICAM (Planetary Ion CAMera*, part of the *SERENA* sensor suite) was switched on 44 hours prior to the closest approach and continued its operation until 44 hours afterwards. During this interval, *PICAM* monitored the solar wind, which proved to be very dynamic and dense. The long interval in the solar wind also provided a great opportunity for *PICAM* to collect data of high scientific importance. The magnetosphere of Mercury was very responsive and *PICAM* observed ions of planetary source, for the first time since the launch of the mission. The high-time resolution data by *PICAM* is now being analyzed, providing more details on bow shock and magnetopause crossings, as well as inner-magnetosphere ion dynamics.

Furthermore, the magnetometers *MPO-MAG* (under IWF technical management) and *Mio-MGF* (under IWF PI-ship) aboard *BepiColombo* were operational during the flyby. These instruments provided valuable scientific measurements of Mercury's internal magnetic field and its interaction with the solar wind. During *BepiColombo's* cruise phase configuration, however, the magnetometers are severely affected by magnetic disturbance from the *Mercury Transfer Module (MTM)*, which carries the two orbiters to Mercury. An intentional data cleaning process, utilizing measurements from both magnetometers (*MAG* and *MGF*), has been initiated to deliver high-quality data. This effort aims to ensure the availability of reliable scientific data for the analysis of Mercury's highly dynamic magnetosphere.

The figure displays a comprehensive plot featuring the *MGF* magnetic field (red line) over-plotted on a *PICAM* ion energy spectrogram observed during the third Mercury flyby. The peak in the total magnetic field, coupled with the observation of high-energy ions, signifies the closest approach during the swingby maneuver around 19:34 UTC. The white lines indicate the plasma boundary crossings. Around 18:44 UTC, there was a sudden increase in the magnetic field and a broadening of the ion energy spectrum, signaling the encounter of the nightside magnetosheath region. As *BepiColombo* approached the planet, the magnetic field decreased just before the magnetopause crossing around 19:14 UTC. The weak magnetic field and low ion energy observations 20 min before the closest approach are indicative of the magnetotail region. Post-closest approach, *BepiColombo* traversed the magnetopause around 19:44 UTC, entering the dayside magnetosheath region and crossed the bow shock eight minutes later, re-entering the solar wind.

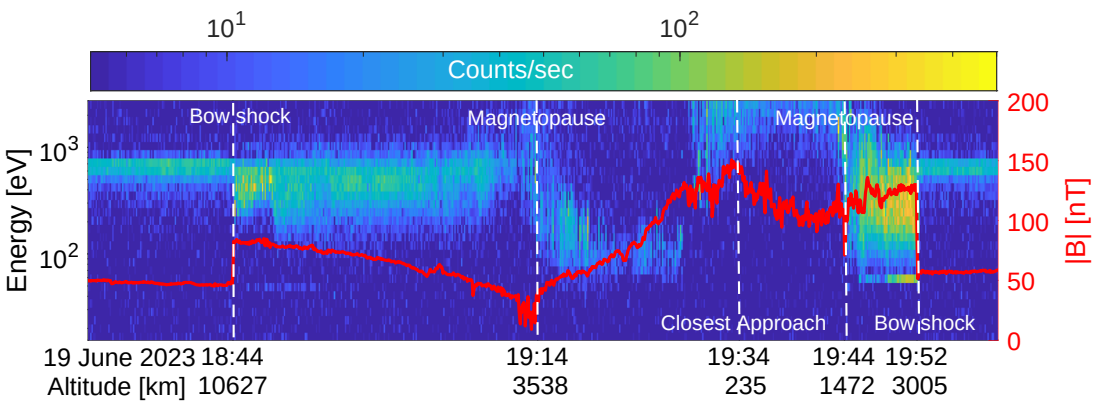

Magnetic field and ion energy spectrogram measured by *MGF* and *PICAM* aboard *BepiColombo* during the third Mercury flyby.

VENUS & MARS

Venus and Mars are Earth's neighbors at a distance of approximately 0.7 astronomical units (au) and 1.5 au from the Sun, respectively. They have orbital periods around the Sun of 224 and 687 days, respectively. While Venus is approximately the same size as the Earth, Mars only has about half the size of the Earth. Where Venus has a very dense and hot atmosphere, Mars's is tenuous and cold. Both planets do not have an internal magnetic field, however, their interaction with the solar wind creates a so-called induced magnetosphere.

TIANWEN-1

Tianwen-1 ("questions to heaven") is China's first Mars mission, consisting of an orbiter and a rover named *Zhurong*. The mission is designed to conduct a comprehensive remote sensing of the Red Planet, as well as surface investigations. The IWF contributed to a magnetometer aboard the orbiter.

Since the switch-on of the *Mars Orbiter MAGnetometer (MOMAG)* on 13 November 2021, it has been in continuous operation with two operational modes: 32 Hz for 120 min around periapsis and for 60 min around apoapsis, and 1 Hz for the rest of the 8-hour orbit. *MOMAG* demonstrated good performance, nevertheless all measurements indicated various spacecraft magnetic effects due to the lack of a magnetic cleanliness program and the rather short 3.2 m boom. The two-sensor gradiometer formation, where the outboard sensor is located at the end of the boom and the inboard sensor at 0.9 m from the outboard, is used to remove the spacecraft magnetic effects. The zero offset has been successfully calibrated using the magnetic field data in the solar wind or in the Martian magnetosheath. The cleaned scientific data have been publicly released in 2023.

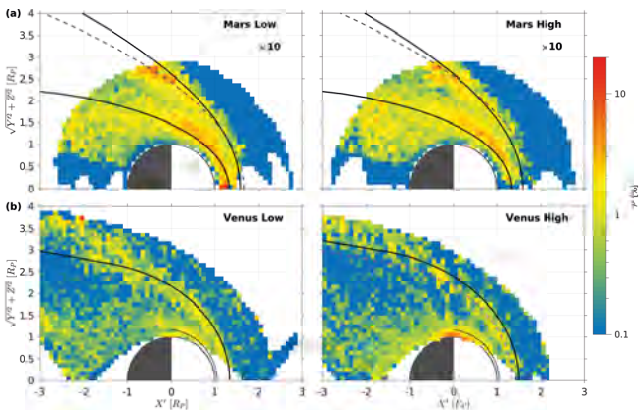

Probability of occurrence of MiMos at Mars from *MAVEN* data (a) with probabilities multiplied by 10 and Venus from *VEX* data (b) in cylindrical coordinates, with the X axis planet-Sun direction. MiMos are concentrated behind the shock region and closer to the planets, with Martian MiMos occurring on average 10 times less than Venus MiMos.

MIRROR-MODE STRUCTURES AT MARS AND VENUS

Mars and Venus have their magneto-environment pervaded by ultra-low-frequency (ULF) waves of different make and origin, which participate in the energy and momentum transfer between the solar wind and the induced magnetospheric plasma. The seeding of these waves takes place in the buffer zone between these two regions, the so-called magnetosheath, where turbulence at small and large scales typically occurs and the plasma instability at the origin of the waves can grow. Mirror Modes (MiMo) are such wave structures which are born from a sizable plasma temperature anisotropy in a weakly magnetized environment, a condition that is expected to occur downstream of the bow shock or close to the interface between the magnetosheath and the induced magnetosphere (a.k.a. the Induced Magnetospheric Boundary or IMB).

Using the datasets gathered by two space missions, *MAVEN* at Mars between 2014 and 2021 and *Venus Express (VEX)* at Venus between 2006 and 2014, and the same data analysis technique based on magnetic field-only measurements, a survey of MiMo structures was carried out, which lead to two separate studies. Results showed that MiMos have occurrence probabilities ranging from a few percent (Mars) to about 10 percent (Venus) in the overall datasets and, similarly for both planets, are indeed mainly confined to two regions, one immediately downstream of the shock, the other just upstream of the IMB.

In agreement with observations at Earth, quasi-perpendicular shock conditions were found to be more conducive to the appearance of MiMos. Moreover, lower solar activity conditions at Mars lead to slightly larger probabilities, a behavior which was suggested to be linked to the anticorrelation between solar activity and solar wind plasma beta, hence globally hindering the growth of the instability. In contrast, at Venus, larger probabilities were registered by *VEX* in solar maximum condition (albeit during a solar cycle different from that covered with *MAVEN*): this was tentatively linked to increased photoionization and local plasma beta variations. Many questions remain as to the differences in behavior at the two planets: they shall be investigated in the future by the same team.

Simon Wedlund, Volwerk et al., Ann. Geophys., 41, 225-251, 2023.
Volwerk, Simon Wedlund et al., Ann. Geophys., 41, 389-408, 2023.

JUPITER

Jupiter, together with Saturn one of the two gas giants, is the largest planet in our solar system, located at 5.2 au from the Sun. One Jupiter year is 11.86 Earth years and one Jupiter day varies between 9h50′ around the equator, 9h55′40.6″ for latitudes greater than 10° and 9h55′29.71″ for the magnetic field. Jupiter also has the most satellites of any planet in our solar system, with the four large Galilean satellites as the best known. Three of these, Europa, Ganymede and Callisto will be the targets of the recently launched ESA mission *JUICE*. Whereas Europa will also be the target of the NASA mission *Europa Clipper*, Io, the innermost moon will not be studied because of the intense radiation environment around this moon. However, the NASA mission *Juno* has recently targeted Io.

During a three months long commissioning phase, following *JUICE's* launch, all antennas and deployment mechanisms were brought into flight configuration and the scientific instruments were checked out in space for the first time. By the end of 2023, *JUICE* has completed about 8% of its journey to Jupiter.

JUNO

NASA's *Juno* mission to Jupiter arrived in July 2016, to study the gravitational field, the magnetosphere and the atmosphere. After 7 years orbiting Jupiter, the spacecraft is scheduled to dive into the gas planet in 2025. The orbit has been adjusted and *Juno* is moving more and more into the inner magnetosphere, encountering the volcanic moon Io.

JUICE

The JUpiter ICy moons Explorer (JUICE) is an ESA L(arge)-class interplanetary mission to the Jupiter system that was launched on 14 April 2023 from Kourou, French Guiana. Its powerful instrument package will make in-situ and remote sensing measurements of Jupiter and the Galilean moons during a three-year science operation phase starting in July 2031. The tour in the Jupiter system will include a high-latitude phase, fly-bys of Callisto, Ganymede and Europa culminating in elliptical and circular orbits around Ganymede down to an altitude of 200 km in 2035. Detection and characterization of potential sub-surface oceans on Europa and Ganymede are a key science goal of the mission as is the interaction between Ganymede's internal field with the Jovian magnetic field.

The IWF participates on Co-Investigator basis in three of the ten scientific instruments aboard *JUICE*: *J-MAG*, *PEP* and *RPWI*.

The *Jupiter MAGnetometer (J-MAG)* is led by Imperial College London and measures the magnetic field vector and magnitude in the spacecraft vicinity in the bandwidth DC to 64 Hz. It is a conventional dual sensor fluxgate configuration combined with an absolute scalar sensor based on quantum-interference technology. Science outcome from *J-MAG* will contribute to a much better understanding of the formation of the Galilean satellites, an improved characterization of their oceans and interiors, and will provide deep insight into the behavior of rapidly rotating magnetic bodies. The IWF supplied the atomic scalar sensor *(MAGSCA)* for *J-MAG*, which was developed in close collaboration with TU Graz.

The absolute highlight for the *MAGSCA* activities in 2023 were the verification of its perfect performance in space a few weeks after launch in May. It included the very first detection of a quantum interference signal used to measure magnetic fields at a distance of five million kilometers from Earth.

The *Particle Environment Package (PEP)* is a suite of different kind of sensors to characterize the plasma environment of the Jovian system and the composition of the exospheres of Callisto, Ganymede, and Europa. *PEP* is led by the Swedish Institute of Space Physics and the IWF participates in the *PEP* consortium with scientific studies related to the plasma interaction and exosphere formation of the Jovian satellites. The IWF has also been responsible for the calibration of the radio antennas of the *Radio and Plasma Wave Investigation (RPWI)*. Besides the three dipole radio antennas, *RPWI* also harbors a search-coil magnetometer and four Langmuir probes. *RPWI* will cover the Jovian radio spectrum in the frequency range from DC to 45 MHz, and the magnetic field measurements will go from DC to 20 kHz. The Langmuir probes on the tips of four 3 m long booms will perform plasma and 3D electric field measurements. Both, *PEP* and *RPWI* performed extremely well during the first test phase after launch.

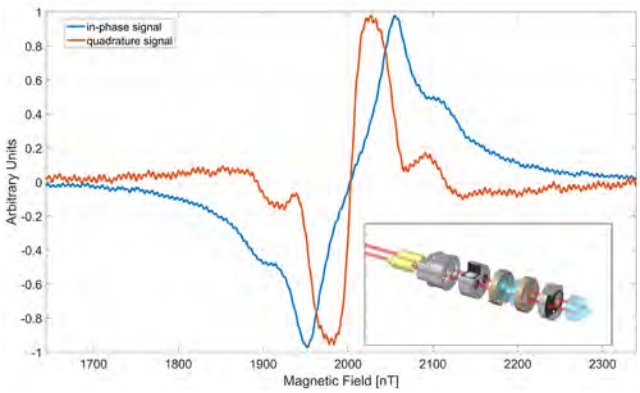

Quantum interference signal which is used to measure the ambient magnetic field with its zero crossing. In this test case it is the field from an auxiliary at the location of the glass cell within the *MAGSCA* sensor (lower right). It has confirmed the perfect functioning of the *MAGSCA* instrument after launch.

ICY MOONS & COMETS

The study of icy moons and comets has intensified in the last few years as it can give answers to some important questions in the areas of solar system and planetary formation and habitability with potential application to exoplanets. Comets are assumed to be the remainders of the building blocks of the solar system. Missions as *Rosetta*, *OSIRIS-Rex* (asteroid sample return) and *Comet Interceptor*, provide a look into the ancient history of the solar system. On the other hand, the study of icy moons, which might harbor an ocean below their kilometers-thick icy surfaces, can give information on the habitability of (exo-)solar system objects. Missions like *Galileo* (discovered the oceans under the icy surface of Europa and Ganymede), *Juno*, *JUICE* and *Europa Clipper* give invaluable data with their high-quality instruments during encounters with the Jovian icy moons Callisto, Ganymede and Europa. This might give indications whether these moons can have a habitable shell inside of them, and could extend the concept of the so-called habitable zone around stars, if sub-surface habitats can exist.

COMET INTERCEPTOR

Comet Interceptor, ESA's first F(ast)-class mission, is well underway in instrument development and building. The mission will consist of three spacecraft: mother spacecraft *A* and daughter spacecraft *B2* under the responsibility of ESA and daughter spacecraft *B1* under the responsibility of JAXA.

After the formal adoption by ESA in 2022, the prime contractors that will build the spacecraft were selected: OHB will be responsible for spacecraft *A* and SENER for spacecraft *B2*.

The envisioned launch date is 2029, depending on the launch date of the *ARIEL* mission, on which *Comet Interceptor* will have a piggy-bag position. The goal of the mission is to have multi-point observations of a dynamically new comet, its nucleus and its environment. This will be the first time that multiple spacecraft will visit a comet simultaneously.

The IWF contributes hardware to two instruments on *Comet Interceptor*. On spacecraft *A* the Data Processing Unit (DPU) for the *Mass Analyzer for Neutrals and ions at Comets (MANiaC*, lead institute University of Bern) is being developed and built. On spacecraft *B* the electronics for the *Flux Gate magnetometer (BFG*, lead institute Imperial College London) is being developed and built, which is part of the *Dust Field and Particles suite (DFP*, lead institute Space Research Center of the Polish Academy of Sciences, CBK).

In 2023, the *BFG* electronics of the first Engineering Model (EM1) was delivered to CBK along with the structural models of the sensor and boards, where they were integrated into their dedicated boxes (electronics box and Structural and Thermal Model box). Further development and testing of the Electrical Functional Model (EFM, equivalent to a Qualification Model) were successfully performed. The actual EFM sensors and boards were successfully tested with in thermal-vacuum, vibration as well as calibrated in Braunschweig (Germany), which paved the way for the upcoming *Comet Interceptor* Flight Model. The sturdiness of the sensor can be seen in the pictures below, showing that the fine copper wires survive the vibration test without any damage.

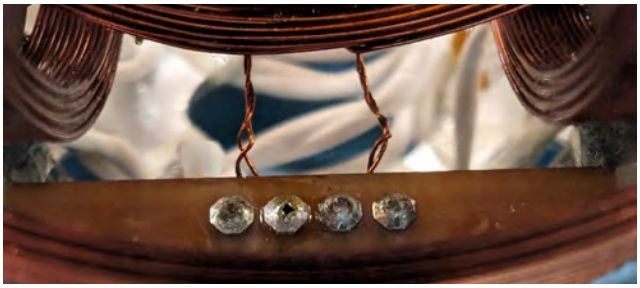

BFG EFM sensors after vibration test (© OeAW/IWF/Valavanoglou).

EM1 and EM2 of the *MANiaC* DPU were manufactured at the IWF, and the functional tests for EM1 started in November. The team aims for a delivery of the EM1 in early 2024 to the University of Bern where early test with the rest of the instrument will take place. EM2 will be delivered later next year. In parallel, the Boot Software for the DPU has been completed, and its first version was validated and released. Work on the Application Software (ASW) also started but was delayed due to continuous requirement changes, resulting in the Software Preliminary Design Review in late November. Nevertheless, the team is working towards the release of an early version of the ASW together with the EM1 delivery.

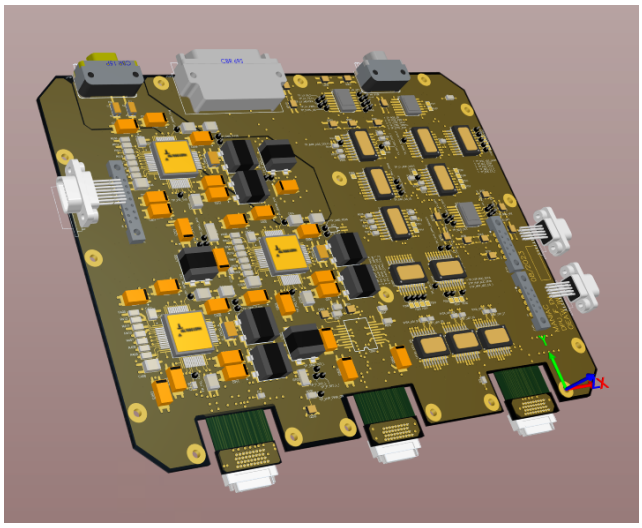

Interface printed circuit board for the *MANiaC* DPU.

MIDAS SCIENCE

The enormous wealth of *Rosetta* data is still leading to new scientific results. The *MIDAS (Micro-Imaging Dust Analysis System)* atomic force microscope on board the *Rosetta* comet orbiter investigated and measured the 3D topography of dust particles of comet 67P/Churyumov-Gerasimenko with sizes from a few hundred nm to tens of µm, with a resolution down to a few nm. The measurements give insights into the physical processes of the early solar system.

The shapes of the cometary dust particles collected by *MIDAS* were analyzed on the basis of a recently updated particle catalog, with the aim to determine which structural properties remained pristine (see figure below).

A set of shape descriptors and metrics such as aspect ratio, elongation, circularity, convexity, and particle surface and volume distribution, which can be used to describe the distribution of particle shapes, have been developed.

Furthermore, the structure of the *MIDAS* dust particles and the clusters, in which the particles were deposited, were compared to those found in previous laboratory experiments and by *Rosetta's COmetary Secondary Ion Mass Analyzer*.

Finally, the findings were combined to calculate a pristineness score for *MIDAS* particles and determine the most pristine particles and their properties. It was found that the morphological properties of all cometary dust particles at the micrometer scale are surprisingly homogeneous despite originating from diverse cometary environments. It was also found that most types of clusters measured by *MIDAS* show good agreement with those defined by previous laboratory experiments.

Kim et al., A&A, 673, A129, 2023.
Kim et al., A&A, 678, A179, 2023.

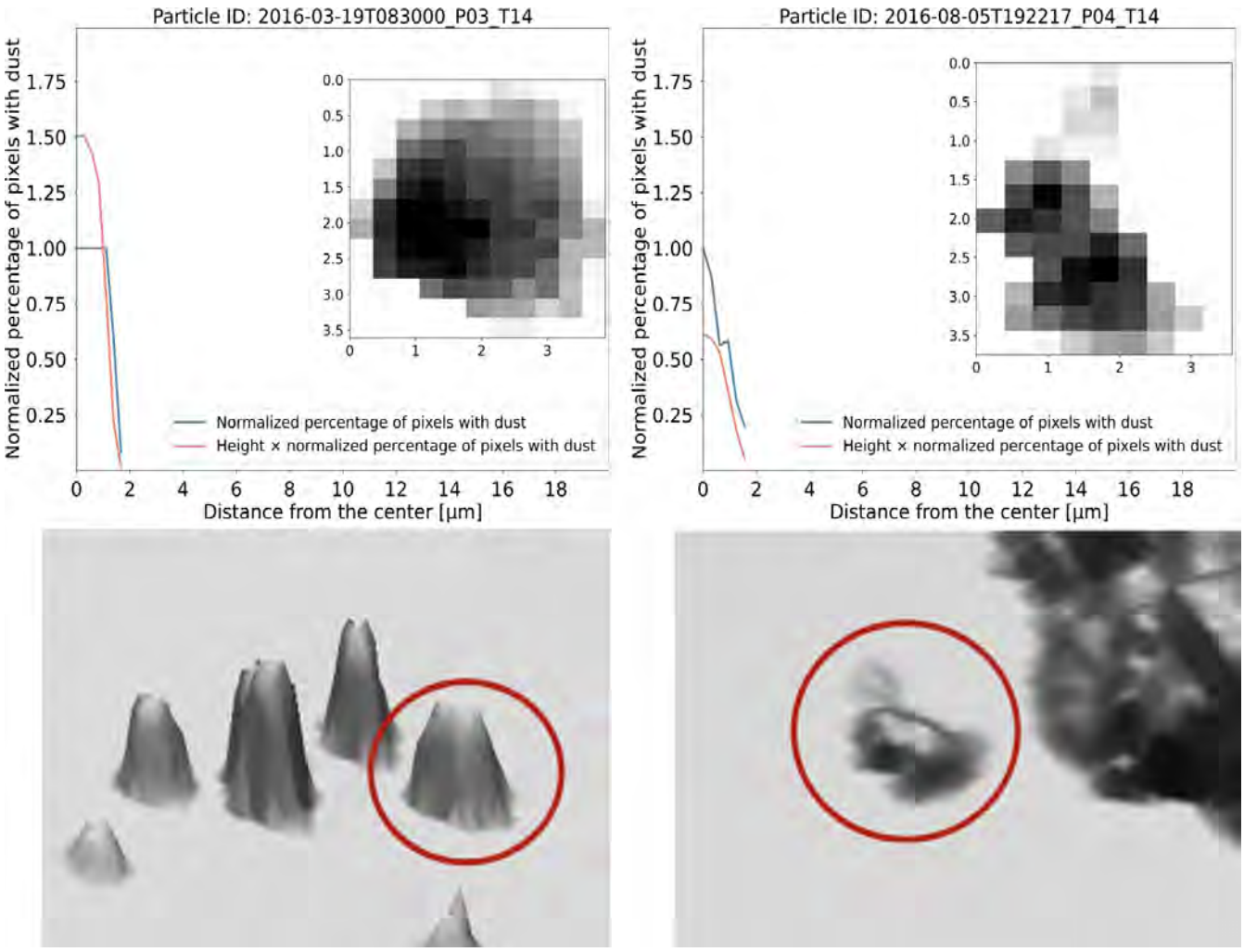

Example of particle surface and volume distribution of *MIDAS* Single particles (e.g., typically a solid, roundish bulk, showing a plateau in the particle surface distribution; top left) and *MIDAS* Pile particles (e.g., elongated shapes, fringed rims, showing no plateau; top right). Corresponding 3D images of the *MIDAS* Single (bottom left) and Pile (bottom right) particles are marked with red circles.

ASTRO-LABORATORY: GAS DIFFUSION EXPERIMENTS AND SIMULATION WITH THEORETICAL MODELS

On both comets and icy moons, the gas transport through the porous surface material plays a major role in the formation and replenishment of their comae and atmospheres/exospheres, respectively. Sublimated water ice and other volatile components from layers below the surface can escape the surface material only if it is sufficiently permeable. Due to the weak gravity of these celestial objects, the gas pressures above the surface are very low. Therefore, gas particles that reach the surface from deeper layers mainly experience collisions with the pore walls of the surface material, while the number of intermolecular collisions is negligible. The net gas flow occurs by diffusion of the particles through the pores, the so-called Knudsen diffusion. For the diffusion process the size and structure of the pores play a crucial role.

Although Knudsen diffusion has been studied for more than a century, there are still many open questions, especially about the influence of the pore structure. Therefore, in recent years corresponding experiments have been carried out in connection with the above-mentioned applications in space research. After developing a precise methodology for separating Knudsen diffusion and viscous flow in experiments, Finite Element Method (FEM) simulations were applied to identify changes to the experimental setup that lead to a further increase in measurement accuracy.

Laddha et al., Meas. Sci. Technol. 34, 045012, 2023.

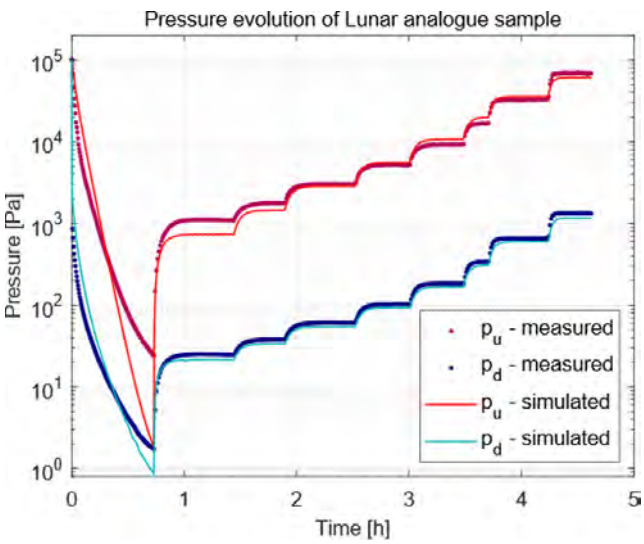

Measurements and FEM simulations for the upstream and downstream pressure (p_u and p_d) of the gas flow through a porous sample of analog material.

In addition to the experimental research with associated FEM simulations, an expansion of the theoretical foundations was initiated. Based on a stochastic description of gas particle transport through plane porous layers, two main results could be obtained. On the one hand, a relation was derived between the probability of a gas particle to penetrate a porous layer and the Knudsen diffusion coefficient, which describes the diffusion process. On the other hand, a mathematical expression of these coefficients in terms of material parameters was inferred, which is closer to the experimental measurements than previous classical formulas. These analytical models were confirmed by Direct Simulation Monte Carlo (DSMC) computations. The stochastic approach is valid for homogenous packing and isotropic surface element distribution, and the mentioned simulations were performed for monodisperse sphere packing. Extensions to polydisperse and angular grains, as well as spatial variations, are planned for the near future. They are extremely important in order to render gas transport on comets and icy moons more realistically.

Güttler et al., MNRAS, 524, 4, 6114, 2023.

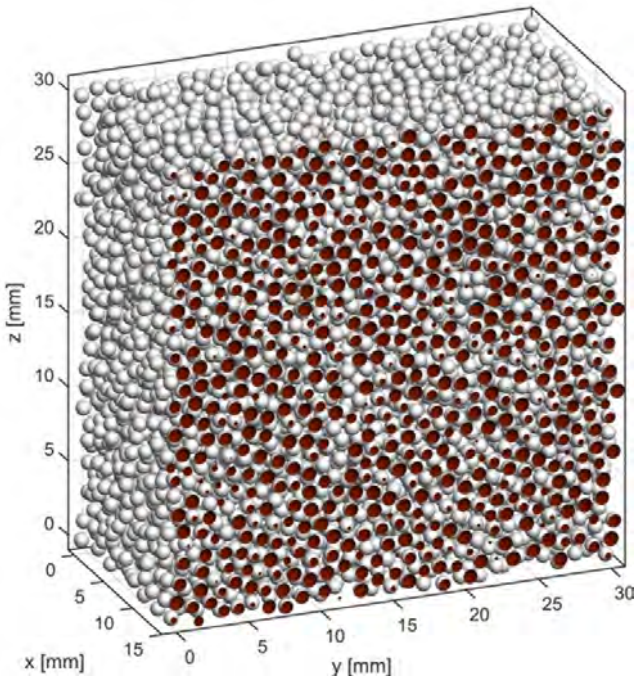

Cross section of sphere packing for 65% porosity, as used for DSMC gas flow simulations.

EXOPLANETS & DISKS

The field of exoplanet research - i.e., investigation of planets orbiting stars other than the Sun - has developed strongly in the past decades. The first exoplanet orbiting a Sun-like star, 51 Peg b, was detected in 1995. More than 5000 exoplanets, most in planetary systems, are now known. Improved instrumentation and analysis techniques have led to the detection of smaller and lighter planets, particularly orbiting bright, nearby stars, which therefore enable in-depth structure and atmospheric characterization. Although hot Neptunes and (ultra-) hot Jupiters are still prime targets for atmospheric characterization, smaller planets are entering the realm of the planets for which the atmosphere can be directly probed. This is particularly thanks to the advent of the *James Webb Space Telescope (JWST)*. With its large collecting area and broad suite of instruments, *JWST* is driving a revolution in our view of exoplanetary atmospheres and of the cosmos at large. The IWF has been involved in the early science release.

The main exoplanet missions in which the IWF is involved with hardware and/or science are *CHEOPS*, *CUTE*, *PLATO*, *ARIEL*, and *NEWATHENA*.

The European consortium in charge of the majority of *CHEOPS* observing time made use of *CHEOPS* observations to publish about 20 refereed publications. Among those, the team published the first *CHEOPS* Nature paper, which carries significant IWF contribution and has been listed among the top six Nature papers of all times in terms of media coverage. The first results of NASA's *CUTE* mission have been published, and ESA's *ARIEL* mission passed Preliminary Design Review.

The IWF focuses on the study and characterization of planetary atmospheres and of star-planet interaction phenomena using both theory and observations, in particular on the analysis of planet formation, atmospheric clouds, evolution, and mass-loss processes. The research is based on collecting and analyzing ground- and space-based observations to constrain the models, as well as on modeling of planetary atmospheres and of planet formation from first principles.

With the aim of constraining the properties of the middle and upper atmosphere, near-ultraviolet transits of the hot Jupiter HD 189733 b have been observed with the *Hubble Space Telescope*. The planet's near-ultraviolet spectrum is rather flat, consistent with what measured in the optical and infrared, except for two broad absorption regions concomitant with the location of lines of ionized Fe. Surprisingly, no ionized Mg has been detected in the planetary upper atmosphere, while it has been observed in all other planets so far characterized at near-ultraviolet wavelengths.

CHEOPS

CHEOPS (CHaracterising ExOPlanet Satellite), successfully launched in December 2019, started regular science operations in April 2020. The mission aims at studying exoplanets by means of ultra-high precision photometry. The primary science goals are to precisely measure the radii of Neptune- to Earth-sized planets to constrain the internal composition and atmospheric evolution, study the atmospheric properties of transiting giant planets, and look for new planets particularly in already known systems.

In 2023, *CHEOPS* started operations of the first extended mission until the end of 2026, demonstrating that the satellite performs and ages as expected. A possible further extension until the end of 2029 would enable overlaps of *CHEOPS* with *PLATO*, and possibly *ARIEL*.

The IWF contributed the *Back-End-Electronics* that is one of the two onboard computers and it is responsible for controlling the data flow and the thermal stability of the telescope structure. The institute also developed and maintains the mission's signal-to-noise calculator. Within the Guaranteed Time Observations of the *CHEOPS* consortium, the IWF chairs the task force coordinating the effort towards obtaining ground-based radial velocity observations for planetary mass measurements, coordinates the re-analysis of archival observations from other facilities to better constrain planetary transit ephemerides prior to *CHEOPS* observations and the efforts towards modeling eclipse and phase curves observations. The institute hosts two members of the *CHEOPS* board, as well as two *CHEOPS* science team members.

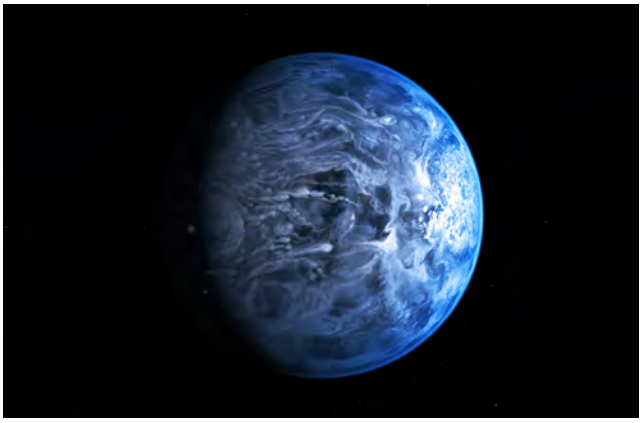

Artist's impression of the deep blue planet HD 189733 b (© ESA/ Hubble).

CUTE

CUTE (Colorado Ultraviolet Transit Experiment) is a NASA-funded 6U-form CubeSat led by the University of Colorado that was launched in 2021. *CUTE* performs low-resolution transmission spectroscopy of transiting exoplanets at near-ultraviolet wavelengths. It studies the upper atmosphere of short-period exoplanets with the aim of observationally constraining atmospheric escape processes, which are key to understand planetary evolution, and detect heavy metals, which constrain the presence and composition of aerosols in the lower atmosphere. Following a rather long commissioning phase, the first scientific results have been published in 2023.

The IWF is the only technological contributor to the mission outside of the University of Colorado (Boulder), where *CUTE* was developed. The institute is responsible for the data simulator, the data signal-to-noise calculator, the ground data reduction software, the data analysis procedures, and the algorithms defining the onboard data reduction software.

In 2023, the IWF finalized the development of the data analysis pipeline and of the signal-to-noise calculator, which is extensively used for target selection and scheduling of *CUTE* observations. The *CUTE* signal-to-noise calculator is an offshoot of the *CUTE* data simulator, which has been developed at the IWF in previous years. The code reads the input parameters to generate a spectrum of the target star in the *CUTE* band by employing a library of synthetic photospheric stellar fluxes. The *CUTE* spectrograph also covers the MgII h&k resonance lines, which in late-type stars present chromospheric line core emission with a strength proportional to the stellar activity. The code automatically estimates the MgII h&k line core emission from the input given by the user. The stellar flux at Earth is then derived by scaling for the distance to the star calculated from the parallax provided by the user.

The *CUTE* signal-to-noise calculator also accounts for interstellar medium absorption. In particular, both broadband extinction and interstellar medium line absorption for Mg and Fe have been implemented. Each interstellar medium absorption feature is simulated as a single Voigt profile with a fixed broadening parameter of 3 km s^{-1} and assuming no radial velocity shift between the stellar and interstellar medium features as radial velocity shift has a negligible impact on transit measurements at the *CUTE* resolution. The MgI, MgII, and FeII interstellar medium column densities, which set the strength of the absorption features, are required input from the user. The stellar flux at Earth, optionally modified to account for the interstellar medium absorption, is then converted from erg cm^{-2} s^{-1} $Å^{-1}$ to photons cm^{-2} s^{-1} $Å^{-1}$. The spectra are then trimmed to the relevant wavelength range, multiplied by the effective area of the instrument, and convolved to the spectrograph's resolution, finally obtaining the CCD detector counts.

As a further step, the signal-to-noise calculator converts the counts $Å^{-1}$ s^{-1} to counts $pixel^{-1}$ s^{-1} by taking into account the spectral resolution and the number of pixels per resolution element. Finally, the CCD counts are multiplied by the exposure time to obtain the expected signal from a particular source. The CCD counts are further converted from counts to photo-electrons using the gain provided by the user. As a further feature, the signal-to-noise calculator incorporates error propagation for computing transit depth uncertainties starting from the signal-to-noise of the original spectroscopic observations.

Sreejith et al., Astrophys. & Space Science, 368, 31, 2023.

ARIEL

ARIEL (Atmospheric Remote-sensing Infrared Exoplanet Large-survey) is ESA's fourth M(edium)-class mission, led by University College London, to be launched in 2029. It will investigate the atmospheres of several hundred exoplanets to address fundamental questions on how planetary systems form and evolve. During its four-year mission, *ARIEL* will observe 1000 exoplanets ranging from Jupiter- and Neptune- down to super-Earth-size in the visible and infrared with its meter-class telescope. The analysis of *ARIEL* spectra and photometric data will enable extracting the chemical fingerprints of gases and condensates in planetary atmospheres, including the elemental composition for the most favorable targets, with a particular focus on carbon and oxygen. Thermal and scattering properties of the atmospheres will also be studied.

ARIEL consists of a one-meter telescope feeding two infrared low-resolution spectrographs and the fine guiding sensor (FGS), working in the optical. To improve the satellite's pointing stability, the FGS provides optical photometry of the target in three broad bands that are used to control instrumental systematics, measure intrinsic stellar variability, and constrain the presence of high-altitude aerosols in planetary atmospheres. The IWF co-leads the upper atmosphere working group, is part of the laboratory data working group and is involved in testing the mission's performances, advancing the atmospheric retrieval tools and improving the inference of fundamental parameters (e.g. mass, age) of the host stars.

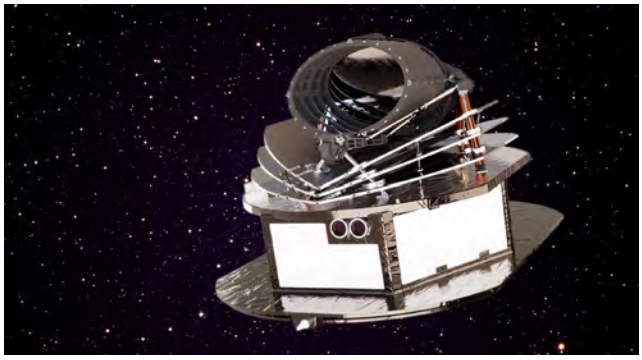

Artist view of *ARIEL* (© Airbus).

PLATO

PLATO (PLAnetary Transits and Oscillations of stars) is ESA's third M(edium)-class mission, led by DLR. Its objective is to find and study a large number of exoplanetary systems, with emphasis on the properties of terrestrial planets in the habitable zone around solar-like stars. *PLATO* has also been designed to investigate seismic activity of stars, enabling the precise characterization of the host star, including its age. Launch is expected in 2026.

The IWF co-leads the work package aiming at studying planetary habitability and leads the work packages studying cloud and gas chemistry, as well as multi-dimensional properties of planetary atmospheres. The institute takes part in two further work packages (on stellar characterization and on planetary evolution) aiming at gaining the knowledge and preparing the tools necessary to best exploit the data. The IWF contributes to the development of the *Instrument Control Unit (ICU)* by delivering the *Router and Data Compression Unit (RDCU)*.

PLATO consists of 24 telescopes for nominal and two telescopes for fast observations. Each telescope has its dedicated front-end-electronics, reading and digitizing the CCD content. Twelve nominal and two fast DPUs collect the data from the front-end-electronics and extract the areas of interest. The *RDCU* is a key element in the data processing chain, providing the communication between the DPUs and the *ICU*. The second task of the *RDCU* is the lossless compression of the science data. For performance reasons, the compression algorithm is implemented in an FPGA.

In 2023, the *RDCU* Engineering Qualification Model (EQM) was completed and delivered to INAF in Italy. It was integrated with the *ICU* and performed nominally. The team also completed the manufacturing of the three Flight Model boards (FM1 as nominal, FM2 as redundant and FM3 as spare). The boards were inspected by an ESA soldering qualification expert in November, and the minor re-works required were implemented. The boards will undergo functional testing in early 2024 before delivery to Italy.

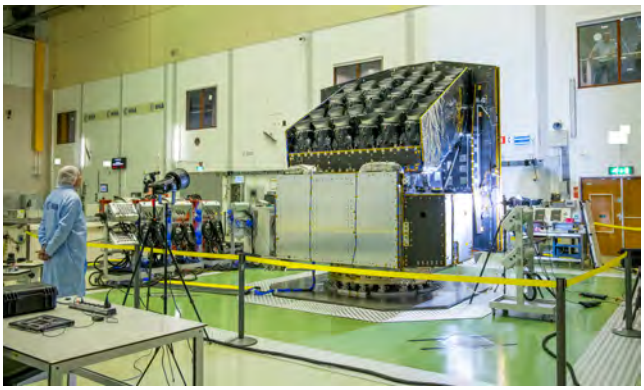

PLATO situated on top of ESA's QUAD shaker to simulate the vibrations encountered during launch (© ESA/G. Porter).

NEWATHENA

ATHENA (Advanced Telescope for High-ENergy Astrophysics) was ESA's second L(arge)-class mission in the Cosmic Vision 2015-2025 plan. It was reformulated in 2023 due to cost overrun. The now approved mission is called *NEWATHENA*. Most of the scientific objectives of *ATHENA* remain, namely: (1) the study of hot gas in clusters and groups of galaxies and in the intergalactic medium to determine how ordinary matter assembles into large-scale structures and (2) the study of black holes growth and their impact on the universe. Thus, *NEWATHENA* remains an observatory in the X-ray range of the electromagnetic spectrum with the aim of understanding the high energetic processes close to the event horizon of black holes and provide more details for the baryonic component locked in ultra-hot gas. The science redefinition team, however, added stars hosting exoplanets to the *NEWATHENA* science drivers, addressing the contribution of stellar activity to exoplanet habitability.

The institute is part of the consortium for the *Wide Field Imager (WFI)* and will provide the Data Processing Unit (DPU) as part of the *Instrument Control Unit (ICU)*. In 2023, design work for the DPU prototype has started, the finalization and manufacturing is expected to be completed next year.

OTHER TELESCOPES

Members of the institute obtained 16.5 hours of observing time with the *NIRSpec* and *MIRI* instruments on board the *James Webb Space Telescope*. The observations will cover two transits of the warm Jupiter WASP-69 b in the 2.8-12.0 μm wavelength range to make an exhaustive inventory of chemical species in the atmosphere of this planet. Measuring the concentration of multiple atmospheric species with *JWST* will enable disentangling the impact of the different chemical processes at play in the planetary atmosphere.

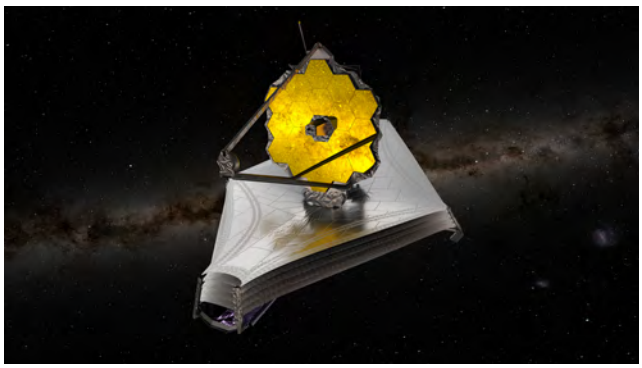

JWST sees farther into our origins: from the formation of stars and planets, to the birth of the first galaxies in the early Universe (© ESA/ATG medialab).

NEPTUNIAN PLANET TOI-1055 b CHARACTERIZED WITH HARPS, TESS, AND CHEOPS

Sub-Neptunes and super-Earths are primary targets for the *CHEOPS* mission. This is because exoplanets in the mass range between Earth and Saturn show a large radius, and thus density, spread for a given mass. Therefore, the precise measurement of the radii of these planets is key to constrain and further understand planetary internal structure and planet formation and evolution.

TOI-1055 is an active Sun-like star known to host a transiting Neptune-sized planet on a 17.5-day orbit (TOI-1055 b) for which past radial velocity measurements led to significantly different planetary masses. A newly developed analysis tool, able to account and correct for stellar activity, has been used to re-analyze the radial velocity observations and thus deduce the planetary mass. Two *CHEOPS* light curves have been employed in addition to the already available *TESS* data to measure the planetary radius with a significantly better precision compared to what presented in the literature. The radial velocity data have been analyzed by means of a skew normal function to obtain line centers and additional parameters to be used for correcting the signal coming from stellar activity through the breakpoint algorithm. The joint photometric and radial velocity analysis, performed using a Markov chain Monte Carlo scheme, led to the firm detection of TOI-1055 b, deriving a planetary mass of 20.4 +/- 2.6 Earth masses, which is in agreement with one of the two literature estimates, but it is significantly more precise. The photometry led to derive a planetary radius of 3.490 +/- 0.070 Earth radii. The mass and radius measurements imply a mean density of 2.65 +/- 0.37 g cm^{-3}. Planetary structure models run with the measured planetary parameters led to the conclusion that TOI-1055 b is very likely to host a substantial gas envelope with a mass of 0.41 +/- 0.34 Earth masses and a thickness of 1.05 +/- 0.30 Earth radii.

Bonfanti et al., A&A, 671, L8, 2023.

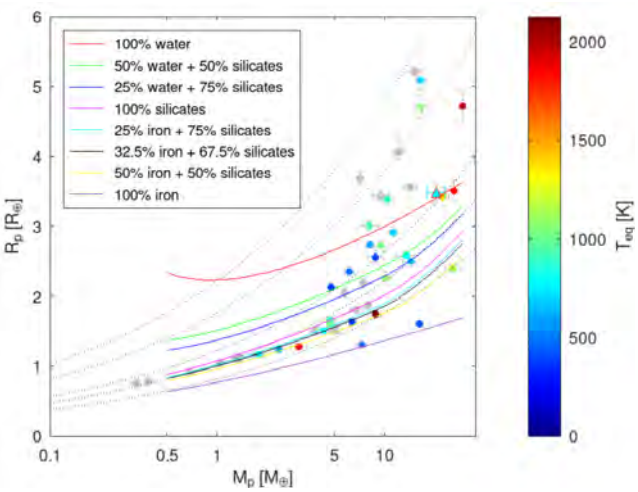

Left: Mass-radius diagram showing exoplanets with mass smaller than 30 Earth masses, whose estimated mean density is more precise than 15%. TOI-1055 b is represented by a triangle. All markers are color-coded according to the planetary equilibrium temperature, where available. Dotted black lines represent the loci of constant average density equal to 0.5, 1, 3, 5, and 10 g cm^{-3} (from top to bottom). Solid lines represent different planet composition models (as explained in the legend) computed for an equilibrium temperature of 750 K, namely that of TOI–1055 b.

ESCAPING METALS IN THE UPPER ATMOSPHERE OF WASP-189 b

With the arrival of the first science data, the IWF led the first scientific publication. Ultraviolet observations of ultra-hot Jupiters, exoplanets with temperatures over 2000 K, such as those gathered by *CUTE*, provide an opportunity to investigate if and how atmospheric escape shapes their upper atmosphere. In particular, near-ultraviolet transit spectroscopy offers a unique tool to study this process owing to the presence of strong metal lines and a bright photospheric continuum as the light source against which the absorbing gas is observed. WASP-189 b is one of the hottest planets discovered to date, with a dayside temperature of about 3400 K orbiting a bright A-type star. WASP-189 b was one of the *CUTE* early science targets and was observed during three consecutive transits in March 2022. The *CUTE* observations led to the measurement of a near-ultraviolet (2500-3300 Å) broadband transit depth (1.08±0.08%) of about twice the visual transit depth indicating that the planet has an extended, hot upper atmosphere with a temperature of about 15,000 K and a moderate mass-loss rate of about 4 x 10^8 kg s^{-1}. The *CUTE* observations also revealed absorption by the MgII h&k resonance lines beyond the Roche lobe at more than 4σ in the transmission spectrum at a resolution of 10 Å. At a lower resolution of 100 Å, the data present a quasi-continuous absorption signal consistent with a "forest" of low-ionization metal absorption dominated by FeII. The suggested upper atmospheric temperature of about 15,000 K is higher than that predicted by current state-of-the-art hydrodynamic models, indicating the possible presence of additional heating and/or cooling mechanisms not considered so far.

Sreejith et al., Astrophys. J. Lett., 954, L23, 2023.

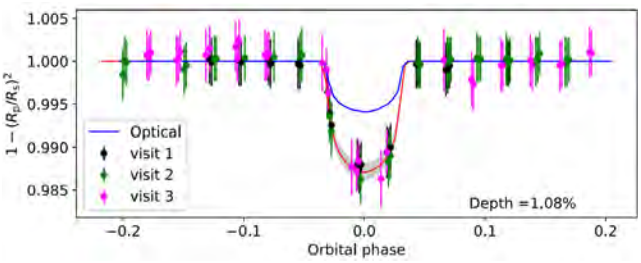

Broadband *CUTE* near-ultraviolet light curve of WASP-189 b for a 800 Å bin centered at 2900 Å.

GEOMETRIC ALBEDO OF THE HOT JUPITER HD 189733 b MEASURED WITH CHEOPS

The second primary goal of the *CHEOPS* mission is deepening our understanding of the atmospheres of giant exoplanets through phase curve and secondary eclipse (i.e. occultation) measurements. In particular, measurements of the occultation of an exoplanet at visible wavelengths allow one to determine the reflective properties of a planetary atmosphere. The observed occultation depth can be then translated into a geometric albedo. This in turn aids in characterizing the structure and composition of an atmosphere by providing additional information on the wavelength-dependent reflective qualities of the aerosols in the atmosphere. Thirteen occultations observed with *CHEOPS* of the hot Jupiter HD 189733 b have been analyzed to infer the geometric albedo accounting for the contribution of thermal emission from the planet. The *CHEOPS* data led to the measurement of an occultation depth of 24.7±4.5 ppm, corresponding to a geometric albedo of 0.076±0.016, which is consistent with models assuming the atmosphere of the planet to be cloud-free at the scattering level and absorption in the *CHEOPS* band to be dominated by the resonant doublet of neutral sodium. Taking into account previous optical-light occultation observations obtained with the Hubble Space Telescope, both measurements combined are consistent with a super-stellar sodium elemental abundance in the dayside atmosphere of HD 189733 b. Furthermore, the data constrain the planetary Bond albedo to lie between 0.013 and 0.42.

Krenn et al., A&A, 672, A24, 2023.

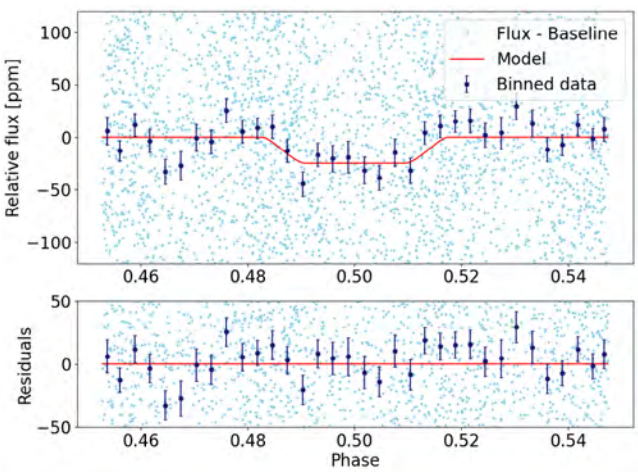

Close-up of the phase-folded, detrended, and fitted occultations of HD 189733b observed by *CHEOPS* (top) and the residuals of the fitted model (bottom). The light blue points represent the individual data points, the dark blue points the 5 min bins, and the red line the model.

ORIGIN OF THE NON-DETECTION OF METASTABLE HeI IN THE ATMOSPHERE OF WASP-80 b

Because of its proximity to an active K-type star, the hot Jupiter WASP-80 b is a possible excellent target for detecting and measuring HeI absorption in the upper atmosphere, but previous observations led to a non-detection. X-ray flux measurements of WASP-80 and recent scaling relations accounting for the coronal [Fe/O] abundance ratio were used to constrain the extreme-ultraviolet (EUV) stellar flux in the 200-504 Å range, which controls the formation of metastable HeI. Three-dimensional (magneto)hydrodynamic simulations of the expanding planetary upper atmosphere interacting with the stellar wind have been used to study the impact on the HeI absorption of the stellar high-energy emission, the He/H abundance ratio, the stellar wind, and the possible presence of a planetary magnetic field up to 1 G. For low stellar EUV emission, which is favored by the observations, the HeI non-detection can be explained by a solar He/H abundance ratio in combination with a strong stellar wind, by a subsolar He/H abundance ratio, or by a combination of the two. For a high stellar EUV emission, the non-detection implies a subsolar He/H abundance ratio. A planetary magnetic field is unlikely to be the cause of the non-detection.

Fossati et al., A&A, 673, A37, 2023.

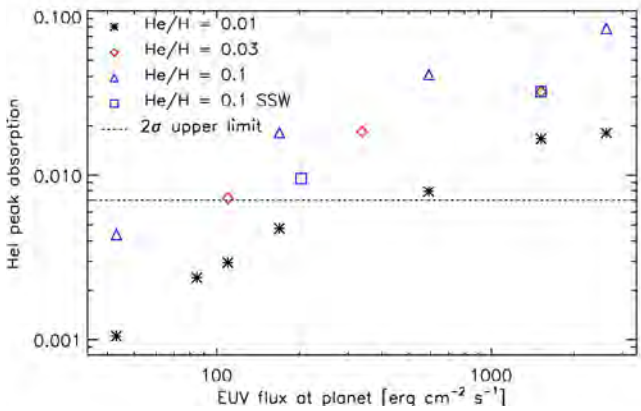

HeI peak absorption resulting from the simulations as a function of stellar EUV flux assuming different He/H abundance ratios. Blue squares are for a strong stellar wind. The horizontal dashed line marks the observed 2σ upper limit. The vertical dotted lines correspond to the two possible values of the stellar EUV flux.

IMPACT OF MgII INTERSTELLAR MEDIUM ABSORPTION ON NEAR-ULTRAVIOLET EXOPLANET TRANSITS

Ultraviolet (UV) transmission spectroscopy probes atmospheric escape, which has a significant impact on planetary atmospheric evolution. If unaccounted for, interstellar medium (ISM) absorption at the position of specific UV lines might bias transit depth measurements, and thus potentially affect the (non-)detection of features in transmission spectra. A parametric study quantifying the impact of unresolved or unconsidered ISM absorption in transit depth measurements at the position of the MgII h&k resonance lines in the near-ultraviolet spectral range has been presented. The parameter study covers main-sequence stars of different spectral types as well as shape and amount of chromospheric emission, ISM absorption, planetary absorption, and their relative velocities. An open-source tool enabling one to quantify the impact of unresolved or unconsidered MgII ISM absorption in transit depth measurements has been developed and applied to a few already or soon to be observed systems. On average, it is found that ignoring ISM absorption leads to biases in the MgII transit depth measurements comparable to the uncertainties obtained from the observations published to date. However, considering the bias induced by ISM absorption might become necessary when analyzing observations obtained with the next generation space telescopes with UV coverage, such as NASA's *Habitable Worlds Observatory*.

Sreejith et al., MNRAS, 519, 2101, 2023.

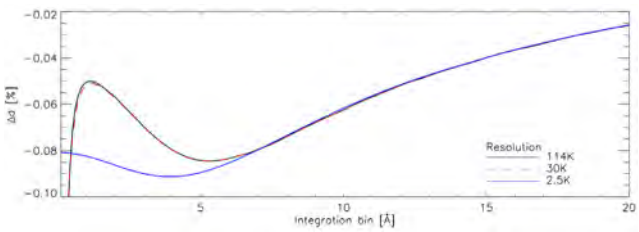

Transit depth difference, in %, obtained between considering and ignoring ISM absorption at the position of the MgII h&k resonance lines as a function of integration bin, in Å, for three spectral resolutions of 114000 (black), 30000 (red dashed), and 2500 (blue).

THE HUBBLE NEAR-UV TRANSMISSION SPECTRUM OF HD 189733 b

The benchmark hot Jupiter HD 189733 b has been a key target to lay out the foundations of comparative planetology for giant exoplanets. As such, HD 189733 b has been extensively studied across the electromagnetic spectrum, except in the near-ultraviolet (NUV). Observation and analysis of three NUV transit light curves of HD 189733 b obtained with the *STIS* spectrograph on board the *Hubble Space Telescope* have been presented. The NUV is a unique window for atmospheric mass-loss studies owing to the strong resonance lines and large stellar photospheric flux. Overall, at low resolution the planet's NUV spectrum is well characterized by a relatively flat baseline, consistent with the optical-infrared transmission, plus two regions at about 2350 and 2600 Å that exhibit a broad excess absorption above the continuum. These features coincide with the expected location of FeII bands. However, solar-abundance hydrodynamic models of the upper atmosphere are not able to reproduce the amplitude of these features considering just iron absorption. An analysis at a higher resolution shows that the transit depths at the core of the magnesium resonance lines are consistent with the surrounding continuum, discarding the presence of MgII absorption in the upper atmosphere.

Cubillos et al., A&A, 671, A170, 2023.

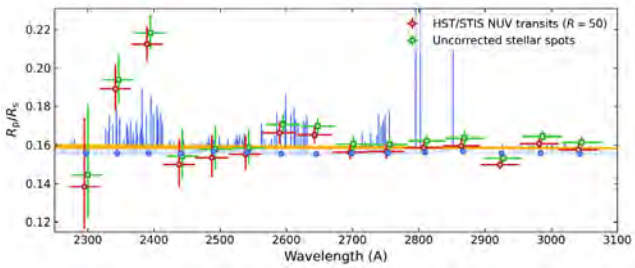

NUV transmission spectrum of HD 189733 b. The red markers with error bars denote the systematics- and stellar-spot corrected transmission spectrum, their 1σ uncertainties, and the span of the spectral bins. The green markers show the results obtained when neglecting spot contamination. The blue line shows a theoretical model of the planet's upper atmosphere and the blue dots show the model integrated over the spectral bins. The orange curve shows an extrapolation from a fit to the optical transmission spectrum of the planet.

H I BALMER LINES TRANSMISSION SPECTROSCOPY AND MODELING OF THE ULTRA-HOT JUPITER KELT-20 b

Ultra-hot Jupiters are prime targets for atmospheric characterization. The H I Balmer line profiles of the ultra-hot Jupiter KELT-20b have been extracted from six transits obtained with the *HARPS-N* high-resolution spectrograph attached to the *Telescopio Nazionale Galileo*. The temperature-pressure profile has been computed employing the HELIOS code in the lower atmosphere and the CLOUDY non-local thermodynamical equilibrium (NLTE) code in the middle and upper atmosphere. CLOUDY has been further used to compute the theoretical planetary transmission spectrum for comparison with observations. The Hα, Hβ, Hγ, and Hδ lines have been detected at more than 4σ. The models predict an isothermal temperature of ≈2200 K at pressures $>10^{-2}$ bar and of ≈7700 K at pressures $<10^{-8}$ bar, with a roughly linear temperature rise in between. The NLTE synthetic transmission spectrum is in good agreement with the observed H I Balmer line profiles, validating the obtained atmospheric structure. Metals appear to be the primary agents leading to the temperature inversion in ultra-hot Jupiters, and the impact of NLTE effects on them increases the magnitude of the inversion.

Fossati et al., A&A, 676, A99, 2023.

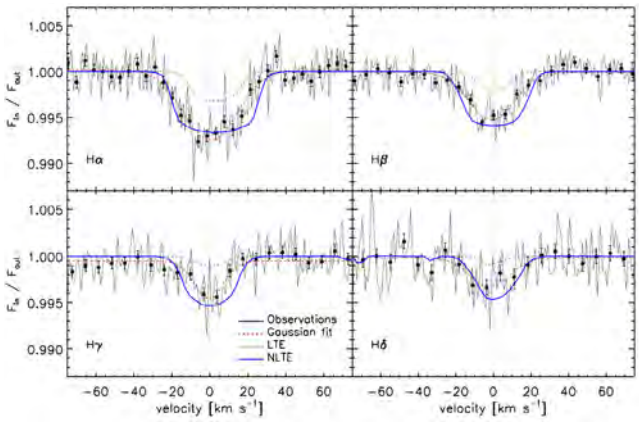

Comparison between observed and synthetic Hα, Hβ, Hγ, and Hδ line profiles. The solid black line shows the observations, while the black dots show the observed profiles re-binned to about 4.5 km s^{-1}. The dashed red line indicates the Gaussian fit to the observations. The solid blue and dash-dotted green lines show the synthetic line profiles computed in NLTE and LTE, respectively.

RADIOACTIVE HEAT BUDGET MODIFICATION OF EARTH-LIKE PLANETS

Radioactive heat producing isotopes in the interior of terrestrial planets are important drivers of the planet's thermal evolution and the related tectonic activity. The initial amount of these elements will later determine if a terrestrial planet evolves to a Venus-like planet or an Earth-like habitat. It is shown that the moderately volatile element potassium with its radioactive isotope ^{40}K can be outgassed from magma oceans into H_2-dominated primordial atmospheres of accreting protoplanets at the time when the gas disc diminishes. In the study of this outgassing, the impact related planetary growth and atmospheric escape is investigated. The assumed impactors consist of depleted and non-depleted material that resembles the same ^{40}K abundance as in average carbonaceous chondrites until the growing protoplanets reach one Earth-mass. Different atmospheric compositions, as a function of pressure and temperature are investigated and the proportion of potassium by Gibbs Free Energy minimization, using the GGCHEM code, is calculated (see figure a). It is found that for H_2-envelopes and for magma ocean surface temperatures that are ≥ 2500 K, no K-related condensates are thermally stable and ^{40}K can populate the escaping primordial atmosphere to a great extent. The escaping H atoms can drag ^{40}K so that a fraction of the isotopes is lost to space (see figure b). Therefore, one can expect different initial abundances of heat producing elements, which will result in various thermal and tectonic histories of terrestrial planets and hence their potential habitability conditions.

Erkaev et al., MNRAS, 518, 3703-3721, 2023.

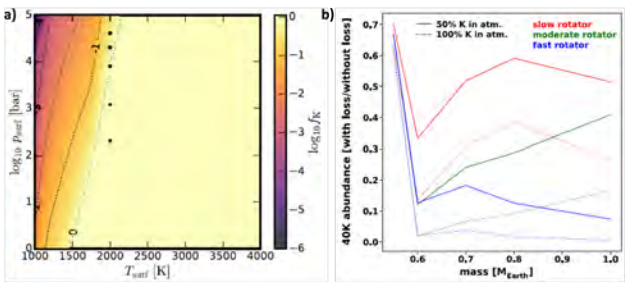

a) K fraction in the gas phase dependent on H_2-pressure between 1000 - 4000 K of an underlying magma ocean. The numbers along the dotted lines indicate no K containing condensate is stable. The black dots indicate the investigated conditions. b) ^{40}K escape results and impact on the final composition as compared to planets without atmospheric escape for 50 % and 100 % of all ^{40}K within the atmosphere. Here, the impactors are assumed to be undepleted. Protoplanets with ≥0.6 M Earth could lose almost all of their ^{40}K, particularly for moderate and fast rotators

INFRARED SPECTRA OF TiO_2 CLUSTERS FOR HOT JUPITER ATMOSPHERES

Clouds appear to be an unavoidable phenomenon in cool and dense environments. Hence, their inclusion is a necessary part of explaining observations of exoplanet atmospheres, most recently those of WASP-96 b with the *James Webb Space Telescope (JWST)*. Understanding the formation of cloud condensation nuclei in non-terrestrial environments is therefore crucial in developing accurate models to interpret current and future observations. To study cloud formation in exoplanet atmospheres observations were supported with infrared spectra for $(TiO_2)_N$ clusters. Vibrational frequencies were derived from quantum-chemical calculations for 123 (TiO_2)-clusters and their isomers. Their line-broadening mechanisms were also evaluated. Cluster spectra were calculated for several atmospheric levels for two example exoplanet atmospheres (WASP-121 b-like and WASP-96 b-like) to identify possible spectral fingerprints for cloud formation.

The rotational motion of clusters and the rotational transitions within them cause significant line broadening, so that individual vibrational lines are broadened beyond the spectral resolution of the medium-resolution mode of the *JWST Mid-InfraRed Instrument (MIRI)* at resolution R = 3000. However, each individual cluster isomer exhibits a 'fingerprint' IR spectrum. In particular, larger (TiO_2) clusters have distinctly different spectra from smaller clusters. The morning and evening terminator for the same planet can exhibit different total absorbances, due to the greater abundance of different cluster sizes. The largest (TiO_2) clusters are not necessarily the most abundant (TiO_2) clusters in the high-altitude regions of ultra-hot Jupiters and different cluster isomers do contribute to the local absorbance. Planets with a considerable day-night asymmetry will be most suitable in the search for (TiO_2) cluster isomers with the goal of improving cloud formation modeling.

Sindel et al., A&A, 680, A65, 2023.

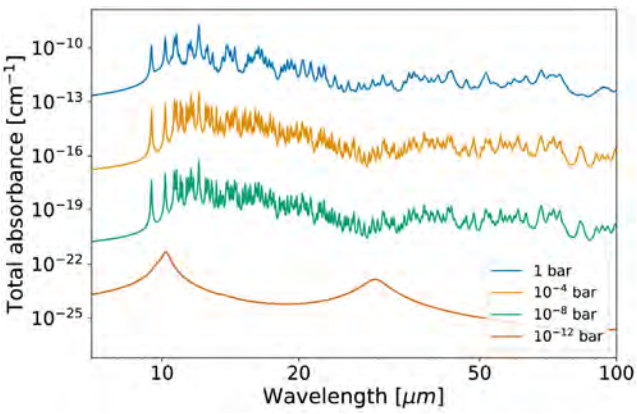

Total absorbance from $(TiO_2)_N$ clusters at different pressure levels of a WASP 121 b-like exoplanet atmosphere as a function of the wavelength; morning terminator.

THE EFFECT OF THERMAL NON-EQUILIBRIUM ON KINETIC NUCLEATION

Nucleation is considered to be the first step in dust and cloud formation in the atmospheres of asymptotic giant branch (AGB) stars, exoplanets, and brown dwarfs. In these environments dust and cloud particles grow to macroscopic sizes when gas phase species condense onto cloud condensation nuclei (CCNs). Understanding the formation processes of CCNs and dust in AGB stars is important because the species that formed in their outflows enrich the interstellar medium. Although widely used, the validity of chemical and thermal equilibrium conditions is debatable in some of these highly dynamical astrophysical environments. A kinetic nucleation model was derived that includes the effects of thermal non-equilibrium by adopting different temperatures for nucleating species, and to quantify the impact of thermal non-equilibrium on kinetic nucleation. Forward and backward rate coefficients were derived as part of a collisional kinetic nucleation theory ansatz. The endothermic backward rates were derived from the law of mass action in thermal non-equilibrium. Elastic collisions were considered as thermal equilibrium drivers.

For homogeneous TiO_2 nucleation and a gas temperature of 1250 K, the differences in the kinetic cluster temperatures as small as 20 K can increase the formation of larger TiO_2 clusters by over an order of magnitude. Conversely, an increase in cluster temperature of around 20 K at gas temperatures of 1000 K can reduce the formation of a larger TiO_2 cluster by over an order of magnitude. This confirms and quantifys the prediction of previous thermal non-equilibrium studies. Small thermal non-equilibria can cause a significant change in the synthesis of larger clusters. Therefore, it is important to use kinetic nucleation models that include thermal non-equilibrium to describe the formation of clusters in environments where even small thermal non-equilibria can be present.

Kiefer et al., A&A, 671, A169, 2023.

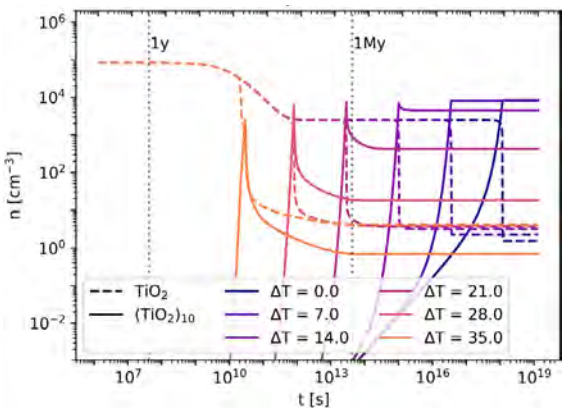

$(TiO_2)_N$ cluster number densities as a function of time under kinetic-to-gas thermal offsets ($T_{kin} = T_{int}$, T_{gas}). Strongest effects occur at T_{gas} = 1000 K where $(TiO_2)_{10}$ increases above the monomer abundance on long time scales.

EXOPLANET WEATHER AND CLIMATE REGIMES WITH CLOUDS AND THERMAL IONOSPHERES

Gaseous exoplanets are the targets that enable us to explore fundamentally our understanding of planetary physics and chemistry. With observational efforts moving from the discovery into the characterization mode, systematic campaigns that cover large ranges of global stellar and planetary parameters will be needed to disentangle the diversity of exoplanets and their atmospheres that all are affected by their formation and evolutionary paths. Pre-calculated 3D global circulation models (GCM) for M, K, G, F host stars are the input for our kinetic cloud model for the formation of nucleation seeds, the growth to macroscopic cloud particles and their evaporation, gravitational settling, element conservation and gas chemistry. Cloud formation trends were studied together with globally changing chemical regimes into which gas-giant exoplanets may fall due to the host star's effect on the thermodynamic structure of their atmospheres. The emergence of an ionosphere as indicator for potentially asymmetric magnetic field effects was examined, providing input for exoplanet missions such as *JWST*, *PLATO*, and *ARIEL*, as well as potential UV instruments like *POLLUX* on NASA's *Habitable Worlds Observatory (HWO)*.

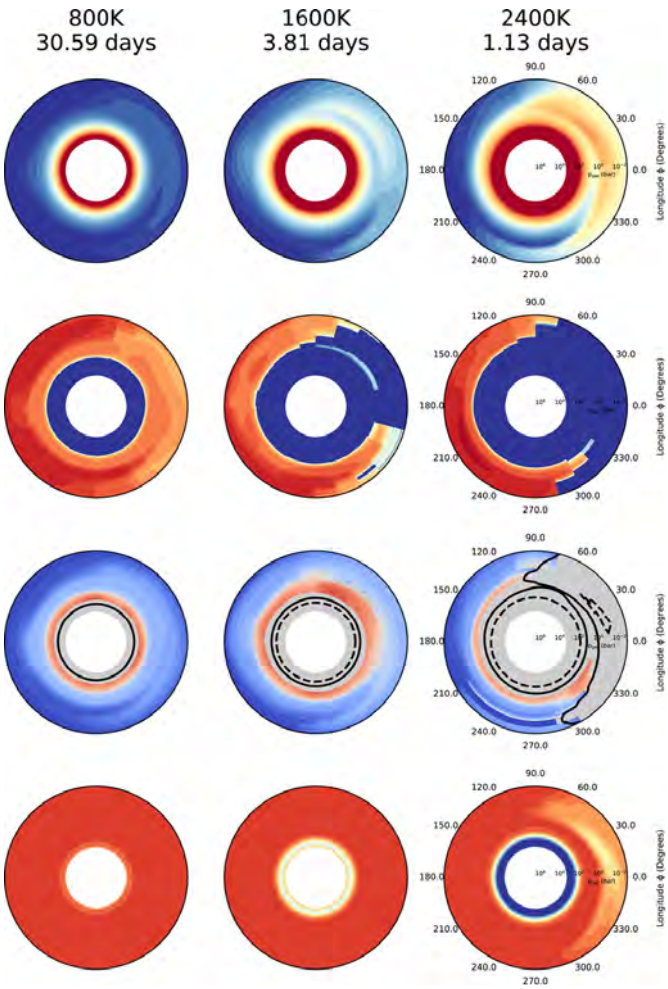

Cool ($T_{eff,P}$ = 800 K), the transient ($T_{eff,P}$ = 1600 K), the hot ($T_{eff,P}$ = 2400 K) exoplanet atmospheres (log g = 3) with an F type host star. 2D equatorial plane slices (θ = 0°) for the 1D profiles extracted from the 3D GCM models: local gas temperature [K], first row; total nucleation rate log(J_*), second row; surface averaged mean particle size log($\langle a \rangle_A$) overlayed with $f_e = 10^{-7}$ (solid line; $f_e = 10^{-6}$ (dashed); third row), mean molecular weight (fourth row).

Gaseous exoplanets fall broadly into three classes: (i) cool planets with homogeneous cloud coverage, (ii) intermediate temperature planets with asymmetric dayside cloud coverage, and (iii) ultra-hot planets without clouds on the dayside. In class (ii), the dayside cloud patterns are shaped by the wind flow and irradiation. Surface gravity and planetary rotation have little effect. For a given effective temperature, planets around K dwarfs are rotating faster compared to G dwarfs leading to larger cloud inhomogeneities in the fast rotating case. Extended atmosphere profiles suggest the formation of mineral haze in form of metal-oxide clusters (e.g. $(TiO_2)_N$).

The dayside cloud coverage is the tell-tale sign for the different planetary regimes and their resulting weather and climate appearance. Class (i) is representative of planets with a very homogeneous cloud particle size and material compositions across the globe (e.g., HATS-6 b, NGTS-1 b), whereas classes (ii) - e.g., WASP-43 b, HD 209458 b - and (iii) - e.g., WASP-121 b, WP 0137 b - have a large day-night divergence of the cloud properties. The C/O ratio is, hence, homogeneously affected in class (i), but asymmetrically in class (ii) and (iii). The atmospheres of class (i) and (ii) planets are little affected by thermal ionization, but class (iii) planets exhibit a deep ionosphere on the dayside. Magnetic coupling will therefore affect different planets differently and will be more efficient on the more extended, cloud-free dayside. How the ionosphere connects atmospheric mass loss at the top of the atmosphere with deep atmospheric layers need to be investigated to coherently interpret high resolution observations of ultra-hot planets.

It was further demonstrated that atmospheric asymmetries on the hot Saturn WASP-96 b, target of *JWST's* Early Release Observations (ERO) should be detectable with the *NIRISS* instrument on board *JWST*.

Helling et al., A&A, 671, A122, 2023.
Samra et al., A&A, 669, A142, 2023.

SIZE-DEPENDENT CHARGING OF DUST PARTICLES IN PROTOPLANETARY DISKS

The dust grains in protoplanetary disks are generally charged. If directly irradiated by the star, the grains charge up positively due to interactions with UV photons (photoeffect), but deeper in the midplane, which is optically thick and shielded from the UV, the grains charge up negatively because of electron attachments (see figure). The latter process is important to understand midplane ionization, as the grains pick up most of the free electrons, leading to a charge equilibrium between negatively charged grains and molecular cations such as NH_4^+, whereas the electron concentration drops well below 10^{-10}.

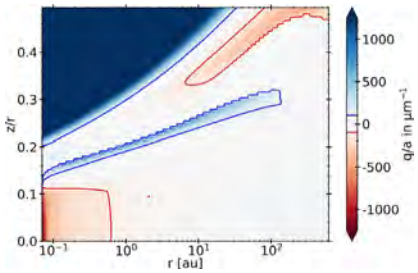

Illustration of how the charge per dust grain radius (q/a) [1/μm] changes in the disk. In large parts of the disk, the dust is found to be only weakly charged. In the upper areas that are directly illuminated by the star, the dust grains are highly charged positively (>100, blue contour lines), but in the midplane areas, especially close to the star, the dust charges very negatively (<-100, red contour lines).

Grain charging as function of grain size was studied, concluding that the quotient (q/a), where q is the charge of a grain and a is its size, has a narrow distribution with a maximum value that is surprisingly constant as function of grain size a under all circumstances. Further, a simple electrification model was developed (see figure 2), where the centrifugal force in turbulent eddies causes a charge separation. However, the electric fields created this way are by orders of magnitude smaller that the critical electric fields needed to kick-start lightning.

Balduin et al., A&A, 678, A192, 2023 .

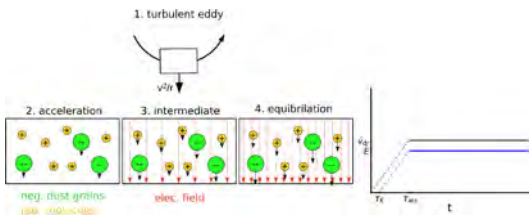

Turbulent electrification model for negatively charged dust grains (green) in a weakly ionized gas containing a few molecular ions (yellow). The centrifugal force in a turbulent eddy leads to charge separation, where the negative grains are accelerated until an electric field builds up that is sufficiently large to make the positive molecular ions drift along with the grains. After an initial acceleration phase, equilibrium values for the electric field E and the drift speed vdr are established.

SUBLIMATION OF REFRACTORY MINERALS IN THE GAS ENVELOPES OF ACCRETING ROCKY PLANETS

The growth of protoplanets by pebble accretion in protoplanetary disks was studied. Due to accretion heating, the temperature in the envelopes around the protoplanets can become high enough to sublimate refractory minerals (see figure). For each snapshot in the evolution, the envelope structure and the sublimation temperatures of a set of mineral species representing different levels of volatility were calculated. It was found that the envelope of the growing planet reaches temperatures high enough to sublimate all considered mineral species when the mass of the protoplanet exceeds 0.4 Earth masses, in which case further pebble accretion becomes impossible, because these solid, about cm-sized particles would sublimate completely, before they can reach the protoplanet. The models are in good agreement with the slightly depleted sulfur abundance of Mars, while the model only slightly over-predicts the strong sulfur depletion of Earth by a factor of ~2. It was shown that a collision with a sulfur-rich body akin to Mars in the moon-forming giant impact lifts the Earth's sulfur abundance to approximately 10% of the solar value for all impactor masses above 0.05 Earth masses.

Steinmeyer et al., A&A, 677, A181, 2023.

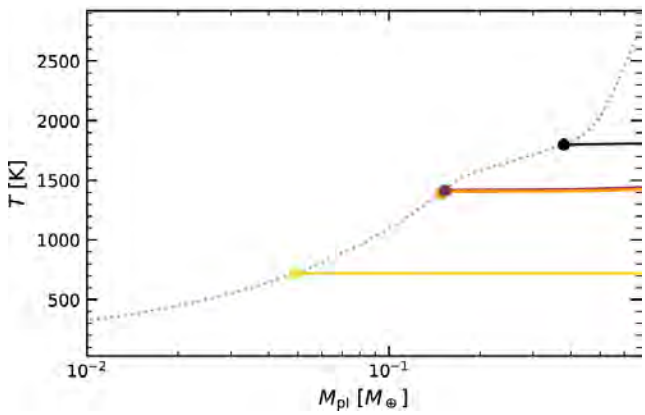

The dotted gray line shows the surface temperature of a protoplanet during its forming in a protoplanetary disk as function of planet mass. The filled circles indicate the sublimation temperatures of selected minerals. For example, when a protoplanet reaches a mass of about 0.05 Earth masses, the pebbles containing troilite (FeS), the most important sulfur containing mineral, would sublimate before they can reach the planet. Therefore, the protoplanet cannot accrete any additional sulfur after it has reached a mass of 0.05 Earth masses.

SATELLITE LASER RANGING

In addition to routinely tracking more than 150 targets, which are equipped with laser retro-reflectors, the Satellite Laser Ranging (SLR) station Graz is working on various international projects. Two new expansion telescope designs were developed for new SLR stations; one based on an aspheric exit lens, the second using the full aperture of a 0.8-meter telescope. Continuous upgrades to the SLR station are deployed such as the new modular observation software Sky Vision. A method for improving the precision of range measurements to *Galileo* satellites is presented.

GALILEO NORMAL POINT IMPROVEMENT

Currently there are four GNSS constellations in the world. The United States' Global Positioning System (GPS) was the first to be established, dating back to 1978. The Russian Global'naya Navigatsionnaya Sputnikovaya Sistema (GLONASS) was launched four years later. China started its *Beidou* system in 2000. The first launch of the *In Orbit Validation (IOV)* satellites of the European *Galileo* system was in 2011. India and Japan have their own regional systems based on satellites in geostationary and geosynchronous orbits. The current generation of *Galileo*, *Beidou* and *GLONASS* satellites carry a Corner Cube Retroreflector (CCR) panel hosting up to 90 reflectors. *Galileo* IOV-type panels include 84 CCRs arranged hexagonally with 33 mm minimum aperture, FOC (Full Orbit Capacity) satellite have only 60 CCRs with 28.2 mm minimum aperture and hence lower optical cross section.

The reflection pattern resulting from each individual uncoated CCR also shows a hexagonal structure - a central spot, with six side lobes. The side lobes appear at an angle of approx. 25 µrad meaning that most of the reflected energy is distributed in this direction. Due to the relative movement between satellite and station, the center of the reflection pattern is shifted in the direction of the satellite movement (velocity aberration). Hence, the observing SLR stations are located somewhere on a 25 µrad circle around the center of the reflection pattern. To avoid that in some orbit geometries SLR stations are in between the higher reflection intensity lobes, the retroreflectors are "clocked": they are rotated by a certain angle and a uniform distribution overall reflection distribution is reached.

However, depending on the geometry between station and spacecraft, this can lead to non-uniform signal distribution detected by satellite laser ranging stations as statistically photons can come from all (e.g. 84) CCRs. Depending on the panel orientation, the mean reflection point can be shifted from true center by a few millimeters, which is then influencing the orbit precision.

The new method overcomes this problem relying on certain orbital orientations of the *Galileo* panel, where multiple CCRs align at constant ranges. Based on the hexagonal structure of the panel, this happens at rotation angles of 0°, 30°, 60° and 90°. These so-called symmetry conditions allow for a very precise determination of the range to each row of CCRs formed this way. Even more, the central row can be identified which corresponds to the true reflection center. These symmetry conditions are predictable and occur multiple times per day for each *Galileo* satellite. A measurement campaign was conducted gathering more than 100 passes, which allowed to prove that normal points generated with the newly invented method are by up to 4 mm more precise than previously generated data. Satellite laser ranging normal point corresponds to statistically averaged range based on all the individual range measurements within a time frame.

The applied methods include analyzing the raw data (left figure) by applying 1) a peak-based method and 2) a correlation-based method. The peak-based method first forms a histogram and smoothed range distribution (middle figure) to detect peaks corresponding to the range of the CCR rows. The correlation method used a simulated Gaussian kernel distribution which is then correlated with the measured data. The right plot of the figure below shows that the improvement for both methods is in the order of 3-4 mm for the measured symmetry pass of *Galileo 102* (NORAD: 33857).

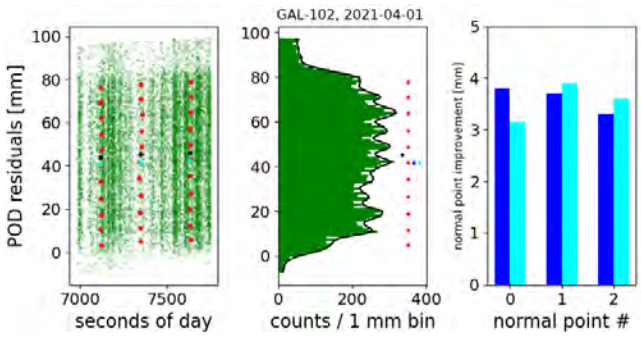

Precise Orbit Determination residuals to *Galileo 102* together with regular normal points (black), peak-based normal points (red, blue) and correlation-based normal point (cyan). Due to the uneven histogram distribution, the regular normal point is clearly off-center; while the central normal points of the new methods are more by more than 3 mm precise.

SLR STATION UPGRADE - SKYVISION

SLR Graz is tracking >150 active or defunct International Laser Ranging Service satellites and >300 uncooperative targets routinely using laser ranging or light curve techniques. It is essential to acquire comprehensive real-time information to judge measurement tasking, satellite scheduling, aircraft avoidance, sun position, cloud coverage or local hardware status.

The new software SkyVision has been developed by the SLR team and is still being upgraded according to ever-changing requirements, e.g. the integration of new tracking cameras, improved satellite scheduling or real-time observation feedback. SkyVision plots a real time schedule of satellite passes which are sorted and color coded dynamically according to time, priority and previously acquired data (see figure). Further details provided to the observers include: orbit information, laser point ahead angle, CPF version, time bias estimation, satellite or space debris visibility and visibility changing time, etc. In addition, during debris tracking the radar cross section values and past tracking records are displayed to give success rate feedback.

SkyVision communicates with an air traffic tracking device which acquires ADS-B, MLAT, FLARM signals to calculate the aircrafts' information near the station. The laser is switched off automatically when any aircraft flies within a predefined cone near the laser beam. The software also gets an actual sky picture from a home-integrated all sky camera to get the current cloud coverage, highlighting areas on the sky which would prohibit laser ranging, and also creates a keogram image to store the weather development of the last 24 hours. Both pictures together with satellite schedule are shared to the observers via Internet to allow them to plan the nightly observation sessions efficiently.

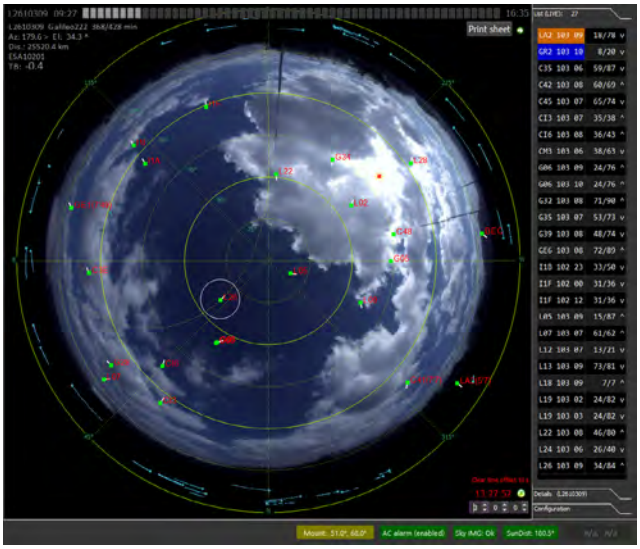

The radar plot of SkyVision illustrates in real-time satellite and debris passes, tracking and aircraft information combined with an all-sky image as background for easier orientation for the observer. Satellites are highlighted in green, aircraft in blue.

SLR EXPANSION TELESCOPE DESIGNS

The IWF is currently involved in building laser and detection packages for several new SLR stations. For two stations new concepts for expansion optics increasing the laser beam diameter were simulated, developed and tested at Graz SLR station. The first station will extend the tracking capabilities of the existing Izana-1 SLR station on Teide, Tenerife, towards space debris laser ranging. Secondly, a station to be deployed in Matera, Italy, is aiming at providing optimized tracking to GNSS satellites.

For the space debris laser ranging upgrade a compact diffraction-limited (simulated Strehl-ratio of 0.98) beam expansion telescope was designed aiming for robustness and flexibility in use. The centerpiece of the telescope is a 20 cm aspheric lens with an extremely low focal length of only 300 mm. This allows for a beam diameter increase from 4 mm to 15 cm in less than 0.5 meters. To reach the magnification and to reduce aberrations a specific design and arrangement of lenses had to be chosen (top figure). Given such extreme expansion, thermal and mechanical stability was simulated using Finite-Element simulations, proving that the construction fulfills the pointing accuracy requirements, even under the various tilting conditions during tracking.

The beam expansion for the GNSS testbed follows an approach to use the full aperture of a 0.8 m Ritchey-Chrétien telescope. After a first beam expansion to 1 cm, the laser is coupled into the system using a two-stage diverging lens system, tailoring the laser beam to fit the size of the primary and secondary mirror. The reflected photons are then gathered with the main SLR telescope at Lustbühel observatory (bottom figure), approximately 10 meters away from the laser beam expansion telescope. This arrangement allows to verify the setup as it will be deployed, using two identical telescopes, one for laser transmission and one for receiving.

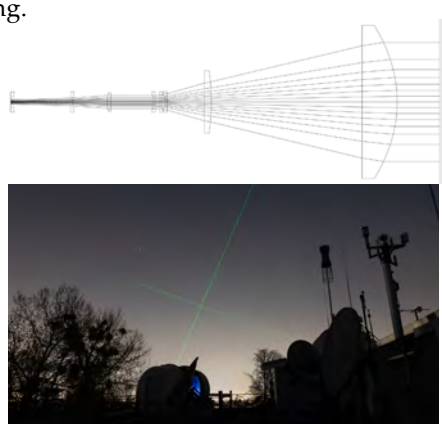

Top: Raytracing simulation for the two-stage aspheric beam expansion telescope. After the first expansion, the beam is collimated to a diameter of 18 mm. In the second expansion stage, the diameter is further increased to 150 mm. Bottom: Laser ranging tests with the new expansion telescope while simultaneously ranging with the standard SLR system.

TECHNOLOGIES

NEW DEVELOPMENTS

One possible aspect to reduce costs of space exploration and hence allowing for more frequent missions is to reduce the spacecraft size and consequently the launch masses. Scientific instruments also have to decrease their resource requirements such as volume, mass, and power, but at the same time achieve at least the same performance as heritage instruments. Therefore, the development of new instrument technologies is essential for competitive and excellent space research.

Machine learning (ML) techniques have shown to be valuable for accelerating data analysis and modeling efforts and may therefore become important in space research and technology. The IWF has started to identify potential application of ML, ranging from laser-ranging data analysis and integrating ML-based data compression with new hardware systems for space missions to modeling planetary disks and characterizing exoplanets. The ML initiative, led by Christiane Helling, identified and worked on ten potential research projects with ML and submitted seven research proposals to the funding agency.

MAGNETOMETER FRONT-END ASIC

The IWF and the Institute of Electrical Measurement and Sensor Systems of the Graz University of Technology (TUG) are collaborating on the next generation of the space proven Magnetometer Front-end ASIC (MFA). It includes the readout electronics for magnetic field sensors which is optimized in terms of size and power consumption. The next generation Application Specific Integrated Circuit (ASIC) shall feature an improved dynamic range and increased radiation hardness. It will be space qualified in the frame of the *FORESAIL* mission.

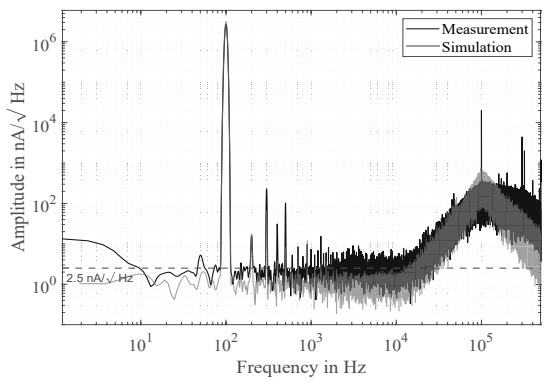

Measured and simulated amplitude spectral density of the output current for the maximum input amplitude of 9 mA in high range.

In 2023, the second prototype microchip (MFA-4.4), which occupies a total silicon area of about 4.6 mm², was received from XFAB Silicon Foundries. One feedback channel is implemented on the MFA-4.4 in order to avoid inter-channel interference and to reduce the complexity of the digital interface. The feedback path includes two dynamic ranges with a peak output current of 9 and 3 mA in high and low range, respectively.

Performance tests revealed a signal-to-noise ratio of 105.2 dB in high range and 103.8 dB in low range. The distortion factor is -94.8 dB and -90 dB. Furthermore, the measured noise floor is less than 2.5 nAHz$^{-0.5}$ for the high range and less than 0.85 nA Hz$^{-0.5}$ for the low range. It could be shown that the measured results agree very well with the simulation.

In addition to the testing of the MFA-4.4 prototype, the design of its successor microchip with e.g., an improvement of the flicker noise at frequencies below 10 Hz was elaborated and the test hardware for radiation tests of the MFA-4.4 planned for early 2024 was developed.

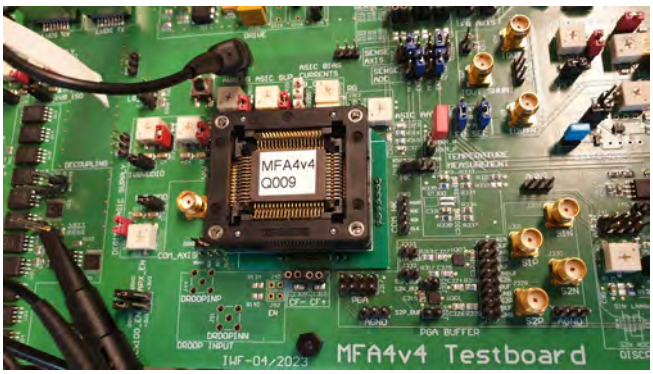

Second prototype microchip (MFA 4.4) mounted in its adapter for functional and performance testing.

OPTICAL VECTOR MAGNETOMETER

As fluxgate magnetometers - the most commonly used instruments to measure static and low frequency magnetic fields in space - suffer temperature and long-term drifts, they are in specific mission cases accompanied by optical magnetometers, which use atomic resonances to provide a reference point for calibration. A recent example is the *Coupled Dark State Magnetometer (CDSM)*, which measures the strength of the magnetic field with the help of a quantum-interference effect called Coherent Population Trapping (CPT). Thereby, the interference between quantum states of rubidium atoms excited by coherent light fields is read out optically.

End of 2022, a PhD project was initiated in the frame of IWF's Young Researcher Program and in cooperation with the Institute of Experimental Physics of TU Graz to study the physical background of utilizing CPT in the so-called Hanle configuration to measure all vector components of the magnetic field. A key aspect of this study is the feasibility of a 3D-Hanle magnetometer to serve as a potential space instrument which can be combined with the existing *CDSM*. On its own, the 3D-Hanle magnetometer would complement the capabilities of the scalar *CDSM* by allowing near-zero magnetic field measurements in all vector components without temperature and long-term offset drifts. A combination of both instruments would yield a sensor that is fully capable of in-flight self-calibration.

The focus in 2023 was on the measurements with a 1D-setup to explore the parameter space of the resonances that arise from the Hanle effect, the investigation of cross-field effects on the Hanle resonances and the definition of first concepts for the realization of a vector magnetometer based on the Hanle effect.

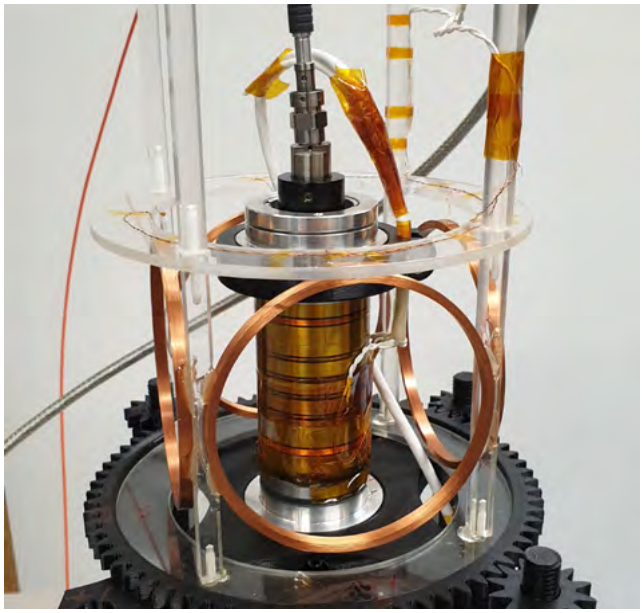

Modified *CDSM* sensor with an additional 3D coil system to run the Hanle mode and to investigate cross field effects.

ANALYZING THE SEDS OF PROTOPLANETARY DISKS WITH MACHINE LEARNING

Spectral energy distributions (SEDs) are commonly used to determine the physical structure and the dust properties of protoplanetary disks. A new innovative approach is presented to fit the observational data from UV to millimeter wavelengths by means of full 2D radiative transfer models, including Bayesian analysis. The key idea is to generate large grids of about 100000 Monte Carlo radiative transfer models, which predict the SED from the physical parameters of the problem, such as the disc mass, its radial extension and shape, dust size and material properties, and stellar properties. Next, a suitable neutral network (NN) is trained on that data to generate one SED within a millisecond with an accuracy of better than 5%, instead of using about 5 min for one original radiative transfer model, i.e. an acceleration of about 300000. This acceleration allows to carry out a full Bayesian analysis, from which all fitted parameter values with uncertainties can be determined, detecting and quantifying parameter degeneracies. A full re-analysis of 30 protoplanetary disks is carried out using SED data collected by the FP7-Space DIANA project. The frequently used analytic relationship between disk dust mass and millimeter flux systematically underestimates the true dust masses for high-mass disks.

Käufer et al., A&A, Volume 672, A30, 2023.

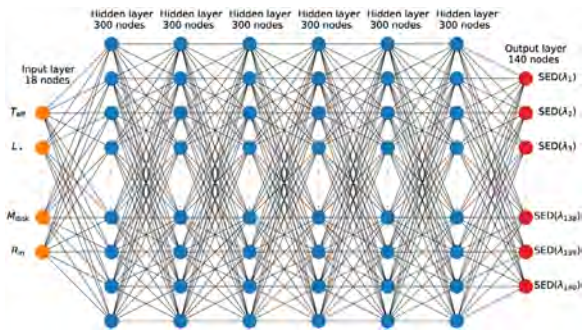

Chosen architecture of the neural network (NN) for the fast prediction of SEDs. The NN consists of an input layer (orange) with 18 neurons (18 free parameters), 6 hidden layers (blue circles) with 300 neurons each, and an output layer (red) with 140 neurons (the resulting flux values at 140 different wavelengths). There are about 500.000 trainable parameters in this network.

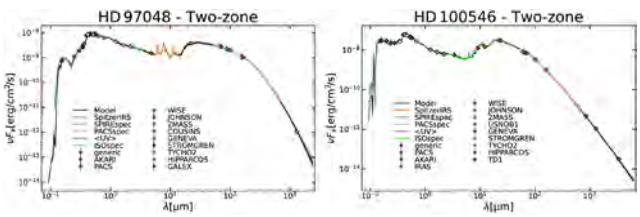

Fitted SEDs for selected objects. The colored points and lines indicate the observations listed in the legend. The SEDs from the posterior distribution are shown in black. The line denotes the median of all model SED, with the dark, medium, and light black areas denoting the 68%, 95%, and 99.9% percentiles, respectively.

INFRASTRUCTURE

Space-born instruments are exposed to harsh environments, e.g., vacuum, large temperature ranges, radiation, and high mechanical loads during launch. They are expected to be highly reliable, providing full functionality over the entire mission duration, which could last for more than a decade.

The IWF operates several test facilities and special infrastructure for the production of flight hardware. A high-performance computer helps the scientists to cope with the enormous data, which have to be analyzed for space missions. For manufacturing and assembly of the electronics, in particular the flight units, very often specific mechanical tools and jigs are necessary.

A new acquisition in 2023 was a washing machine for Printed Circuit Boards (PCB): PBT MiniSwash II.

NEW "DISH WASHER"

After manufacturing and soldering, PCBs require cleaning in order to remove soldering flux and contaminating residuals. This was previously performed manually with a brush; a tedious process exposing the technicians to the fumes of the alcohol-based solution.

The new PBT MiniSwash II uses a water-based, alkaline cleaner (Vigon A201). In order to provide short process times, the device is equipped with a heating system for cleaning (60 °C) and drying (90 °C). Furthermore, the MiniSwash II consists of a combined cleaning chamber for spraying and drying as well as a central control and programming unit. The washing machine will allow for an automatic, consistent and safe cleaning, thus to increase the reliability and quality control of the PCBs manufactured by the IWF and to meet the cleanliness standards of ESA.

Placing of a printed circuit board in the new "dish washer" for cleaning.

UPGRADE OF THE THERMAL-VACUUM FACILITY

The thermal vacuum (TV) chamber of the WF is fitted with two turbo molecular pumps, a dry scroll fore pump, and an ion getter pump, which together achieve a pressure level of 10^{-6} mbar. It allows for a quick change of components and/or devices to be tested. A thermal plate installed in the chamber and are used for thermal cycling in a temperature range between -160 °C and +140 °C. The vertically oriented cylindrical chamber enables a maximum diameter of the device under test of 410 mm and a maximum height of 320 mm. The TV system is essential for a proper and time efficient testing of the flight hardware built by the IWF.

The thermal control hardware for the TV chamber was renewed in 2023 based on an Arduino GIGA R1 controller. The TV control system itself comprises two hardware controllers in cold standby and a software control system on a PC for configuring and running the whole system. An uninterruptible power supply was also implemented to prevent a possible power failure during a test. The software was adapted to comply with the Arduino data protocol. The system upgrade was made to improve the stability of the system and to implement more safety features.

Hardware controller rack of the IWF thermal vacuum test facility.

For further information on the IWF infrastructure refer to www.oeaw.ac.at/en/iwf/institute/infrastructure.

Impressions from the *JUICE* Launch Event at the IWF (© ÖAW/Daniel Hinterramskogler).

IMPACT BEYOND SCIENCE

PUBLIC OUTREACH

The highlight of the year 2023 was the launch of ESA's *JUICE* mission. Together with the Austrian Research Promotion Agency (FFG), Graz University of Technology, Beyond Gravity, Terma and Geosphere Austria, the IWF organized a launch event on 13 April, which was attended by numerous guests, including OeAW President Heinz Faßmann, Rector Harald Kainz and Vice Rector Horst Bischof of TU Graz as well as City Councilor Manfred Eber representing Mayor Elke Kahr. Although the launch itself had to be postponed by one day, the audience listened to several talks, learned all about Austria's contributions to the mission and toasted the team's successes to date.

The scientific questions and results of IWF's exoplanet researchers inspired artists to video and sound installations shown in the mobile pavilion as part of the exhibition SHOWING STYRIA under the title "Atmospheres. Art, Climate and Space Research". In March, the pavilion was opened in Vienna, in April, it moved to Herberstein and in December a mini-version traveled to New York.

Christopher Drexler, Governor of Styria, curator Astrid Kury, Christiane Helling, and Marko Mele, Director of Science at the Universalmuseum Joanneum (v.l.t.r.) during the opening ceremony of the mobile pavilion on 22 March in the Weltmuseum Wien (© Universalmuseum Joanneum/J.J. Kucek).

In the IWF colloquium and seminar series, international guest speakers (colloquium) and local speakers (seminar) inform about current research topics and scientific results. In 2023, 12 colloquia and 8 seminars were given, most of them are available on IWF's YouTube channel. The topics ranged from modeling the near-Earth plasma environment to magnetic fields shaping protoplanetary disks.

With two lectures on exoplanetary research, Christiane Helling and Luca Fossati kicked off the new year of the EAI Academy, which provides a framework to meet online with the European astrobiology community.

The Graz *JUICE* team presented the Jupiter mission and the scalar magnetometer at the Ball der Technik of TU Graz, on 27 January 2023 in the Congress Graz.

Werner Magnes and Irmgard Jernej presenting *JUICE* at the Ball der Technik (© Ball der Technik / Götschmaier).

During her visit on 3 March 2023, Vice President Ulrike Diebold also spoke with IWF's PhD students and PostDocs and was shown around in the laboratories and at the SLR station on Lustbühel.

On 18 April 2023, Bruno Besser opened the exhibition „Astronomica. Meilensteine der historischen Weltraumforschung“ at the University of Klagenfurt with a talk about planets, comets, galaxies, and historical astronomical research in Carinthia.

On 13 June 2023, Christiane Helling presented her research at the Young Academy Roadshow, which aims to showcase the diversity of the OeAW's research areas in short presentations.

Her first visit to Austria took ESA's Director of Science, Carole Mundell, to Graz on 5 September 2023, where she presented the activities and plans of ESA's science program to the Austrian space community.

Christiane Helling, Carole Mundell, and Andreas Geisler, head of the Aerospace Agency of the FFG (f.l.t.r., © IWF/Scherr).

On 20 September 2023, Manfred Steller gave a keynote lecture on the future of space research from the perspective of the IWF during the evening event "Galaktische Perspektiven für Oberösterreich", which was organized in the frame of "communale oö" in Peuerbach.

In 2023, Austria chaired the European Interparliamentary Space Conference (EISC) under the theme "Europe's contribution to an evolving space economy". On 24-25 September 2023, Christiane Helling attended the EISC Plenary Session at the Austrian Parliament in Vienna. She gave the keynote on "Space science as inspirator and pathfinder" and was invited to be panel member for the discussion "From talents to space entrepreneurs".

Christiane Helling and Therese Niss, Member of the National Council of Austria, at the EISC dinner (© Parlamentsdirektion/ Anna Rauchenberger).

During the European Researchers' Night (ERN) held at the University of Applied Arts in Vienna on 29 September 2023, the IWF presented its contributions to *JUICE* to a large number of visitors of all ages.

The IWF team and one of its youngest visitors at ERN in Vienna (© bee produced).

During an exhibition organized by the Austrian Armed Forces on 25 and 26 October in the center of Vienna, the IWF presented the project "SWAP: The Austrian Platform for Space Weather", coordinated by GeoSphere Austria. The stand was also visited by Klaudia Tanner, Federal Minister of Defence and Martin Polaschek, Federal Minister for Education, Science and Research.

Roman Leonhardt from GeoSphere Austria welcomed Minister Polaschek and Tanner at the space weather stand (© OeAW/IWF/Scherr).

In autumn and winter 2023, the astronomy lectures at Urania Graz focused on the *James Webb Space Telescope* and research at the IWF. Under the scientific lead of Christiane Helling, 8 talks were given by IWF members.

As part of the "Talk am Turm" series organized by the Astronomical Association of Carinthia (AVK) Werner Magnes gave a lecture about *JUICE* and the icy moons of Jupiter and Christiane Helling talked about the weather on exoplanets.

During a seminar organized by ARGE NAWI BMHS Niederösterreich on 13 November, Ruth-Sophie Taubner gave a talk on what we can learn from Mars, Venus and the exoplanets with respect to climate change.

At the "Innovationsabend SpaceTech" on 20 November, Christiane Helling discussed Austria's role in space research and industry together with Therese Niss, Member of the National Council, Andreas Geisler, Head of the Aerospace Agency of the FFG, Hermann-Ludwig Möller, Director of the European Space Policy Institute, Dieter Grebner, CEO of Peak Technology, and Thomas Grübler, CEO of OroraTech.

In his lecture at VHS Wien on 7 December, Werner Magnes explained what the scientists expect from *JUICE's* magnetic field measurements in the Jupiter system.

In the space blog of the Austrian newspaper "Der Standard" Helmut Lammer wrote about Austria's role in studying Jupiter's icy moons aboard *JUICE*.

More information and pictures of the events are found at www.oeaw.ac.at/en/iwf/latest/events.

YOUNG RESEARCHER PROGRAM

The Young Researcher Program in interdisciplinary space science and planetary research (YRP@Graz) is a close collaboration between the IWF and the two local universities, Graz University of Technology (TU Graz) and the University of Graz, which helps future researchers to gain first experiences in science.

In the second year of YRP@Graz two PhD positions were funded by the two universities:

- Laboratory astrophysics: High resolution spectroscopy of exoplanetary gas species
  PhD student: Elisa Ehl
  Supervisors: Birgitta Schultze-Bernhardt (TU Graz), Luca Fossati (IWF)
- Coronal dimming diagnostics of solar and stellar mass ejections
  PhD student: Amaia Razquin Lizarraga
  Supervisors: Astrid Veronig (University of Graz), Helmut Lammer (IWF)

To foster networking within YRP@Graz, a kick-off meeting (20 January), a tour at the IWF (6 June), and a Jamboree (30 November) were organized.

The first year PhD students and their supervisors during the YRP@Graz kick-off meeting (© OeAW/IWF/Scherr).

During summer time, two students from TU Wien and University of Graz performed a two-months internship, funded by the City of Graz. They worked on the habitability of nearby stellar systems and on interplanetary shocks and plasma turbulence using supercomputing simulations.

Additionally, three high-school students conducted an internship at the IWF. They tested the electronic boards for the *PLATO* mission, optimized the functional parameters of the *JUICE* magnetometer, and measured the field homogeneity in a magnetic shielding chamber. Two more students from the Europagymnasium Klagenfurt and the Informatik Mittelschule (iMS) Jennersdorf completed their practical work experience days at the IWF.

Jonas Halb from iMS Jennersdorf spent his first practical day at the Lustbühel Observatory (© Markus Halb).

As part of Science Garden, the IWF presented itself at the Faszination Technik Challenge at the Styrian Chamber of Commerce in May and at the 2. MINT-Forum Steiermark at the Kunsthaus Weiz in November.

Following the OeAW young science initiative "Akademie im Klassenzimmer" Luca Fossati visited VS 9 Fellach and VS Kühnsdorf and together with Alexandra Scherr VS Hüttenberg and VS Hörzendorf, Günter Kargl BG Lerchenfeld, Ruth-Sophie Taubner HTL Wien West and BRG Kapfenberg, and Martin Volwerk and Daniel Schmid HTL Kaindorf.

Luca Fossati during his classroom lecture on exoplanets held in VS Hüttenberg (© OeAW/IWF/Scherr).

RECOGNITION

IWF Director Christiane Helling was nominated for Austria 23 in the category "research" by the daily newspaper "Die Presse".

Daria Kubyshkina was awarded a Schrödinger Fellowship, which will take her to the University of Bern in 2024. Yasuhito Narita was appointed Professor of Theoretical Physics at Technische Universität Braunschweig and Owen Wyn Roberts was appointed Lecturer in Physics at Aberystwyth University.

MEETINGS

Christiane Helling served as chair of the Program Committee of the Summer School Alpbach, which took place from 11 to 20 July and was dedicated to "Exoplanets: Understanding alien worlds in diverse environments". Every year, 60 students and about 25 lecturers and tutors from ESA's member states are invited to this meeting.

At the CHAMELEON School III, the Early Stage Researchers presented their scientific results to date.

The Graz-Vienna Exoplanet Scientist Meeting (GVESM) is a series of meetings, focused on strengthening connections between researchers working in Austria in the field of exoplanet science. The meetings take place twice a year, alternating between Graz and Vienna. GVSEM II was held on 5 May at the IWF.

Graz in Space is a biennial public lecture series in which scientists and engineers present their different research areas. The first event was organized in 2002 in cooperation with the University of Graz. After a forced break of five years due to the pandemic, the 10th edition took place at the IWF. On 7 and 8 September, 16 scientists presented an overview of various space topics. Guided tours at the IWF and the Lustbühel Observatory provided additional insights into space research in Graz.

Helmut Rucker, the long-standing scientific director of Graz in Space, has handed over his position to Christiane Helling (© OeAW/IWF/Taubner).

From 11-13 September, the *PLATO* Workshop on 3D Climate and Clouds was held at the IWF, bringing together scientists who are interested in the detailed characterization and modeling of exoplanet atmospheres.

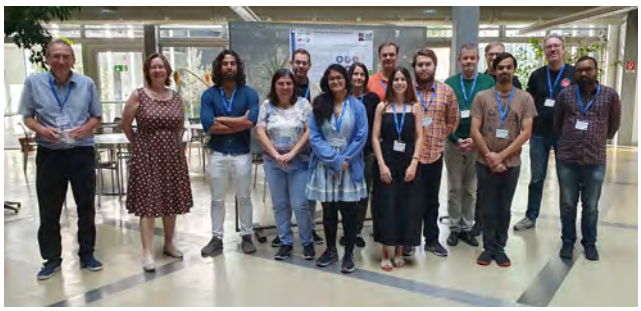

IWF director Christiane Helling (2nd f.l.) and organizer Ludmila Carone (4th f.l.) together with the participants of the *PLATO* Workshop (© OeAW/IWF/Scherr).

B.P. Besser, M. Boudjada, P. Bourdin, L. Carone, Ch. Helling, G. Kargl, R. Nakamura, E. Panov, M. Scherf, M. Steindorfer, R.-S. Taubner, M. Volwerk, and S. Zenitani were members of 21 scientific program and/or organizing committees at 13 international meetings.

LECTURING

In summer 2023 and in winter term 2023/2024 IWF members gave (online) lectures at the University of Graz, Graz University of Technology, FH Wiener Neustadt, TU Braunschweig, and University of Jena.

THESES

Besides lecturing, IWF members are supervising Bachelor, Diploma, Master, and PhD Theses. In 2023, the following supervised theses have been completed:

Amateis, I.: Digging in the Dirt: Measuring Planetary Fundamental Parameters in the Presence of Stellar Activity. The Case of TOI-396, Master Thesis, Università degli studi di Torino, 120 pages, 2023. Supervisor: A. Bonfanti, L. Fossati

Barth, P.: Tracing the Chemistry of High-Energy Processes in Planetary Atmospheres, PhD Thesis, University of St Andrews , 117 pages, 2023. Supervisors: Ch. Helling, E.E. Stueeken

Blazovnik, L.: Numerical Simulation and Optimization of Fluxgate Sensors, Master Thesis, Technische Universität Graz, 74 pages, 2023. Supervisor: W. Renhart

Haberz, D.: Reduction of Reactions in the Cluster Formation of TiO_2, Bachelor Thesis, Technische Universität Graz, 35 pages, 2023. Supervisor: S. Kiefer, Ch. Hellling

Ley, T.: Characterization of Titanium Oxide Nanoclusters, Bachelor Thesis, Technische Universität Graz, 35 pages, 2023. Supervisor: H. Lecoq Molinos, Ch. Hellling

Nadrag, L.: Exploring Observable Consequences of Mixed-Material Clouds in the JWST Era, Bachelor Thesis, Technische Universität Graz, 31 pages, 2023. Supervisor: D. Samra, Ch. Helling

Reisinger, N.: Occurrence of Electron Scale Current Sheet in Dipolarization Front and Signatures of Reconnection, Master Thesis, Universität Graz, 98 pages, 2023. Supervisor: R. Nakamura

Sindel, J.P.: Cloud Formation in Exoplanet Atmospheres - Nucleation of Small Molecular Clusters, PhD Thesis, Katholieke Universiteit Leuven, 128 pages, 2023. Supervisors: Ch. Helling, L. Decin, D. Gobrecht

Trummer, N.M.: Simulation and Classification of Space Debris Light Curves, Master Thesis, Universität Graz, 100 pages, 2023. Supervisor: S. Krauss, M. Steindorfer

Zivithal, S.: Experimental Characterisation of the Gas-Flow Properties of Dry Refractories in the Context of Cometary Physics, Master Thesis, Universität Graz, 102 pages, 2023. Supervisor: G. Kargl, H. Lammer

NEW PROJECTS

In 2023, the following third party projects with a budget greater than 100,000 EUR were acquired:

Project	Lead
FWF - ML supported Exoplanet Cloud Formation Modelling	Ch. Helling
FWF - Formation and Evolution of Planets orbiting Low-mass Stars	D. Kubyshkina
FWF - Compressible Turbulence in the Heliosphere	Z. Vörös
FWF - Redox Disequilibrium in the Clouds of Venus – A Sign of Life	P. Woitke
FFG - *NEWATHENA* Magnetometer	G. Giono
ESA - *MANiaC* DPU ProtoFlight Model & Flight Spare	G. Giono
ESA - *Comet Interceptor*, Magnetometer *FGM B2*	W. Magnes
DiGOS - New SLR Station TU Berlin	M. Steindorfer
DiGOS - New SLR Station Matera	M. Steindorfer

GOODBYE AND HELLO

In 2023, Gabriel Giono joined the IWF, leading the On-board Computers group. He followed long-time Group Leader (2002-2022) Manfred Steller.

Manfred Steller studied electrical engineering at the Graz University of Technology, and graduated in 1984 with a diploma thesis on a microprocessor-controlled instrument for data acquisition. Soon afterwards, on 1 August 1984, he joined the IWF. He initially worked on the Soviet missions *Vega 1* and *2*, which performed swingbys at planet Venus mid of June 1985, released landers and balloons, and headed for a flyby at comet Halley in March 1986. Following the launch of these probes in December 1984, he started to work on instruments for the Soviet missions *Phobos 1* and *2* to planet Mars, launched in July 1988. Manfred was involved in the design and construction of the mass spectrometers *TAUS* and *SOWICOMS*. Both made very successful particle measurements in orbit around Mars.

In preparation of the *AUSTROMIR* mission of Austrian cosmonaut Franz Viehböck in October 1991, Manfred led a group at the Institute of Applied Systems (IAS) of the Styrian Forschungsgesellschaft Joanneum, which developed and implemented the central computer system *DATAMIR* for controlling, handling and storing data from the Austrian instruments on board the Soviet/Russian *Mir* space station.

In 1992, with the same group at IAS, Manfred started to develop the *Aerosol Collector and Pyrolyzer (ACP)* for the *Huygens* probe as part of the *Cassini* mission to Saturn and its moon Titan, to chemically analyze aerosol particles in Titan's atmosphere. *Huygens* was an exciting mission, offering several highlights. To reach Titan, the probe on board *Cassini* travelled over 55 billion kilometers for 6.7 years. The images taken during the descent revealed an absolutely fascinating world 1.2 billion kilometers from Earth, where deep-frozen water ice plays the role of soil and rock, while liquid and gaseous methane are the main components of the atmosphere.

Starting in 1996, Manfred contributed to the *Micro-Imaging Dust Analysis System (MIDAS)* aboard ESA's comet chaser *Rosetta*. In 2000, he completed his doctoral study at TU Graz with a thesis on the development of processor systems and investigations on compression algorithms for particle analyzers.

With his contributions to the 2D photometer aboard the French space telescope *CoRoT* he participated in IWF's first exoplanetary mission, launched in 2006. *CoRoT* discovered 34 exoplanets within its mission period of 6 years. Manfred's "favorite" is CoRot-7 b, the smallest known exoplanet at the time of discovery, with a diameter of 1.58 Earth radii. Due to its proximity to its host star, the orbital period is 20 hours and it is a rather inhospitable world, with temperatures of over 1300 Kelvin on the day side and only a few Kelvin on the night side.

In 2007, Manfred's group started to build the electron gun and detector electronics for the *Electron Drift Instrument (EDI)* for NASA's *MMS* mission, launched in 2015. They developed the on-board computer for the *Radio and Plasma Waves (RPW)* instrument on board *Solar Orbiter* and the data processing unit for the *Back End Electronics (BEE)* of ESA's space telescope *CHEOPS* designed to characterize exoplanets in detail.

The most recent contributions are the electronics box for *SMILE* and the router and data compression unit for *PLATO*, scheduled for launch in 2025 and 2026, respectively.

Besides his efforts in engineering and science, Manfredwas actively engaged in public outreach. His self-built launch pad for paper rockets will hopefully inspire young and old for many years to come.

Symbolic handover of a *MANiaC* test box (© OeAW/IWF/Ottacher).

Gabriel Giono studied physics at the "Université Claude Bernard Lyon 1" in France and graduated with a master degree in "Astrophysics and Sub-atomic physics" in 2012 after completion of his thesis at ESA/ESTEC. He moved to Japan in 2013 for his doctoral degree, where he worked at the National Astronomical Observatory of Japan. During the PhD, he carried out the optical alignment and the polarization calibration of the *Chromsopheric Lyman-Alpha SpectroPolarimeter (CLASP)*, a sounding-rocket instrument to observe the solar chromosphere in the far-ultraviolet. Gabriel completed his PhD in 2016 and then moved to the Royal Institute of Technology in Sweden, where he stayed until 2020. During these four years, he worked on a number of space instruments for atmospheric, plasma and auroral sciences, on sounding rockets, cubesats and larger satellites. As an highlight, he calibrated the *Radio and Plasma Wave Instrument* onboard *JUICE*. Afterwards, he worked for two years at the Galileo Competence Center of the German Aerospace Center (DLR) in Oberpfaffenhofen, developing procedure for the assembly, integration and testing for the *COMPASSO* project, a demonstrator for the future generation of optical atomic clocks, which will be deployed outside the *International Space Station*. "I enjoy being between science and engineering, building instruments to continue our exploration of the cosmos. For that, the IWF is the perfect place!", he says.

PUBLICATIONS

REFEREED ARTICLES

Abend, S., B. Allard, A.S. Arnold, T. Ban, L. Barry, B. Battelier, A. Bawamia, Q. Beaufils, S. Bernon, A. Bertoldi, A. Bonnin, P. Bouyer, A. Bresson, O.S. Burrow, B. Canuel, B. Desruelle, G. Drougakis, R. Forsberg, N. Gaaloul, A. Gauguet, M. Gersemann, P.F. Griffin, H. Heine, V.A. Henderson, W. Herr, S. Kanthak, M. Krutzik, M.D. Lachmann, R. Lammegger, W. Magnes, G. Mileti, M.W. Mitchell, S. Mottini, D. Papazoglou, F. Pereira dos Santos, A. Peters, E. Rasel, E. Riis, C. Schubert, S.T. Seidel, G.M. Tino, M. Van Den Bossche, W. von Klitzing, A. Wicht, M. Witkowski, N. Zahzam, M. Zawada: Technology roadmap for cold-atoms based quantum inertial sensor in space, *AVS Quantum Sci.*, **5**, 019201, doi, 2023.

Affolter, L., C. Mordasini, A.V. Oza, D. Kubyshkina, L. Fossati: Planetary evolution with atmospheric photoevaporation. II. Fitting the slope of the radius valley by combining boil-off and XUV-driven escape, *Astron. Astrophys.*, **676**, A119, doi, 2023.

Ahrer, E.-M., K.B. Stevenson, M. Mansfield, S.E. Moran, J. Brande, G. Morello, C.A. Murray, N.K. Nikolov, D.J.M. Petit dit de la Roche, E. Schlawin, P.J. Wheatley, S. Zieba, N.E. Batalha, M. Damiano, J.M. Goyal, M. Lendl, J.D. Lothringer, S. Mukherjee, K. Ohno, N.M. Batalha, M.P. Battley, J.L. Bean, T.G. Beatty, B. Benneke, Z.K. Berta-Thompson, A.L. Carter, P.E. Cubillos, T. Daylan, N. Espinoza, P. Gao, N.P. Gibson, S. Gill, J. Harrington, R. Hu, L. Kreidberg, N.K. Lewis, M.R. Line, M. López-Morales, V. Parmentier, D.K. Powell, D.K. Sing, S.-M. Tsai, H.R. Wakeford, L. Welbanks, M.K. Alam, L. Alderson, N.H. Allen, D.R. Anderson, J.K. Barstow, D. Bayliss, T.J. Bell, J. Blecic, E.M. Bryant, M.R. Burleigh, L. Carone, S.L. Casewell, Q. Changeat, K.L. Chubb, I.J.M. Crossfield, N. Crouzet, L. Decin, J.-M. Désert, A.D. Feinstein, L. Flagg, J.J. Fortney, J.E. Gizis, K. Heng, N. Iro, E.M.-R. Kempton, S. Kendrew, J. Kirk, H.A. Knutson, T.D. Komacek, P.-O. Lagage, J. Leconte, J. Lustig-Yaeger, R.J. MacDonald, L. Mancini, E.M. May, N.J. Mayne, Y. Miguel, T. Mikal-Evans, K. Molaverdikhani, E. Palle, C. Piaulet, B.V. Rackham, S. Redfield, L.K. Rogers, P.-A. Roy, Z. Rustamkulov, E.L. Shkolnik, K.S. Sotzen, J. Taylor, P. Tremblin, G.S. Tucker, J.D. Turner, M. de Val-Borro, O. Venot, X. Zhang: Early release science of the exoplanet WASP-39b with JWST NIRCam, *Nature*, **614**, 653-658, doi, 2023.

Ahrer, E.-M., L. Alderson, N.M. Batalha, N.E. Batalha, J.L. Bean, T.G. Beatty, T.J. Bell, B. Benneke, Z.K. Berta-Thompson, A.L. Carter, I.J.M. Crossfield, N. Espinoza, A.D. Feinstein, J.J. Fortney, N.P. Gibson, J.M. Goyal, E.M.-R. Kempton, J. Kirk, L. Kreidberg, M. López-Morales, M.R. Line, J.D. Lothringer, S.E. Moran, S. Mukherjee, K. Ohno, V. Parmentier, C. Piaulet, Z. Rustamkulov, E. Schlawin, D.K. Sing, K.B. Stevenson, H.R. Wakeford, N.H. Allen, S.M. Birkmann, J. Brande, N. Crouzet, P.E. Cubillos, M. Damiano, J.-M. Désert, P. Gao, J. Harrington, R. Hu, S. Kendrew, H.A. Knutson, P.-O. Lagage, J. Leconte, M. Lendl, R.J. MacDonald, E.M. May, Y. Miguel, K. Molaverdikhani, J.I. Moses, C.A. Murray, M. Nehring, N.K. Nikolov, D.J.M. Petit dit de la Roche, M. Radica, P.-A. Roy, K.G. Stassun, J. Taylor, W.C. Waalkes, P. Wachiraphan, L. Welbanks, P.J. Wheatley, K. Aggarwal, M.K. Alam, A. Banerjee, J.K. Barstow, J. Blecic, S.L. Casewell, Q. Changeat, K.L. Chubb, K.D. Colón, L.-P. Coulombe, T. Daylan, M. de Val-Borro, L. Decin, L.A. Dos Santos, L. Flagg, K. France, G. Fu, A. García. Muñoz, J.E. Gizis, A. Glidden, D. Grant, K. Heng, T. Henning, Y.-C. Hong, J. Inglis, N. Iro, T. Kataria, T.D. Komacek, J.E. Krick, E.K.H. Lee, N.K. Lewis, J. Lillo-Box, J. Lustig-Yaeger, L. Mancini, A.M. Mandell, M. Mansfield, M.S. Marley, T. Mikal-Evans, G. Morello, M.C. Nixon, K. Ortiz Ceballos, A.A.A. Piette, D. Powell, B.V. Rackham, L. Ramos-Rosado, E. Rauscher, S. Redfield, L.K. Rogers, M.T. Roman, G.M. Roudier, N. Scarsdale, E.L. Shkolnik, J. Southworth, J.J. Spake, M.E. Steinrueck, X. Tan, J.K. Teske, P. Tremblin, S.-M. Tsai, G.S. Tucker, J.D. Turner, J.A. Valenti, O. Venot, I.P. Waldmann, N.L. Wallack, X. Zhang, S. Zieba: Identification of carbon dioxide in an exoplanet atmosphere, *Nature*, **614**, 649-652, doi, 2023.

Alberti, T., W. Sun, A. Varsani, D. Heyner, S. Orsini, A. Milillo, J.A. Slavin, J.M. Raines, A. Aronica, H.-U. Auster, S. Barabash, E. De Angelis, I. Dandouras, R. Jarvinen, H. Jeszenszky, E. Kallio, A. Kazakov, G. Laky, S. Livi, V. Mangano, S. Massetti, M. Moroni, A. Mura, R. Noschese, C. Plainaki, F. Plaschke, I. Richter, R. Rispoli, R. Sordini, P. Wurz: High-energy particle enhancements in the solar wind upstream Mercury during the first BepiColombo flyby: SERENA/PICAM and MPO-MAG observations, *Astron. Astrophys.*, **669**, A35, doi, 2023.

Alderson, L., H.R. Wakeford, M.K. Alam, N.E. Batalha, J.D. Lothringer, J. Adams Redai, S. Barat, J. Brande, M. Damiano, T. Daylan, N. Espinoza, L. Flagg, J.M. Goyal, D. Grant, R. Hu, J. Inglis, E.K.H. Lee, T. Mikal-Evans, L. Ramos-Rosado, P.-A. Roy, N.L. Wallack, N.M. Batalha, J.L. Bean, B. Benneke, Z.K. Berta-Thompson, A.L. Carter, Q. Changeat, K.D. Colón, I.J.M. Crossfield, J.-M. Désert, D. Foreman-Mackey, N.P. Gibson, L. Kreidberg, M.R. Line, M. López-Morales, K. Molaverdikhani, S.E. Moran, G. Morello, J.I. Moses, S. Mukherjee, E. Schlawin, D.K. Sing, K.B. Stevenson, J. Taylor, K. Aggarwal, E.-M. Ahrer, N.H. Allen, J.K. Barstow, T.J. Bell, J. Blecic, S.L. Casewell, K.L. Chubb, N. Crouzet, P.E. Cubillos, L. Decin, A.D. Feinstein, J.J. Fortney, J. Harrington, K. Heng, N. Iro, E.M.-R. Kempton, J. Kirk, H.A. Knutson, J. Krick, J. Leconte, M. Lendl, R.J. MacDonald, L. Mancini, M. Mansfield, E.M. May, N.J. Mayne, Y. Miguel, N.K. Nikolov, K. Ohno, E. Palle, V. Parmentier, D.J.M. Petit dit de la Roche, C. Piaulet, D. Powell, B.V. Rackham, S. Redfield, L.K. Rogers, Z. Rustamkulov, X. Tan, P. Tremblin, S.-M. Tsai, J.D. Turner, M. de Val-Borro, O. Venot, L. Welbanks, P.J. Wheatley, X.

Zhang: Early release science of the exoplanet WASP-39b with JWST NIRSpec G395H, *Nature*, **614**, 664-669, doi, 2023.

Alonso, R., S. Hoyer, M. Deleuil, A.E. Simon, M. Beck, W. Benz, H.-G. Florén, P. Guterman, L. Borsato, A. Brandeker, D. Gandolfi, T.G. Wilson, T. Zingales, Y. Alibert, G. Anglada, T. Bárczy, D. Barrado Navascues, S.C.C. Barros, W. Baumjohann, T. Beck, N. Billot, X. Bonfils, Ch. Broeg, S. Charnoz, A. Collier Cameron, C. Corral van Damme, Sz. Csizmadia, P.E. Cubillos, M.B. Davies, A. Deline, L. Delrez, O.D.S. Demangeon, B.-O. Demory, D. Ehrenreich, A. Erikson, A. Fortier, L. Fossati, M. Fridlund, M. Gillon, M. Güdel, M.N. Günther, A. Heitzmann, Ch. Helling, K.G. Isaak, L.L. Kiss, E. Kopp, K.W.F. Lam, J. Laskar, A. Lecavelier des Étangs, M. Lendl, D. Magrin, P.F.L. Maxted, Ch. Mordasini, V. Nascimbeni, G. Olofsson, R. Ottensamer, I. Pagano, E. Pallé, G. Peter, G. Piotto, D. Pollacco, D. Queloz, R. Ragazzoni, N. Rando, H. Rauer, I. Ribas, N.C. Santos, G. Scandariato, D. Ségransan, A.M.S. Smith, S.G. Sousa, M. Stalport, Gy.M. Szabó, N. Thomas, S. Udry, B. Ulmer, V. Van Grootel, J. Venturini, F. Verrecchia, N.A. Walton: No random transits in CHEOPS observations of HD 139139, *Astron. Astrophys.*, **680**, A78, doi, 2023.

Alqeeq, S.W., O. Le Contel, P. Canu, A. Retinò, T. Chust, L. Mirioni, A. Chuvatin, R. Nakamura, N. Ahmadi, F.D. Wilder, D.J. Gershman, Yu.V. Khotyaintsev, P.-A. Lindqvist, R.E. Ergun, J.L. Burch, R.B. Torbert, S.A. Fuselier, C.T. Russell, H.Y. Wei, R.J. Strangeway, K.R. Bromund, D. Fischer, B.L. Giles, Y. Saito: Two classes of equatorial magnetotail dipolarization fronts observed by Magnetospheric Multiscale mission: A statistical overview, *J. Geophys. Res. Space Phys.*, **128**, e2023JA031738, doi, 2023.

Amtmann, C., R. Lammegger, A. Betzler, M. Agú, M. Ellmeier, C. Hagen, I. Jernej, W. Magnes, A. Pollinger, W.E. Ernst: Experimental and theoretical investigations on the modulation capabilities of a sample of vertical cavity surface emitting laser diodes for atomic vapour applications, *Appl. Phys. B*, **129**, 31, doi, 2023.

Anger, M., P. Niemelä, K. Cheremetiev, B. Clayhills, A. Fetzer, V. Lundén, M. Hiltunen, T. Kärkkäinen, M. Mayank, L. Turc, A. Osmane, M. Palmroth, E. Kilpua, P. Oleynik, R. Vainio, P. Virtanen, P. Toivanen, P. Janhunen, D. Fischer, G. Le Bonhomme, A. Slavinskis, J. Praks: Foresail-2: Space physics mission in a challenging environment, *Space Sci. Rev.*, **219**, 66, doi, 2023.

Arkhypov, O.V., M.L. Khodachenko: Tachocline Alfvén waves manifested in stellar activity, *Astron. Astrophys.*, **673**, A22, doi, 2023.

Balduin, T., P. Woitke, U.G. Jørgensen, W.-F. Thi, Y. Narita: Size-dependent charging of dust particles in protoplanetary disks. Can turbulence cause charge separation and lightning?, *Astron. Astrophys.*, **678**, A192, doi, 2023.

Balikhin, M.A., M. Gedalin, S.N. Walker, O.V. Agapitov, T.-L. Zhang: Structure of a quasi-parallel shock front, *Astrophys. J.*, **959**, 130, doi, 2023.

Barnes, J.R., M.R. Standing, C.A. Haswell, D. Staab, J.P.J. Doherty, M. Waller-Bridge, L. Fossati, M. Soto, G. Anglada-Escude, J. Llama, C. McCune, F.W. Lewis: DMPP-4: Candidate sub-Neptune mass planets orbiting a naked-eye star, *MNRAS*, **524**, 5196–5212, doi, 2023.

Barth, P., E.E. Stüeken, Ch. Helling, L. Rossmanith, Y. Peng, W. Walters, M. Claire: Isotopic constraints on lightning as a source of fixed nitrogen in Earth's early biosphere, *Nat. Geosci.*, **16**, 478–484, doi, 2023.

Baumjohann, W., R.A. Treumann: ECMI resonance in AKR revisited: Hyperbolic resonance, harmonics, and wave-wave interaction, *Front. Physics*, **11**, 1174557, doi, 2023.

Bertini, L., V. Roccatagliata, M. Kim: Flybys in debris disk systems with Gaia eDR3, *Astron. Astrophys.*, **671**, L2, doi, 2023.

Blanco-Cano, X., D. Rojas-Castillo, P. Kajdič, L. Preisser: Jets and mirror mode waves in Earth's magnetosheath, *J. Geophys. Res. Space Phys.*, **128**, e2022JA031221, doi, 2023.

Blasl, K.A., T.K.M. Nakamura, R. Nakamura, A. Settino, H. Hasegawa, Z. Vörös, M. Hosner, D. Schmid, M. Volwerk, O.W. Roberts, E.V. Panov, Y.-H. Liu, F. Plaschke, J.E. Stawarz, J.C. Holmes: Electron-scale reconnecting current sheet formed within the lower-hybrid wave-active region of Kelvin-Helmholtz waves, *Geophys. Res. Lett.*, **50**, e2023GL104309, doi, 2023.

Boldog, A., Gy.M. Szabó, L. Kriskovics, A. Brandeker, F. Kiefer, A. Bekkelien, P. Guterman, G. Olofsson, A.E. Simon, D. Gandolfi, L.M. Serrano, T.G. Wilson, S.G. Sousa, A. Lecavelier des Etangs, Y. Alibert, R. Alonso, G. Anglada, T. Bandy, T. Bárczy, D. Barrado, S.C.C. Barros, W. Baumjohann, M. Beck, T. Beck, W. Benz, N. Billot, X. Bonfils, C. Broeg, M. Buder, J. Cabrera, S. Charnoz, A. Collier Cameron, C. Corral van Damme, Sz. Csizmadia, M.B. Davies, A. Deline, M. Deleuil, L. Delrez, O.D.S. Demangeon, B.-O. Demory, D. Ehrenreich, A. Erikson, J. Farinato, A. Fortier, L. Fossati, M. Fridlund, M. Gillon, M. Güdel, K. Heng, S. Hoyer, K.G. Isaak, L.L. Kiss, J. Laskar, M. Lendl, C. Lovis, D. Magrin, P.F.L. Maxted, M. Mecina, V. Nascimbeni, R. Ottensamer, I. Pagano, E. Pallé, G. Peter, G. Piotto, D. Pollacco, D. Queloz, R. Ragazzoni, N. Rando, H. Rauer, I. Ribas, N.C. Santos, G. Scandariato, D. Ségransan, A.M.S. Smith, M. Steller, N. Thomas, S. Udry, V. Van Grootel, N.A. Walton: Glancing through the debris disk: Photometric analysis of DE Boo with CHEOPS, *Astron. Astrophys.*, **671**, A127, doi, 2023.

Bonfanti, A., D. Gandolfi, J.A. Egger, L. Fossati, J. Cabrera, A. Krenn, Y. Alibert, W. Benz, N. Billot, H.-G. Florén, M. Lendl, V. Adibekyan, S. Salmon, N.C. Santos, S.G. Sousa, T.G. Wilson, O. Barragán, A. Collier Cameron, L. Delrez, M. Esposito, E. Goffo, H. Osborne, H.P. Osborn, L.M. Serrano, V. Van Eylen, J. Alarcon, R. Alonso, G. Anglada, T. Bárczy, D. Barrado Navascues, S.C.C. Barros, W. Baumjohann, M. Beck, T. Beck, M. Bedell, X. Bonfils, L. Borsato, A. Brandeker, C. Broeg, S. Charnoz, C. Corral Van Damme, Sz. Csizmadia, P.E. Cubillos, M.B. Davies, M. Deleuil, O.D.S. Demangeon, B.-O. Demory, D. Ehrenreich, A. Erikson, A. Fortier, M. Fridlund, M. Gillon, M. Güdel, S. Hoyer, K.G. Isaak, F. Kerschbaum, L.L. Kiss, J. Laskar, A. Lecavelier des Etangs, D. Lorenzo-Oliveira, C. Lovis, D. Magrin, L. Marafatto, P.F.L. Maxted, J. Meléndez, C. Mordasini, V. Nascimbeni, G. Olofsson, R. Ottensamer, I.

Pagano, E. Pallé, G. Peter, D. Piazza, G. Piotto, D. Pollacco, D. Queloz, R. Ragazzoni, N. Rando, H. Rauer, I. Ribas, G. Scandariato, D. Ségransan, A.E. Simon, A.M.S. Smith, M. Steller, Gy.M. Szabó, N. Thomas, S. Udry, B. Ulmer, V. Van Grootel, J. Venturini, N.A. Walton: TOI-1055 b: Neptunian planet characterised with HARPS, TESS, and CHEOPS, *Astron. Astrophys.*, **671**, L8, doi, 2023.

Boudjada, M.Y., H.U. Eichelberger, E. Al-Haddad, W. Magnes, P.H.M. Galopeau, X. Zhang, A. Pollinger, H. Lammer: Case study of radio emission beam associated to very low frequency signal recorded onboard CSES satellite, *Adv. Radio Sci.*, **20**, 77-84, doi, 2023.

Bourrier, V., O. Attia, M. Mallonn, A. Marret, M. Lendl, P.-C. Konig, A. Krenn, M. Cretignier, R. Allart, G. Henry, E. Bryant, A. Leleu, L. Nielsen, G. Hebrard, N. Hara, D. Ehrenreich, J. Seidel, L. dos Santos, C. Lovis, D. Bayliss, H.M. Cegla, X. Dumusque, I. Boisse, A. Boucher, F. Bouchy, F. Pepe, B. Lavie, J. Rey Cerda, D. Ségransan, S. Udry, T. Vrignaud: DREAM I. Orbital architecture orrery, *Astron. Astrophys.*, **669**, A63, doi, 2023.

Brandt, P.C., E. Provornikova, S.D. Bale, A. Cocoros, R. DeMajistre, K. Dialynas, H.A. Elliott, S. Eriksson, B. Fields, A. Galli, M.E. Hill, M. Horanyi, T. Horbury, S. Hunziker, P. Kollmann, J. Kinnison, G. Fountain, S.M. Krimigis, W.S. Kurth, J. Linsky, C.M. Lisse, K.E. Mandt, W. Magnes, R.L. McNutt, J. Miller, E. Moebius, P. Mostafavi, M. Opher, L. Paxton, F. Plaschke, A.R. Poppe, E.C. Roelof, K. Runyon, S. Redfield, N. Schwadron, V. Sterken, P. Swaczyna, J. Szalay, D. Turner, H. Vannier, R. Wimmer-Schweingruber, P. Wurz, E.J. Zirnstein: Future exploration of the outer heliosphere and very local interstellar medium by Interstellar Probe, *Space Sci. Rev.*, **219**, 18, doi, 2023.

Broeren, T., K.G. Klein, J.M. TenBarge, I. Dors, O.W. Roberts, D. Verscharen: Corrigendum: Magnetic field reconstruction for a realistic multi-point, multi-scale spacecraft observatory, *Front. Astron. Space Sci.*, **10**, 1197352, doi, 2023.

Burch, J.L., K.J. Genestreti, S.V. Heuer, A. Chasapis, R.B. Torbert, D.J. Gershman, R. Bandyopadhyay, C.J. Pollock, W.H. Matthaeus, T.K.M. Nakamura, J. Egedal: Electron energy dissipation in a magnetotail reconnection region, *Phys. Plasmas*, **30**, 082903, doi, 2023.

Cabrera, J., D. Gandolfi, L.M. Serrano, Sz. Csizmadia, J.A. Egger, Ph. Baumeister, A. Krenn, W. Benz, A. Deline, H.-G. Florén, A. Collier Cameron, V. Adibekyan, Y. Alibert, S.E. Bellomo, L. Delrez, L. Fossati, A. Fortier, S. Grziwa, S. Hoyer, A. Bonfanti, S. Salmon, S.G. Sousa, T.G. Wilson, J. Alarcón, R. Alonso, G. Anglada Escudé, T. Bárczy, O. Barragán, D. Barrado, S.C.C. Barros, W. Baumjohann, M. Beck, T. Beck, L.M. Bernabò, N. Billot, X. Bonfils, L. Borsato, A. Brandeker, C. Broeg, O. Carrión.-González, S. Charnoz, D.R. Ciardi, W.D. Cochran, K.A. Collins, K.I. Collins, D.M. Conti, M.B. Davies, H.J. Deeg, M. Deleuil, O.D.S. Demangeon, B.-O. Demory, D. Ehrenreich, A. Erikson, M. Esposito, M. Fridlund, M. Gillon, E. Goffo, M. Güdel, E.W. Guenther, J.-V. Harre, K. Heng, M.J. Hooton, K.G. Isaak, J.M. Jenkins, L.L. Kiss, E. Knudstrup, K.W.F. Lam, J. Laskar, A. Lecavelier des Etangs, M. Lendl, C. Lovis, R. Luque, D. Magrin, P.F.L. Maxted, A. Muresan, V. Nascimbeni, G. Olofsson, H.P. Osborn, H.L.M. Osborne, R. Ottensamer, I. Pagano, E. Pallé, C.M. Persson, G. Peter, G. Piotto, D. Pollacco, D. Queloz, R. Ragazzoni, N. Rando, H. Rauer, S. Redfield, I. Ribas, G.R. Ricker, F. Rodler, N.C. Santos, G. Scandariato, S. Seager, D. Ségransan, A.E. Simon, A.M.S. Smith, M. Steller, Gy.M. Szabó, N. Thomas, N. Tosi, J.D. Twicken, S. Udry, V. Van Eylen, V. Van Grootel, N.A. Walton, J.N. Winn: The planetary system around HD 190622 (TOI-1054). Measuring the gas content of low-mass planets orbiting F-stars, *Astron. Astrophys.*, **675**, A183, doi, 2023.

Chen, Y.J., M.Y. Wu, S.D. Xiao, G.Q. Wang, Y.Q. Chen, Y.Q. Lou, A.M. Du, T.-L. Zhang: Observations of occurrence rates of small-scale magnetic holes in the Martian magnetosheath, *Chin. J. Geophys.*, **66**, 871-880, doi, 2023.

Chen, Y.Q., M.Y. Wu, Y.J. Chen, S.D. Xiao, G.Q. Wang, T.-L. Zhang: Responses of the field-aligned currents in the plasma sheet boundary layer to a geomagnetic storm, *Earth Planet. Phys.*, **7**, 558-564, doi, 2023.

Cheng, L., R. Lillis, Y. Wang, A. Mittelholz, S. Xu, D.L. Mitchell, C. Johnson, Z. Su, J.S. Halekas, B. Langlais, T.-L. Zhang, G. Wang, S. Xiao, Z. Zou, Z. Wu, Y. Chi, Z. Pan, K. Liu, X. Hao, Y. Li, M. Chen, J. Espley, F. Eparvier: Martian bow shock oscillations driven by solar wind variations: Simultaneous observations from Tianwen-1 and MAVEN, *Geophys. Res. Lett.*, **50**, e2023GL104769, doi, 2023.

Chi, Y., C. Shen, J. Liu, Z. Zhong, M. Owens, C. Scott, L. Barnard, B. Yu, D. Heyner, H.-U. Auster, I. Richter, Y. Wang, T.-L. Zhang, J. Guo, B. Sánchez-Cano, Z. Pan, Z. Zou, M. Xu, L. Cheng, Z. Su, D. Mao, Z. Zhang, C. Wang, Z. Wu, G. Wang, S. Xiao, K. Liu, X. Hao, Y. Li, M. Chen, M. Lockwood: The dynamic evolution of multipoint interplanetary coronal mass ejections observed with BepiColombo, Tianwen-1, and MAVEN, *Astrophys. J. Lett.*, **951**, L14, doi, 2023.

Chi, Y., C. Shen, L. Cheng, B. Yu, B. Miao, Y. Wang, T.-L. Zhang, Z. Zou, M. Xu, Z. Pan, Z. Su, J. Guo, D. Mao, Z. Zhong, Z. Zhang, J. Liu, C. Wang, Z. Wu, G. Wang, S. Xiao, K. Liu, X. Hao, Y. Li, M. Chen, Y. Du: Interplanetary coronal mass ejections and stream interaction regions observed by Tianwen-1 and MAVEN at Mars, *Astrophys. J. Suppl. Ser.*, **267**, 3, doi, 2023.

Chiappetta, F., E. Yordanova, Z. Vörös, F. Lepreti, V. Carbone: Energy conversion through a fluctuation-dissipation relation at kinetic scales in the Earth's magnetosheath, *Astrophys. J.*, **957**, 98, doi, 2023.

Collinson, G.A., H. Hietala, F. Plaschke, T. Karlsson, L.B. Wilson III, M. Archer, M. Battarbee, X. Blanco-Cano, C. Bertucci, D. Long, M. Opher, N. Sergis, C. Gasque, T. Liu, S. Raptis, S. Burne, R. Frahm, T.-L. Zhang, Y. Futaana: Shocklets and Short Large Amplitude Magnetic Structures (SLAMS) in the high Mach foreshock of Venus, *Geophys. Res. Lett.*, **50**, e2023GL104610, doi, 2023.

Collinson, G.A., R.A. Frahm, A. Glocer, L. Daldorff, E. Thiemann, S.-B. Kang, G. Gronoff, Y. Futaana, T.-L. Zhang: A survey of strong electric potential drops in the ionosphere of Venus, *Geophys. Res. Lett.*, **50**, e2023GL104989, doi, 2023.

Coulombe, L.-P., B. Benneke, R. Challener, A.A.A. Piette, L.S. Wiser, M. Mansfield, R.J. MacDonald, H. Beltz, A.D. Feinstein, M. Radica, A.B. Savel, L.A. Dos Santos, J.L. Bean, V. Parmentier, I. Wong, E. Rauscher, T.D. Komacek, E.M.-R. Kempton, X. Tan, M. Hammond, N.T. Lewis, M.R. Line, E.K.H. Lee, H. Shivkumar, I.J.M. Crossfield, M.C. Nixon, B.V. Rackham, H.R. Wakeford, L. Welbanks, X. Zhang, N.M. Batalha, Z.K. Berta-Thompson, Q. Changeat, J.-M. Désert, N. Espinoza, J.M. Goyal, J. Harrington, H.A. Knutson, L. Kreidberg, M. López-Morales, A. Shporer, D.K. Sing, K.B. Stevenson, K. Aggarwal, E.-M. Ahrer, M.K. Alam, T.J. Bell, J. Blecic, C. Caceres, A.L. Carter, S.L. Casewell, N. Crouzet, P.E. Cubillos, L. Decin, J.J. Fortney, N.P. Gibson, K. Heng, T. Henning, N. Iro, S. Kendrew, P.-O. Lagage, J. Leconte, M. Lendl, J.D. Lothringer, L. Mancini, T. Mikal-Evans, K. Molaverdikhani, N.K. Nikolov, K. Ohno, E. Palle, C. Piaulet, S. Redfield, P.-A. Roy, S.-M. Tsai, O. Venot, P.J. Wheatley: A broadband thermal emission spectrum of the ultra-hot Jupiter WASP-18b, *Nature*, **620**, 292-298, doi , 2023.

Cubillos, P.E., L. Fossati, T. Koskinen, C. Huang, A.G. Sreejith, K. France, P. Wilson Cauley, C.A. Haswell: The Hubble/STIS near-ultraviolet transmission spectrum of HD 189733 b, *Astron. Astrophys.*, **671**, A170, doi, 2023.

Dandouras, I., M.G.G.T. Taylor, J. De Keyser, Y. Futaana, R.A. Bamford, G. Branduardi-Raymont, J.-Y. Chaufray, D. Constantinescu, E. De Angelis, P. Devoto, J. Eastwood, M. Echim, P. Garnier, B. Grison, D. Hercik, H. Lammer, A. Laurens, F. Leblanc, A. Milillo, R. Nakamura, L. Přech, E. Roussos, Š. Štverák, J. Forest, A. Trouche, S.L.G. Hess, J.-C. Mateo-Vélez, J. Carpenter, J. Winter: Space plasma physics science opportunities for the lunar orbital platform - Gateway, *Front. Astron. Space Sci.*, **10**, 1120302, doi, 2023.

Dang, T., B. Zhang, M. Yan, J. Lyon, Z. Yao, S. Xiao, T.-L. Zhang, J. Lei: A new tool for understanding the solar wind-Venus interaction: Three-dimensional multifluid MHD model, *Astrophys. J.*, **945**, 91, doi, 2023.

Deibert, E.K., E.J.W. de Mooij, R. Jayawardhana, J.D. Turner, A. Ridden-Harper, C.E. Hood, J.J. Fortney, L. Flagg, L. Fossati, R. Allart, M. Brogi, R.J. MacDonald: ExoGemS high-resolution transmission spectroscopy of WASP-76b with GRACES, *Astron. J.*, **166**, 141, doi, 2023.

Delrez, L., A. Leleu, A. Brandeker, M. Gillon, M.J. Hooton, A. Collier Cameron, A. Deline, A. Fortier, D. Queloz, A. Bonfanti, V. Van Grootel, T.G. Wilson, J.A. Egger, Y. Alibert, R. Alonso, G. Anglada, J. Asquier, T. Bárczy, D. Barrado y. Navascues, S.C.C. Barros, W. Baumjohann, M. Beck, T. Beck, W. Benz, N. Billot, X. Bonfils, L. Borsato, C. Broeg, M. Buder, J. Cabrera, V. Cessa, S. Charnoz, Sz. Csizmadia, P.E. Cubillos, M.B. Davies, M. Deleuil, O.D.S. Demangeon, B.-O. Demory, D. Ehrenreich, A. Erikson, L. Fossati, M. Fridlund, D. Gandolfi, M. Güdel, J. Hasiba, S. Hoyer, K.G. Isaak, J.M. Jenkins, L.L. Kiss, J. Laskar, D.W. Latham, A. Lecavelier des Etangs, M. Lendl, C. Lovis, R. Luque, D. Magrin, P.F.L. Maxted, C. Mordasini, V. Nascimbeni, G. Olofsson, R. Ottensamer, I. Pagano, E. Pallé, G. Peter, G. Piotto, D. Pollacco, R. Ragazzoni, N. Rando, H. Rauer, I. Ribas, G. Ricker, N.C. Santos, G. Scandariato, S. Seager, D. Ségransan, A.E. Simon, A.M.S. Smith, S.G. Sousa, M. Steller, Gy.M. Szabó, N. Thomas, S. Udry, R. Vanderspek, J. Venturini, V. Viotto, N.A. Walton, J.N. Winn: Refining the properties of the TOI-178 system with CHEOPS and TESS, *Astron. Astrophys.*, **678**, A200, doi, 2023.

Demory, B.-O., S. Sulis, E. Meier Valdés, L. Delrez, A. Brandeker, N. Billot, A. Fortier, S. Hoyer, S.G. Sousa, K. Heng, M. Lendl, A. Krenn, B.M. Morris, J.A. Patel, Y. Alibert, R. Alonso, G. Anglada, T. Bárczy, D. Barrado, S.C.C. Barros, W. Baumjohann, M. Beck, T. Beck, W. Benz, X. Bonfils, C. Broeg, M. Buder, J. Cabrera, S. Charnoz, A. Collier Cameron, H. Cottard, Sz. Csizmadia, M.B. Davies, M. Deleuil, O.D.S. Demangeon, D. Ehrenreich, A. Erikson, L. Fossati, M. Fridlund, D. Gandolfi, M. Gillon, M. Güdel, K.G. Isaak, L.L. Kiss, J. Laskar, A. Lecavelier des Etangs, C. Lovis, A. Luntzer, D. Magrin, L. Marafatto, P.F.L. Maxted, V. Nascimbeni, G. Olofsson, R. Ottensamer, I. Pagano, E. Pallé, G. Peter, G. Piotto, D. Pollacco, D. Queloz, R. Ragazzoni, N. Rando, F. Ratti, H. Rauer, I. Ribas, N.C. Santos, G. Scandariato, D. Ségransan, A.E. Simon, A.M.S. Smith, M. Steller, Gy.M. Szabó, N. Thomas, S. Udry, V. Van Grootel, N.A. Walton: 55 Cancri e's occultation captured with CHEOPS, *Astron. Astrophys.*, **669**, A64, doi, 2023.

Divin, A., I. Zaitsev, I. Paramonik, V.S. Semenov, D. Korovinskiy, A. Mao, J.P. Dargent, S. Toledo-Redondo, J. Deca: Cold ion crescent echoes in the exhaust of symmetric magnetic reconnection, *Phys. Plasmas*, **30**, 062901, doi, 2023.

Du, A., Y. Ge, H. Wang, H. Li, Y. Zhang, H. Luo, C. Huang, L. Shan, F. Han, Y. Liu, Y. Zou, C. Wang, Y. Pan, Q. Liu, R.N. Mitchell, Y. Jia, B. Chen, S. Jin, Y. Jiang, T.-L. Zhang, R. Zhu, D. Gubbins, K. Zhang: Ground magnetic survey on Mars from the Zhurong rover, *Nat. Astron.*, **7**, 1037-1047, doi, 2023.

Echim, M., H. Lamy, C. Simon-Wedlund, J. De Keyser, G. Cessateur: Probing the magnetospheric generator of quiet electrostatic auroral arcs from ground based optical observations and magnetosphere-ionosphere coupling modeling, *Geophys. Res. Lett.*, **50**, e2023GL103689, doi, 2023.

Egan, A., N. Nell, A. Suresh, K. France, B. Fleming, A.G. Sreejith, J. Lambert, N. DeCicco: The on-orbit performance of the Colorado Ultraviolet Transit Experiment mission, *Astron. J.*, **165**, 64, doi, 2023.

Ehrenreich, D., L. Delrez, B. Akinsanmi, T.G. Wilson, A. Bonfanti, M. Beck, W. Benz, S. Hoyer, D. Queloz, Y. Alibert, S. Charnoz, A. Collier Cameron, A. Deline, M. Hooton, M. Lendl, G. Olofsson, S.G. Sousa, V. Adibekyan, R. Alonso, G. Anglada, D. Barrado, S.C.C. Barros, W. Baumjohann, T. Beck, A. Bekkelien, M. Bergomi, N. Billot, X. Bonfils, A. Brandeker, C. Broeg, T. Bárczy, Z.K. Berta-Thompson, J. Cabrera, C. Corral Van Damme, S. Csizmadia, M.B. Davies, M. Deleuil, O. Demangeon, B.-O. Demory, J.P. Doty, A. Erikson, M.M. Fausnaugh, H.-G. Florén, A. Fortier, L. Fossati, M. Fridlund, D. Futyan, D. Gandolfi, M. Gillon, P. Guterman, M. Güdel, K. Heng, K.G. Isaak, A. Jäckel, J.M. Jenkins, L.L. Kiss, J. Laskar, D.W. Latham, A. Lecavelier des Etangs, A.M. Levine, C. Lovis, D. Magrin, P.F.L. Maxted, E.H. Morgan, V. Nascimbeni, H.P. Osborn, R. Ottensamer, I. Pagano, E. Pallé, G. Peter, G. Piotto, D. Pollacco, R. Ragazzoni, N. Rando, H. Rauer, I. Ribas, G.R. Ricker, S. Salmon, N.C. Santos, G. Scandariato, A.E. Simon,

A.M.S. Smith, M. Steinberger, M. Steller, G.M. Szabó, D. Ségransan, A. Shporer, N. Thomas, M. Tschentscher, S. Udry, R. Vanderspek, V. Van Grootel, N.A. Walton: A full transit of ν2 Lupi d and the search for an exomoon in its Hill sphere with CHEOPS, *Astron. Astrophys.*, **671**, A154, doi, 2023.

Ellmeier, M., C. Amtmann, A. Pollinger, W. Magnes, C. Hagen, A. Betzler, I. Jernej, M. Agú, L. Windholz, R. Lammegger: Frequency shift compensation for single and dual laser beam pass sensors of a coherent population trapping resonance based coupled dark state magnetometer, *Meas.: Sens.*, **25**, 100606, doi, 2023.

Erkaev, N.V., M. Scherf, O. Herbort, H. Lammer, P. Odert, D. Kubyshkina, M. Leitzinger, P. Woitke, C. O'Neill: Modification of the radioactive heat budget of Earth-like exoplanets by the loss of primordial atmospheres, *MNRAS*, **518**, 3703-3721, doi, 2023.

Feinstein, A.D., M. Radica, L. Welbanks, C.A. Murray, K. Ohno, L.-P. Coulombe, N. Espinoza, J.L. Bean, J.K. Teske, B. Benneke, M.R. Line, Z. Rustamkulov, A. Saba, A. Tsiaras, J.K. Barstow, J.J. Fortney, P. Gao, H.A. Knutson, R.J. MacDonald, T. Mikal-Evans, B.V. Rackham, J. Taylor, V. Parmentier, N.M. Batalha, Z.K. Berta-Thompson, A.L. Carter, Q. Changeat, L.A. dos Santos, N.P. Gibson, J.M. Goyal, L. Kreidberg, M. López-Morales, J.D. Lothringer, Y. Miguel, K. Molaverdikhani, S.E. Moran, G. Morello, S. Mukherjee, D.K. Sing, K.B. Stevenson, H.R. Wakeford, E.-M. Ahrer, M.K. Alam, L. Alderson, N.H. Allen, N.E. Batalha, T.J. Bell, J. Blecic, J. Brande, C. Caceres, S.L. Casewell, K.L. Chubb, I.J.M. Crossfield, N. Crouzet, P.E. Cubillos, L. Decin, J.-M. Désert, J. Harrington, K. Heng, T. Henning, N. Iro, E.M.-R. Kempton, S. Kendrew, J. Kirk, J. Krick, P.-O. Lagage, M. Lendl, L. Mancini, M. Mansfield, E.M. May, N.J. Mayne, N.K. Nikolov, E. Palle, D.J.M. Petit dit de la Roche, C. Piaulet, D. Powell, S. Redfield, L.K. Rogers, M.T. Roman, P.-A. Roy, M.C. Nixon, E. Schlawin, X. Tan, P. Tremblin, J.D. Turner, O. Venot, W.C. Waalkes, P.J. Wheatley, X. Zhang: Early release science of the exoplanet WASP-39b with JWST NIRISS, *Nature*, **614**, 670–675, doi, 2023.

Fletcher, L.N., T. Cavalié, D. Grassi, R. Hueso, L.M. Lara, Y. Kaspi, E. Galanti, T.K. Greathouse, P.M. Molyneux, M. Galand, C. Vallat, O. Witasse, R. Lorente, P. Hartogh, F. Poulet, Y. Langevin, P. Palumbo, G.R. Gladstone, K.D. Retherford, M.K. Dougherty, J.-E. Wahlund, S. Barabash, L. Iess, L. Bruzzone, H. Hussmann, L.I. Gurvits, O. Santolik, I. Kolmasova, G. Fischer, I. Müller-Wodarg, G. Piccioni, T. Fouchet, J.-C. Gérard, A. Sánchez-Lavega, P.G.J. Irwin, D. Grodent, F. Altieri, A. Mura, P. Drossart, J. Kammer, R. Giles, S. Cazaux, G. Jones, M. Smirnova, E. Lellouch, A.S. Medvedev, R. Moreno, L. Rezac, A. Coustenis, M. Costa: Jupiter science enabled by ESA's Jupiter Icy Moons Explorer, *Space Sci. Rev.*, **219**, 53, doi, 2023.

Fossati, L., F. Biassoni, G.M. Cappello, F. Borsa, D. Shulyak, A.S. Bonomo, D. Gandolfi, F. Haardt, T. Koskinen, A.F. Lanza, V. Nascimbeni, D. Sicilia, M. Young, G. Aresu, A. Bignamini, M. Brogi, I. Carleo, R. Claudi, R. Cosentino, G. Guilluy, C. Knapic, L. Malavolta, L. Mancini, D. Nardiello, M. Pinamonti, L. Pino, E. Poretti, M. Rainer, F. Rigamonti, A. Sozzetti: The GAPS programme at TNG. XLV. HI Balmer lines transmission spectroscopy and NLTE atmospheric modelling of the ultra-hot Jupiter KELT-20b/MASCARA-2b, *Astron. Astrophys.*, **676**, A99, doi, 2023.

Fossati, L., I. Pillitteri, I.F. Shaikhislamov, A. Bonfanti, F. Borsa, I. Carleo, G. Guilluy, M.S. Rumenskikh: Possible origin of the non-detection of metastable HeI in the upper atmosphere of the hot Jupiter WASP-80b, *Astron. Astrophys.*, **673**, A37, doi, 2023.

France, K., B. Fleming, A. Egan, J.-M. Desert, L. Fossati, T.T. Koskinen, N. Nell, P. Petit, A.A. Vidotto, M. Beasley, N. DeCicco, A.G. Sreejith, A. Suresh, J. Baumert, P. Wilson Cauley, C. Villarreal D'Angelo, K. Hoadley, R. Kane1, R. Kohnert, J. Lambert, S. Ulrich: The Colorado Ultraviolet Transit Experiment mission overview, *Astron. J.*, **165**, 63, doi, 2023.

Galopeau, P.H.M., A.S. Maxworth, M.Y. Boudjada, H.U. Eichelberger, M. Meftah, P.F. Biagi, K. Schwingenschuh: A VLF/LF facility network for preseismic electromagnetic investigations, *Geosci. Instrum. Method. Data Syst.*, **12**, 231-237, doi, 2023.

Garai, Z., H.P. Osborn, D. Gandolfi, A. Brandeker, S.G. Sousa, M. Lendl, A. Bekkelien, C. Broeg, A. Collier Cameron, J.A. Egger, M.J. Hooton, Y. Alibert, L. Delrez, L. Fossati, S. Salmon, T.G. Wilson, A. Bonfanti, A. Tuson, S. Ulmer-Moll, L.M. Serrano, L. Borsato, R. Alonso, G. Anglada, J. Asquier, D. Barrado y. Navascues, S.C.C. Barros, T. Bárczy, W. Baumjohann, M. Beck, T. Beck, W. Benz, N. Billot, F. Biondi, X. Bonfils, M. Buder, J. Cabrera, V. Cessa, S. Charnoz, Sz. Csizmadia, P.E. Cubillos, M.B. Davies, M. Deleuil, O.D.S. Demangeon, B.-O. Demory, D. Ehrenreich, A. Erikson, V. Van Eylen, A. Fortier, M. Fridlund, M. Gillon, V. Van Grootel, M. Güdel, M.N. Günther, S. Hoyer, K.G. Isaak, L.L. Kiss, M.H. Kristiansen, J. Laskar, A. Lecavelier des Etangs, C. Lovis, A. Luntzer, D. Magrin, P.F.L. Maxted, C. Mordasini, V. Nascimbeni, G. Olofsson, R. Ottensamer, I. Pagano, E. Pallé, G. Peter, G. Piotto, D. Pollacco, D. Queloz, R. Ragazzoni, N. Rando, H. Rauer, I. Ribas, N.C. Santos, G. Scandariato, D. Ségransan, A.E. Simon, A.M.S. Smith, M. Steller, Gy.M. Szabó, N. Thomas, S. Udry, J. Venturini, N. Walton: Refined parameters of the HD22946 planetary system and the true orbital period of planet d, *Astron. Astrophys.*, **674**, A44, doi, 2023.

Gasman, D., E.F. van Dishoeck, S.L. Grant, M. Temmink, B. Tabone, T. Henning, I. Kamp, M. Güdel, P.-O. Lagage, G. Perotti, V. Christiaens, M. Samland, A.M. Arabhavi, I. Argyriou, A. Abergel, O. Absil, D. Barrado, A. Boccaletti, J. Bouwman, A. Caratti o. Garatti, V. Geers, A.M. Glauser, R. Guadarrama, H. Jang, J. Kanwar, F. Lahuis, M. Morales-Calderón, M. Mueller, C. Nehmé, G. Olofsson, É. Pantin, N. Pawellek, T.P. Ray, D. Rodgers-Lee, S. Scheithauer, J. Schreiber, K. Schwarz, B. Vandenbussche, M. Vlasblom, R.L.B.F.M. Waters, G. Wright, L. Colina, T.R. Greve, G. Östlin: MINDS. Abundant water and varying C/O across the disk of Sz 98 as seen by JWST/MIRI, *Astron. Astrophys.*, **679**, A117, doi, 2023.

Genestreti, K.J., C.J. Farrugia, S. Lu, S.K. Vines, P.H. Reiff, T. Phan, D.N. Baker, T.W. Leonard, J.L. Burch, S.T. Bingham, I.J. Cohen, J.R. Shuster, D.J. Gershman, C.G. Mouikis,

A.J. Rogers, R.B. Torbert, K.J. Trattner, J.M. Webster, L.-J. Chen, B.L. Giles, N. Ahmadi, R.E. Ergun, C.T. Russell, R.J. Strangeway, R. Nakamura: Multiscale observation of magnetotail reconnection onset: 1. Macroscopic dynamics, *J. Geophys. Res. Space Phys.*, **128**, e2023JA031758, doi, 2023.

Genestreti, K.J., C.J. Farrugia, S. Lu, S.K. Vines, P.H. Reiff, T. Phan, D.N. Baker, T.W. Leonard, J.L. Burch, S.T. Bingham, I.J. Cohen, J.R. Shuster, D.J. Gershman, C.G. Mouikis, A.J. Rogers, R.B. Torbert, K.J. Trattner, J.M. Webster, L.-J. Chen, B.L. Giles, N. Ahmadi, R.E. Ergun, C.T. Russell, R.J. Strangeway, R. Nakamura, D.L. Turner: Multi-scale observation of magnetotail reconnection onset: 2. Microscopic dynamics, *J. Geophys. Res. Space Phys.*, **128**, e2023JA031760, doi, 2023.

Goetz, C., L. Scharré, C. Simon Wedlund, A. Moeslinger, H. Nilsson, E. Odelstad, M.G.G.T. Taylor, M. Volwerk: Solar wind protons in the diamagnetic cavity at comet 67P/Churyumov-Gerasimenko, *J. Geophys. Res. Space Phys.*, **128**, e2022JA031249, doi, 2023.

Goffo, E., D. Gandolfi, J.A. Egger, A.J. Mustill, S.H. Albrecht, T. Hirano, O. Kochukhov, N. Astudillo-Defru, O. Barragan, L.M. Serrano, A.P. Hatzes, Y. Alibert, E. Guenther, F. Dai, K.W.F. Lam, S. Csizmadia, A.M.S. Smith, L. Fossati, R. Luque, F. Rodler, M.L. Winther, J.L. Rørsted, J. Alarcon, X. Bonfils, W.D. Cochran, H.J. Deeg, M. Jenkins, J. Korth, J.H. Livingston, A. Meech, F. Murgas, J. Orell-Miquel, H.L.M. Osborne, E. Palle, C.M. Persson, S. Redfield, G.R. Ricker, S. Seager, R. Vanderspek, V. Van Eylen, J.N. Winn: Company for the ultra-high density, ultra-short period sub-Earth GJ 367 b: Discovery of two additional low-mass planets at 11.5 and 34 days, *Astrophys. J. Lett.*, **955**, L3, doi, 2023.

Grant, S.L., E.F. van Dishoeck, B. Tabone, D. Gasman, T. Henning, I. Kamp, M. Güdel, P.-O. Lagage, G. Bettoni, G. Perotti, V. Christiaens, M. Samland, A.M. Arabhavi, I. Argyriou, A. Abergel, O. Absil, D. Barrado, A. Boccaletti, J. Bouwman, A. Caratti o. Garatti, V. Geers, A.M. Glauser, R. Guadarrama, H. Jang, J. Kanwar, F. Lahuis, M. Morales-Calderón, M. Mueller, C. Nehmé, G. Olofsson, E. Pantin, N. Pawellek, T.P. Ray, D. Rodgers-Lee, S. Scheithauer, J. Schreiber, K. Schwarz, M. Temmink, B. Vandenbussche, M. Vlasblom, L.B.F.M. Waters, G. Wright, L. Colina, T.R. Greve, K. Justannont, G. Östlin: MINDS. The detection of 13CO_2 with JWST-MIRI indicates abundant CO_2 in a protoplanetary disk, *Astrophys. J. Lett.*, **947**, L6, doi, 2023.

Grasser, N., K. Kislyakova, M. Scherf, H. Lammer, G. Van Looveren: Evolution of Earth's oxygen, nitrogen, and carbon polar outflow in the Archean eon, *Earth Planet. Sci. Lett.*, **623**, 118442, doi, 2023.

Grigorenko, E.E., A.Y. Malykhin, E.A. Kronberg, E.V. Panov: Quasi-parallel whistler waves and their interaction with resonant electrons during high-velocity bulk flows in the Earth's magnetotail, *Astrophys. J.*, **943**, 169, doi, 2023.

Grimmich, N., F. Plaschke, M.O. Archer, D. Heyner, J.Z.D. Mieth, R. Nakamura, D.G. Sibeck: Study of extreme magnetopause distortions under varying solar wind conditions, *J. Geophys. Res. Space Phys.*, **128**, e2023JA031603, doi, 2023.

Gunnarson, J.L., K.M. Sayanagi, G. Fischer, T. Barry, A. Wesley, U.A. Dyudina, S.P. Ewald, A.P. Ingersoll: Multiple convective storms within a single cyclone on Saturn, *Icarus*, **389**, 115228, doi, 2023.

Güttler, C., M. Rose, H. Sierks, W. Macher, S. Zivithal, J. Blum, S. Laddha, B. Gundlach, G. Kargl: Simulation and experiment of gas diffusion in a granular bed, *MNRAS*, **524**, 6114–6123, doi, 2023.

Harre, J.-V., A.M.S. Smith, S.C.C. Barros, G. Boué, Sz. Csizmadia, D. Ehrenreich, H.-G. Florén, A. Fortier, P.F.L. Maxted, M.J. Hooton, B. Akinsanmi, L.M. Serrano, N.M. Rosário, B.-O. Demory, K. Jones, J. Laskar, V. Adibekyan, Y. Alibert, R. Alonso, D.R. Anderson, G. Anglada, J. Asquier, T. Bárczy, D. Barrado y. Navascues, W. Baumjohann, M. Beck, T. Beck, W. Benz, N. Billot, F. Biondi, A. Bonfanti, X. Bonfils, A. Brandeker, C. Broeg, J. Cabrera, V. Cessa, S. Charnoz, A. Collier Cameron, M.B. Davies, M. Deleuil, L. Delrez, O.D.S. Demangeon, A. Erikson, L. Fossati, M. Fridlund, D. Gandolfi, M. Gillon, M. Güdel, C. Hellier, K. Heng, S. Hoyer, K.G. Isaak, L.L. Kiss, A. Lecavelier des Etangs, M. Lendl, C. Lovis, A. Luntzer, D. Magrin, V. Nascimbeni, G. Olofsson, R. Ottensamer, I. Pagano, E. Pallé, C.M. Persson, G. Peter, G. Piotto, D. Pollacco, D. Queloz, R. Ragazzoni, N. Rando, H. Rauer, I. Ribas, G.R. Ricker, S. Salmon, N.C. Santos, G. Scandariato, S. Seager, D. Ségransan, A.E. Simon, S.G. Sousa, M. Steller, Gy.M. Szabó, N. Thomas, S. Udry, B. Ulmer, V. Van Grootel, N.A. Walton, T.G. Wilson, J.N. Winn, B. Wohler: Examining the orbital decay targets KELT-9 b, KELT-16 b, and WASP-4 b, and the transit-timing variations of HD97658 b, *Astron. Astrophys.*, **669**, A124, doi, 2023.

Hasegawa, H., R.E. Denton, K. Dokgo, K.-J. Hwang, T.K.M. Nakamura, J.L. Burch: Ion-scale magnetic flux rope generated from electron-scale magnetopause current sheet: Magnetospheric multiscale observations, *J. Geophys. Res. Space Phys.*, **128**, e2022JA031092, doi, 2023.

Hawthorn, F., D. Bayliss, T.G. Wilson, A. Bonfanti, V. Adibekyan, Y. Alibert, S.G. Sousa, K.A. Collins, E.M. Bryant, A. Osborn, D.J. Armstrong, L. Abe, J.S. Acton, B.C. Addison, K. Agabi, R. Alonso, D.R. Alves, G. Anglada-Escudé, T. Bárczy, T. Barclay, D. Barrado, S.C.C. Barros, W. Baumjohann, P. Bendjoya, W. Benz, A. Bieryla, X. Bonfils, F. Bouchy, A. Brandeker, C. Broeg, D.J.A. Brown, M.R. Burleigh, M. Buttu, J. Cabrera, D.A. Caldwell, S.L. Casewell, D. Charbonneau, S. Charnoz, R. Cloutier, A. Collier Cameron, K.I. Collins, D.M. Conti, N. Crouzet, S. Czismadia, M.B. Davies, M. Deleuil, E. Delgado-Mena, L. Delrez, O.D.S. Demangeon, B.-O. Demory, G. Dransfield, X. Dumusque, J. Ann Egger, D. Ehrenreich, P. Eigmüller, A. Erickson, Z. Essack, A. Fortier, L. Fossati, M. Fridlund, M.N. Günther, M. Güdel, D. Gandolfi, H. Gillard, M. Gillon, C. Gnilka, M.R. Goad, R.F. Goeke, T. Guillot, A. Hadjigeorghiou, C. Hellier, B.A. Henderson, K. Heng, M.J. Hooton, K. Horne, S.B. Howell, S. Hoyer, J.M. Irwin, J.S. Jenkins, J.M. Jenkins, E.L.N. Jensen, S.R. Kane, A. Kendall, J.F. Kielkopf, L.L. Kiss, G. Lacedelli, J. Laskar, D.W. Latham, A. Lecavalier des Etangs, A. Leleu, M. Lendl, J. Lillo-Box, C. Lovis, D. Mékarnia, B. Massey, T. Masters, P.F.L. Maxted, V. Nascimbeni, L.D. Nielsen, S.M. O'Brien, G. Olofsson, H.P. Osborn, I. Pagano, E. Pallé, C.M. Persson,

G. Piotto, P. Plavchan, D. Pollacco, D. Queloz, R. Ragazzoni, H. Rauer, I. Ribas, G. Ricker, D. Ségransan, S. Salmon, A. Santerne, N.C. Santos, G. Scandariato, F.-X. Schmider, R.P. Schwarz, S. Seager, A. Shporer, A.E. Simon, A.M.S. Smith, G. Srdoc, M. Steller, O. Suarez, G.M. Szabó, J. Teske, N. Thomas, R.H. Tilbrook, A.H.M.J. Triaud, S. Udry, V. Van Grootel, N. Walton, S.X. Wang, P.J. Wheatley, J.N. Winn, R.A. Wittenmyer, H. Zhang: TOI-836: A super-Earth and mini-Neptune transiting a nearby K-dwarf, *MNRAS*, **520**, 3649–3668, doi, 2023.

Hayakawa, H., E.W. Cliver, F. Clette, Y. Ebihara, S. Toriumi, I. Ermolli, T. Chatzistergos, K. Hattori, D.J. Knipp, S.P. Blake, G. Cauzzi, K. Reardon, Ph.-A. Bourdin, D. Just, M. Vokhmyanin, K. Matsumoto, Y. Miyoshi, J.R. Ribeiro, A.P. Correia, D.M. Willis, M.N. Wild, S.M. Silverman: The extreme space weather event of 1872 February: Sunspots, magnetic disturbance, and auroral displays, *Astrophys. J.*, **959**, 23, doi, 2023.

Hayakawa, H., R. Arlt, T. Iju, B.P. Besser: Karl von Lindener's sunspot observations during 1800-1827: Another long-term dataset for the Dalton Minimum, *J Space Weather Space Clim*, **13**, 33, doi, 2023.

Helling, Ch., D. Samra, D. Lewis, R. Calder, G. Hirst, P. Woitke, R. Baeyens, L. Carone, O. Herbort, K.L. Chubb: Exoplanet weather and climate regimes with clouds and thermal ionospheres. A model grid study in support of large-scale observational campaigns, *Astron. Astrophys.*, **671**, A122, doi, 2023.

Huang, C., T. Koskinen, P. Lavvas, L. Fossati: A hydrodynamic study of the escape of metal species and excited hydrogen from the atmosphere of the Hot Jupiter WASP-121b, *Astrophys. J.*, **951**, 123, doi, 2023.

Hughes, A.C.G., M. Chaffin, E. Mierkiewicz, J. Deighan, R.D. Jolitz, E. Kallio, G. Gronoff, V. Shematovich, D. Bisikalo, J. Halekas, C. Simon Wedlund, N. Schneider, B. Ritter, Z. Girazian, S. Jain, J.-C. Gérard, B. Hegyi: Advancing our understanding of Martian proton aurora through a coordinated multi-model comparison campaign, *J. Geophys. Res. Space Phys.*, **128**, e2023JA031838, doi, 2023.

Hwang, K.-J., C.-P. Wang, K. Nykyri, H. Hasegawa, M.B. Tapley, J.L. Burch, S.A. Fuselier, J. Goldstein, K. Dokgo, T.K.M. Nakamura, M. Sitnov, X. Ma, Y. Lin, X. Wang: Kelvin-Helmholtz instability-driven magnetopause dynamics as turbulent pathway for the solar wind-magnetosphere coupling and the flank-central plasma sheet communication, *Front. Astron. Space Sci.*, **10**, 1151869, doi, 2023.

Hwang, K.-J., R. Nakamura, J.P. Eastwood, S.A. Fuselier, H. Hasegawa, T.K.M. Nakamura, B. Lavraud, K. Dokgo, D.L. Turner, R.E. Ergun, P.H. Reiff: Cross-scale processes of magnetic reconnection, *Space Sci. Rev.*, **219**, 71, doi, 2023.

Janssen, L.J., P. Woitke, O. Herbort, M. Min, K.L. Chubb, Ch. Helling, L. Carone: The sulfur species in hot rocky exoplanet atmospheres, *Astron. Nachr.*, **344**, e20230075, doi, 2023.

Kaeufer, T., P. Woitke, M. Min, I. Kamp, C. Pinte: Analysing the SEDs of protoplanetary disks with machine learning, *Astron. Astrophys.*, **672**, A30, doi, 2023.

Kenworthy, M., S. Lock, G. Kennedy, R. van Capelleveen, E. Mamajek, L. Carone, F.-J. Hambsch, J. Masiero, A. Mainzer, J.D. Kirkpatrick, E. Gomez, Z. Leinhardt, J. Dou, P. Tanna, A. Sainio, H. Barker, S. Charbonnel, O. Garde, P. Le Dû, L. Mulato, T. Petit, M. Rizzo Smith: A planetary collision afterglow and transit of the resultant debris cloud, *Nature*, **622**, 251-254, doi, 2023.

Kiefer, F., V. Van Grootel, A. Lecavelier des Etangs, Gy.M. Szabó, A. Brandeker, C. Broeg, A. Collier Cameron, A. Deline, G. Olofsson, T.G. Wilson, S.G. Sousa, D. Gandolfi, G. Hébrard, Y. Alibert, R. Alonso, G. Anglada, T. Bárczy, D. Barrado, S.C.C. Barros, W. Baumjohann, M. Beck, T. Beck, W. Benz, N. Billot, X. Bonfils, J. Cabrera, S. Charnoz, Sz. Csizmadia, M.B. Davies, M. Deleuil, L. Delrez, O.D.S. Demangeon, B.-O. Demory, D. Ehrenreich, A. Erikson, A. Fortier, L. Fossati, M. Fridlund, M. Gillon, M. Güdel, K. Heng, S. Hoyer, K.G. Isaak, L.L. Kiss, J. Laskar, M. Lendl, C. Lovis, D. Magrin, P.F.L. Maxted, M. Munari, V. Nascimbeni, R. Ottensamer, I. Pagano, E. Pallé, G. Peter, D. Piazza, G. Piotto, D. Pollacco, D. Queloz, R. Ragazzoni, N. Rando, F. Ratti, H. Rauer, C. Reimers, I. Ribas, N.C. Santos, G. Scandariato, D. Ségransan, A.E. Simon, A.M.S. Smith, M. Steller, N. Thomas, S. Udry, I. Walter, N.A. Walton: Hint of an exocomet transit in the CHEOPS light curve of HD172555, *Astron. Astrophys.*, **671**, A25, doi, 2023.

Kiefer, S., D. Gobrecht, L. Decin, Ch. Helling: The effect of thermal non-equilibrium on kinetic nucleation, *Astron. Astrophys.*, **671**, A169, doi, 2023.

Kim, M., T. Mannel, P.D. Boakes, M.S. Bentley, A. Longobardo, H. Jeszenszky, R. Moissl, MIDAS Team: Cometary dust collected by MIDAS on board Rosetta. I. Dust particle catalog and statistics, *Astron. Astrophys.*, **673**, A129, doi, 2023.

Kim, M., T. Mannel, J. Lasue, A. Longobardo, M.S. Bentley, R. Moissl, MIDAS Team: Cometary dust collected by MIDAS on board Rosetta II. Particle shape descriptors and pristineness evaluation, *Astron. Astrophys.*, **677**, A179, doi, 2023.

Kislyakova, K.G., L. Noack, E. Sanchis, L. Fossati, G.G. Valyavin, G.J. Golabek, M. Güdel: Induction heating of planetary interiors in white dwarf systems, *Astron. Astrophys.*, **677**, A109, doi, 2023.

Klein, K.G., H. Spence, O. Alexandrova, M. Argall, L. Arzamasskiy, J. Bookbinder, T. Broeren, D. Caprioli, A. Case, B. Chandran, L.-J. Chen, I. Dors, J. Eastwood, C. Forsyth, A. Galvin, V. Genot, J. Halekas, M. Hesse, B. Hine, T. Horbury, L. Jian, J. Kasper, M. Kretzschmar, M. Kunz, B. Lavraud, O. Le Contel, A. Mallet, B. Maruca, W. Matthaeus, J. Niehof, H. O'Brien, C. Owen, A. Retinò, C. Reynolds, O.W. Roberts, A. Schekochihin, R. Skoug, C. Smith, S. Smith, J. Steinberg, M. Stevens, A. Szabo, J. TenBarge, R. Torbert, B. Vasquez, D. Verscharen, P. Whittlesey, B. Wickizer, G. Zank, E. Zweibel: HelioSwarm: A multipoint, multiscale mission to characterize turbulence, *Space Sci. Rev.*, **219**, 74, doi, 2023.

Koller, F., F. Plaschke, M. Temmer, L. Preisser, O.W. Roberts, Z. Vörös: Magnetosheath jet formation influenced by parameters in solar wind structures, *J. Geophys. Res. Space Phys.*, **128**, e2023JA031339, doi, 2023.

Korovinskiy, D., E.V. Panov, R. Nakamura, S. Kiehas, M. Hosner, D. Schmid, I. Ivanov: Electron magnetohydrodynamics Grad-Shafranov reconstruction of the magnetic reconnection electron diffusion region, *Front. Astron. Space Sci.*, **10**, 1069888, doi, 2023.

Kraus, I., Ph.-A. Bourdin, J. Zender, M. Bergmann, A. Hanslmeier: Coronal bright point statistics. I. Lifetime, shape, and coronal co-rotation, *Astron. Astrophys.*, **678**, A184, doi, 2023.

Krenn, A.F., M. Lendl, J.A. Patel, L. Carone, M. Deleuil, S. Sulis, A. Collier Cameron, A. Deline, P. Guterman, D. Queloz, L. Fossati, A. Brandeker, K. Heng, B. Akinsanmi, V. Adibekyan, A. Bonfanti, O.D.S. Demangeon, D. Kitzmann, S. Salmon, S.G. Sousa, T.G. Wilson, Y. Alibert, R. Alonso, G. Anglada, T. Bárczy, D. Barrado Navascues, S.C.C. Barros, W. Baumjohann, M. Beck, T. Beck, W. Benz, N. Billot, L. Blecha, X. Bonfils, L. Borsato, C. Broeg, J. Cabrera, S. Charnoz, C. Corral van Damme, Sz. Csizmadia, P.E. Cubillos, M.B. Davies, L. Delrez, B.-O. Demory, D. Ehrenreich, A. Erikson, J. Farinato, A. Fortier, M. Fridlund, D. Gandolfi, M. Gillon, M. Güdel, S. Hoyer, K.G. Isaak, L.L. Kiss, E. Kopp, J. Laskar, A. Lecavelier des Etangs, C. Lovis, D. Magrin, P.F.L. Maxted, C. Mordasini, V. Nascimbeni, G. Olofsson, R. Ottensamer, I. Pagano, E. Pallé, G. Peter, G. Piotto, D. Pollacco, R. Ragazzoni, N. Rando, H. Rauer, I. Ribas, N.C. Santos, G. Scandariato, D. Ségransan, A.E. Simon, A.M.S. Smith, M. Steller, Gy.M. Szabó, N. Thomas, S. Udry, B. Ulmer, V. Van Grootel, J. Venturini, N.A. Walton: The geometric albedo of the hot Jupiter HD189733b measured with CHEOPS, *Astron. Astrophys.*, **672**, A24, doi, 2023.

Krtička, J., A. Kawka, Z. Mikulášek, L. Fossati, I. Krtičková, M. Prvák, J. Janík, R. Liptaj, M. Zejda, E. Paunzen: EPIC 206197016: A very hot white dwarf orbited by a strongly irradiated red dwarf, *Astron. Astrophys.*, **674**, A94, doi, 2023.

Laddha, S., W. Macher, G. Kargl, S. Zivithal, J. Blum, B. Gundlach, C. Güttler, H. Sierks, M. Rose: Validation of gas flow experiments for porous media by means of computer simulations, *Meas. Sci. Technol.*, **34**, 045012, doi, 2023.

Lam, K.W.F., J. Cabrera, M.J. Hooton, Y. Alibert, A. Bonfanti, M. Beck, A. Deline, H.-G. Florén, A.E. Simon, L. Fossati, C.M. Persson, M. Fridlund, S. Salmon, S. Hoyer, H.P. Osborn, T.G. Wilson, I.Y. Georgieva, Gr. Nowak, R. Luque, J.A. Egger, V. Abidekyan, R. Alonso, G. Anglada Escudé, T. Bárczy, D. Barrado, S.C.C. Barros, W. Baumjohann, T. Beck, A. Bekkelien, W. Benz, N. Billot, X. Bonfils, A. Brandeker, C. Broeg, S. Charnoz, A. Collier Cameron, Sz. Csizmadia, M.B. Davies, M. Deleuil, L. Delrez, O.D.S. Demangeon, B.-O. Demory, D. Ehrenreich, A. Erikson, A. Fortier, D. Futyan, D. Gandolfi, M. Gillon, M. Guedel, P. Guterman, J. Laskar, D.W. Latham, A. Lecavelier des Etangs, M. Lendl, C. Lovis, K. Heng, K.G. Isaak, L. Kiss, D. Magrin, P.F.L. Maxted, V. Nascimbeni, G. Olofsson, R. Ottensamer, I. Pagano, E. Pallé, G. Peter, G. Piotto, D. Pollacco, D. Queloz, I. Ribas, R. Ragazzoni, N. Rando, H. Rauer, N.C. Santos, G. Scandariato, S. Seager, D. Ségransan, L.M. Serrano, A.M.S. Smith, S.G. Sousa, M. Steller, Gy.M. Szabó, N. Thomas, S. Udry, V. Van Grootel, N.A. Walton, J.N. Winn: Discovery of TOI-1260d and the characterisation of the multi-planet system, *MNRAS*, **519**, 1437-1451, doi, 2023.

Longobardo, A., M. Kim, B. Pestoni, M. Ciarniello, G. Rinaldi, S. Ivanovski, F. Dirri, M. Fulle, V. Della Corte, A. Rotundi, M. Rubin: Main results from the ISSI International Team "Characterization of 67P Cometary Activity", *Universe*, **9**, 446, doi, 2023.

Lotz, S., A.E. Nel, R.T. Wicks, O.W. Roberts, N.E. Engelbrecht, R.D. Strauss, G.J.J. Botha, E.P. Kontar, A. Pitňa, S.D. Bale: The radial variation of the solar wind turbulence spectra near the kinetic break scale from Parker Solar Probe measurements, *Astrophys. J.*, **942**, 93, doi, 2023.

Lou, Y., X. Gu, X. Cao, M. Wu, S. Xiao, G. Wang, B. Ni, T.-L. Zhang: Statistical analysis of lunar 1Hz waves using ARTEMIS observations, *Astrophys. J.*, **943**, 17, doi, 2023.

Lou, Y.Q., X. Cao, M.Y. Wu, B.B. Ni, T.-L. Zhang: Scalings for the Alfvén-cyclotron instability in a bi-kappa plasma, *Earth Planet. Phys.*, **7**, 631-639, doi, 2023.

Louca, A.J., Y. Miguel, D. Kubyshkina: Metallicity and spectral evolution of WASP 39b: The limited role of hydrodynamic escape, *Astrophys. J. Lett.*, **956**, L19, doi, 2023.

Luque, R., H.P. Osborn, A. Leleu, E. Pallé, A. Bonfanti, O. Barragán, T.G. Wilson, C. Broeg, A. Collier Cameron, M. Lendl, P.F.L. Maxted, Y. Alibert, D. Gandolfi, J.-B. Delisle, M.J. Hooton, J.A. Egger, G. Nowak, M. Lafarga, D. Rapetti, J.D. Twicken, J.C. Morales, I. Carleo, J. Orell-Miquel, V. Adibekyan, R. Alonso, A. Alqasim, P.J. Amado, D.R. Anderson, G. Anglada-Escudé, T. Bandy, T. Bárczy, D. Barrado Navascues, S.C.C. Barros, W. Baumjohann, D. Bayliss, J.L. Bean, M. Beck, T. Beck, W. Benz, N. Billot, X. Bonfils, L. Borsato, A.W. Boyle, A. Brandeker, E.M. Bryant, J. Cabrera, S. Carrazco-Gaxiola, D. Charbonneau, S. Charnoz, D.R. Ciardi, W.D. Cochran, K.A. Collins, I.J.M. Crossfield, Sz. Csizmadia, P.E. Cubillos, F. Dai, M.B. Davies, H.J. Deeg, M. Deleuil, A. Deline, L. Delrez, O.D.S. Demangeon, B.-O. Demory, D. Ehrenreich, A. Erikson, E. Esparza-Borges, B. Falk, A. Fortier, L. Fossati, M. Fridlund, A. Fukui, J. Garcia-Mejia, S. Gill, M. Gillon, E. Goffo, Y. Gómez Maqueo Chew, M. Güdel, E.W. Guenther, M.N. Günther, A.P. Hatzes, Ch. Helling, K.M. Hesse, S.B. Howell, S. Hoyer, K. Ikuta, K.G. Isaak, J.M. Jenkins, T. Kagetani, L.L. Kiss, T. Kodama, J. Korth, K.W.F. Lam, J. Laskar, D.W. Latham, A. Lecavelier des Etangs, J.P.D. Leon, J.H. Livingston, D. Magrin, R.A. Matson, E.C. Matthews, C. Mordasini, M. Mori, M. Moyano, M. Munari, F. Murgas, N. Narita, V. Nascimbeni, G. Olofsson, H.L.M. Osborne, R. Ottensamer, I. Pagano, H. Parviainen, G. Peter, G. Piotto, D. Pollacco, D. Queloz, S.N. Quinn, A. Quirrenbach, R. Ragazzoni, N. Rando, F. Ratti, H. Rauer, S. Redfield, I. Ribas, G.R. Ricker, A. Rudat, L. Sabin, S. Salmon, N.C. Santos, G. Scandariato, N. Schanche, J.E. Schlieder, S. Seager, D. Ségransan, A. Shporer, A.E. Simon, A.M.S. Smith, S.G. Sousa, M. Stalport, Gy.M. Szabó, N. Thomas, A. Tuson, S. Udry, A.M. Vanderburg, V. Van

Eylen, V. Van Grootel, J. Venturini, I. Walter, N.A. Walton, N. Watanabe, J.N. Winn, T. Zingales: A resonant sextuplet of sub-Neptunes transiting the bright star HD 110067, *Nature*, **623**, 932-937, doi, 2023.

Marsch, E., Y. Narita: A new route to symmetries through the extended Dirac equation, *Symmetry*, **15**, 492, doi, 2023.

Marsch, E., Y. Narita: Correction to: On isospin and flavour of leptons and quarks, *Eur. Phys. J. Plus*, **138**, 155, doi, 2023.

Meier Valdés, E.A., B.M. Morris, B.-O. Demory, A. Brandeker, D. Kitzmann, W. Benz, A. Deline, H.-G. Florén, S.G. Sousa, V. Bourrier, V. Singh, K. Heng, A. Strugarek, D.J. Bower, N. Jäggi, L. Carone, M. Lendl, K. Jones, A.V. Oza, O.D.S. Demangeon, Y. Alibert, R. Alonso, G. Anglada, J. Asquier, T. Bárczy, D. Barrado Navascues, S.C.C. Barros, W. Baumjohann, M. Beck, T. Beck, N. Billot, X. Bonfils, L. Borsato, C. Broeg, J. Cabrera, S. Charnoz, A. Collier Cameron, Sz. Csizmadia, P.E. Cubillos, M.B. Davies, M. Deleuil, L. Delrez, D. Ehrenreich, A. Erikson, A. Fortier, L. Fossati, M. Fridlund, D. Gandolfi, M. Gillon, M. Güdel, M.N. Günther, S. Hoyer, K.G. Isaak, L.L. Kiss, J. Laskar, A. Lecavelier des Etangs, C. Lovis, D. Magrin, P.F.L. Maxted, C. Mordasini, V. Nascimbeni, G. Olofsson, R. Ottensamer, I. Pagano, E. Pallé, G. Peter, G. Piotto, D. Pollacco, D. Queloz, R. Ragazzoni, N. Rando, H. Rauer, I. Ribas, N.C. Santos, M. Sarajlic, G. Scandariato, D. Ségransan, D. Sicilia, A.E. Simon, A.M.S. Smith, M. Steller, Gy.M. Szabó, N. Thomas, S. Udry, B. Ulmer, V. Van Grootel, J. Venturini, N.A. Walton, T.G. Wilson, D. Wolter: Investigating the visible phase-curve variability of 55 Cnc e, *Astron. Astrophys.*, **677**, A112, doi, 2023.

Milillo, A., M. Sarantos, C. Grava, D. Janches, H. Lammer, F. Leblanc, N. Schorghofer, P. Wurz, B.D. Teolis, G. Murakami: Future directions for the investigation of surface-bounded exospheres in the inner solar system, *Space Sci. Rev.*, **219**, 49, doi, 2023.

Mühlich, N.S., H. Jeszenszky, J. Fries, G. Fremuth, J. Gerger, F. Plesescu, M. Steller, B. Seifert, R. Nakamura, F. Cipriani: Development and coupling test of Active Spacecraft Potential Control - Next Generation (ASPOC-NG), *Adv. Space Res.*, **71**, 1711-1720, doi, 2023.

Nagai, T., I. Shinohara, Y. Saito, A. Ieda, R. Nakamura: Location and timing of magnetic reconnections in Earth's magnetotail: Accomplishments of the 29-year Geotail near-Earth magnetotail survey, *J. Geophys. Res. Space Phys.*, **128**, e2023JA032023, doi, 2023.

Nakamura, T.K.M., W.-L. Teh, S. Zenitani, T. Umeda, M. Oka, H. Hasegawa, A.M. Veronig, R. Nakamura: Spatial and time scaling of coalescing multiple magnetic islands, *Phys. Plasmas*, **30**, 022902, doi, 2023.

Naponiello, L., L. Mancini, A. Sozzetti, A.S. Bonomo, A. Morbidelli, J. Dou, L. Zeng, Z.M. Leinhardt, K. Biazzo, P.E. Cubillos, M. Pinamonti, D. Locci, A. Maggio, M. Damasso, A.F. Lanza, J.J. Lissauer, K.A. Collins, P.J. Carter, E.L.N. Jensen, A. Bignamini, W. Boschin, L.G. Bouma, D.R. Ciardi, R. Cosentino, I. Crossfield, S. Desidera, X. Dumusque, A.F.M. Fiorenzano, A. Fukui, P. Giacobbe, C.L. Gnilka, A. Ghedina, G. Guilluy, A. Harutyunyan, S.B. Howell, J.M. Jenkins, M.B. Lund, J.F. Kielkopf, K.V. Lester, L. Malavolta, A.W. Mann, R.A. Matson, E.C. Matthews, D. Nardiello, N. Narita, E. Pace, I. Pagano, E. Palle, M. Pedani, S. Seager, J.E. Schlieder, R.P. Schwarz, A. Shporer, J.D. Twicken, J.N. Winn, C. Ziegler, T. Zingales: A super-massive Neptune-sized planet, *Nature*, **622**, 255-260, doi, 2023; Author Correction: *Nature*, **623**, E6, doi , 2023.

Narita, Y., S. Toepfer, D. Schmid: Magnetopause as conformal mapping, *Ann. Geophys.*, **41**, 87-91, doi, 2023.

Nascimbeni, V., L. Borsato, T. Zingales, G. Piotto, I. Pagano, M. Beck, C. Broeg, D. Ehrenreich, S. Hoyer, F.Z. Majidi, V. Granata, S.G. Sousa, T.G. Wilson, V. Van Grootel, A. Bonfanti, S. Salmon, A.J. Mustill, L. Delrez, Y. Alibert, R. Alonso, G. Anglada, T. Barczy, D. Barrado, S.C.C. Barros, W. Baumjohann, T. Beck, W. Benz, M. Bergomi, N. Billot, X. Bonfils, A. Brandeker, J. Cabrera, S. Charnoz, A. Collier Cameron, Sz. Csizmadia, P.E. Cubillos, M.B. Davies, M. Deleuil, A. Deline, O.D.S. Demangeon, B.-O. Demory, A. Erikson, A. Fortier, L. Fossati, M. Fridlund, D. Gandolfi, M. Gillon, M. Gudel, K.G. Isaak, L.L. Kiss, J. Laskar, A. Lecavelier des Etangs, M. Lendl, C. Lovis, R. Luque, D. Magrin, P.F.L. Maxted, C. Mordasini, G. Olofsson, R. Ottensamer, E. Palle, G. Peter, D. Piazza, D. Pollacco, D. Queloz, R. Ragazzoni, N. Rando, F. Ratti, H. Rauer, I. Ribas, N.C. Santos, G. Scandariato, D. Segransan, A.E. Simon, A.M.S. Smith, M. Steinberger, M. Steller, Gy.M. Szabo, N. Thomas, S. Udry, J. Venturini, N.A. Walton, D. Wolter: A new dynamical modeling of the WASP-47 system with CHEOPS observations, *Astron. Astrophys.*, **673**, A42, doi, 2023.

Nikolaou, N., I.P. Waldmann, A. Tsiaras, M. Morvan, B. Edwards, K.H. Yip, A. Thompson, G. Tinetti, S. Sarkar, J.M. Dawson, V. Borisov, G. Kasneci, M. Petkovic, T. Stepisnik, T. Al-Ubaidi, R.L. Bailey, M. Granitzer, S. Julka, R. Kern, P. Ofner, S. Wagner, L. Heppe, M. Bunse, K. Morik, L.F. Simoes: Lessons learned from the 1st Ariel Machine Learning Challenge: Correcting transiting exoplanet light curves for stellar spots, *RASTI*, **2**, 695–709, doi, 2023.

Osborn, H.P., G. Nowak, G. Hébrard, T. Masseron, J. Lillo-Box, E. Pallé, A. Bekkelien, H.-G. Florén, P. Guterman, A.E. Simon, V. Adibekyan, A. Bieryla, L. Borsato, A. Brandeker, D.R. Ciardi, A. Collier Cameron, K.A. Collins, J.A. Egger, D. Gandolfi, M.J. Hooton, D.W. Latham, M. Lendl, E.C. Matthews, A. Tuson, S. Ulmer-Moll, A. Vanderburg, T.G. Wilson, C. Ziegler, Y. Alibert, R. Alonso, G. Anglada, L. Arnold, J. Asquier, D. Barrado y. Navascues, W. Baumjohann, T. Beck, A.A. Belinski, W. Benz, F. Biondi, I. Boisse, X. Bonfils, C. Broeg, L.A. Buchhave, T. Bárczy, S.C.C. Barros, J. Cabrera, C. Cardona Guillen, I. Carleo, A. Castro-González, S. Charnoz, J. Christiansen, P. Cortes-Zuleta, S. Csizmadia, S. Dalal, M.B. Davies, M. Deleuil, X. Delfosse, L. Delrez, B.-O. Demory, A.B. Dunlavey, D. Ehrenreich, A. Erikson, R.B. Fernandes, A. Fortier, T. Forveille, L. Fossati, M. Fridlund, M. Gillon, R.F. Goeke, M.V. Goliguzova, E.J. Gonzales, M.N. Günther, M. Güdel, N. Heidari, C.E. Henze, S. Howell, S. Hoyer, J.I. Frey, K.G. Isaak, J.M. Jenkins, F. Kiefer, L. Kiss, J. Korth, P.F.L. Maxted, J. Laskar, A. Lecavelier des Etangs, C. Lovis, M.B. Lund, R. Luque, D. Magrin, J.M. Almenara, E. Martioli, M. Mecina, J.V. Medina, D. Moldovan, M. Morales-Calderón, G. Morello, C. Moutou, F. Murgas, E.L.N. Jensen, V. Nascimbeni, G.

Olofsson, R. Ottensamer, I. Pagano, G. Peter, G. Piotto, D. Pollacco, D. Queloz, R. Ragazzoni, N. Rando, H. Rauer, I. Ribas, G. Ricker, O.D.S. Demangeon, A.M.S. Smith, N. Santos, G. Scandariato, S. Seager, S.G. Sousa, M. Steller, G.M. Szabó, D. Ségransan, N. Thomas, S. Udry, B. Ulmer, V. Van Grootel, R. Vanderspek, N. Walton, J.N. Winn: Two warm Neptunes transiting HIP 9618 revealed by TESS and Cheops, *MNRAS*, **523**, 3069–3089, doi, 2023.

Palmroth, M., T.I. Pulkkinen, U. Ganse, Y. Pfau-Kempf, T. Koskela, I. Zaitsev, M. Alho, G. Cozzani, L. Turc, M. Battarbee, M. Dubart, H. George, E. Gordeev, M. Grandin, K. Horaites, A. Osmane, K. Papadakis, J. Suni, V. Tarvus, H. Zhou, R. Nakamura: Magnetotail plasma eruptions driven by magnetic reconnection and kinetic instabilities, *Nat. Geosci.*, **16**, 570-576, doi, 2023.

Patel, J.A., J.A. Egger, T.G. Wilson, V. Bourrier, L. Carone, M. Beck, D. Ehrenreich, S.G. Sousa, W. Benz, A. Brandeker, A. Deline, Y. Alibert, K.W.F. Lam, M. Lendl, R. Alonso, G. Anglada, T. Bárczy, D. Barrado, S.C.C. Barros, W. Baumjohann, T. Beck, N. Billot, X. Bonfils, C. Broeg, M.-D. Busch, J. Cabrera, S. Charnoz, A. Collier Cameron, Sz. Csizmadia, M.B. Davies, M. Deleuil, L. Delrez, O.D.S. Demangeon, B.-O. Demory, A. Erikson, A. Fortier, L. Fossati, M. Fridlund, D. Gandolfi, M. Gillon, M. Güdel, K. Heng, S. Hoyer, K.G. Isaak, L.L. Kiss, E. Kopp, J. Laskar, A. Lecavelier des Etangs, C. Lovis, D. Magrin, P.F.L. Maxted, V. Nascimbeni, G. Olofsson, R. Ottensamer, I. Pagano, E. Pallé, G. Peter, G. Piotto, D. Pollacco, D. Queloz, R. Ragazzoni, N. Rando, F. Ratti, H. Rauer, I. Ribas, N.C. Santos, G. Scandariato, D. Ségransan, A.E. Simon, A.M.S. Smith, M. Steller, Gy.M. Szabó, N. Thomas, S. Udry, B. Ulmer, V. Van Grootel, V. Viotto, N.A. Walton: CHEOPS and TESS view of the ultra-short-period super-Earth TOI-561 b, *Astron. Astrophys.*, **679**, A92, doi, 2023.

Perotti, G., V. Christiaens, Th. Henning, B. Tabone, L.B.F.M. Waters, I. Kamp, G. Olofsson, S.L. Grant, D. Gasman, J. Bouwman, M. Samland, R. Franceschi, E.F. van Dishoeck, K. Schwarz, M. Güdel, P.-O. Lagage, T.P. Ray, B. Vandenbussche, A. Abergel, O. Absil, A.M. Arabhavi, I. Argyriou, D. Barrado, A. Boccaletti, A. Caratti o. Garatti, V. Geers, A.M. Glauser, K. Justannont, F. Lahuis, M. Mueller, C. Nehmé, E. Pantin, S. Scheithauer, C. Waelkens, R. Guadarrama, H. Jang, J. Kanwar, M. Morales-Calderón, N. Pawellek, D. Rodgers-Lee, J. Schreiber, L. Colina, T.R. Greve, G. Östlin, G. Wright: Water in the terrestrial planet-forming zone of the PDS 70 disk, *Nature*, **620**, 516-520, doi, 2023.

Perrone, D., A. Settino, R. De Marco, R. D'Amicis, S. Perri: Ion kinetic effects linked to magnetic field discontinuities in the slow Alfvénic wind observed by Solar Orbiter in the inner heliosphere, *Front. Astron. Space Sci.*, **10**, 1250219, doi, 2023.

Piaulet, C., B. Benneke, J.M. Almenara, D. Dragomir, H.A. Knutson, D. Thorngren, M.S. Peterson, I.J.M. Crossfield, E.M.-R. Kempton, D. Kubyshkina, A.W. Howard, R. Angus, H. Isaacson, L.M. Weiss, C.A. Beichman, J.J. Fortney, L. Fossati, H. Lammer, P.R. McCullough, C.V. Morley, I. Wong: Evidence for the volatile-rich composition of a 1.5-Earth-radius planet, *Nat. Astron.*, **7**, 206–222, doi, 2023.

Psaridi, A., F. Bouchy, M. Lendl, B. Akinsanmi, K.G. Stassun, B. Smalley, D.J. Armstrong, S. Howard, S. Ulmer-Moll, N. Grieves, K. Barkaoui, J.E. Rodriguez, E.M. Bryant, O. Suárez, T. Guillot, P. Evans, O. Attia, R.A. Wittenmyer, S.W. Yee, K.A. Collins, G. Zhou, F. Galland, L. Parc, S. Udry, P. Figueira, C. Ziegler, C. Mordasini, J.N. Winn, S. Seager, J.M. Jenkins, J.D. Twicken, R. Brahm, M.I. Jones, L. Abe, B. Addison, C. Briceño, J.T. Briegal, K.I. Collins, T. Daylan, P. Eigmüller, G. Furesz, N.M. Guerrero, J. Hagelberg, A. Heitzmann, R. Hounsell, C.X. Huang, A. Krenn, N.M. Law, A.W. Mann, J. McCormac, D. Mékarnia, D. Mounzer, L.D. Nielsen, A. Osborn, Y. Reinarz, R.R. Sefako, M. Steiner, P.A. Strøm, A.H.M.J. Triaud, R. Vanderspek, L. Vanzi, J.I. Vines, C.A. Watson, D.J. Wright, A. Zapata: Three Saturn-mass planets transiting F-type stars revealed with TESS and HARPS. TOI-615b, TOI-622b, and TOI-2641b, *Astron. Astrophys.*, **675**, A39, doi, 2023.

Rackham, B.V., N. Espinoza, S.V. Berdyugina, H. Korhonen, R.J. MacDonald, B.T. Montet, B.M. Morris, M. Oshagh, A.I. Shapiro, Y.C. Unruh, E.V. Quintana, R.T. Zellem, D. Apai, T. Barclay, J.K. Barstow, G. Bruno, L. Carone, S.L. Casewell, H.M. Cegla, S. Criscuoli, C. Fischer, D. Fournier, M.S. Giampapa, H. Giles, A. Iyer, G. Kopp, N.M. Kostogryz, N. Krivova, M. Mallonn, C. McGruder, K. Molaverdikhani, E.R. Newton, M. Panja, S. Peacock, K. Reardon, R.M. Roettenbacher, G. Scandariato, S. Solanki, K.G. Stassun, O. Steiner, K.B. Stevenson, J. Tregloan-Reed, A. Valio, S. Wedemeyer, L. Welbanks, J. Yu, M.K. Alam, J.R.A. Davenport, D. Deming, C. Dong, E. Ducrot, C. Fisher, E. Gilbert, V. Kostov, M. López-Morales, M. Line, T. Močnik, S. Mullally, R.R. Paudel, I. Ribas, J.A. Valenti: The effect of stellar contamination on low-resolution transmission spectroscopy: Needs identified by NASA's Exoplanet Exploration Program Study Analysis Group 21, *RASTI*, **2**, 148–206, doi, 2023.

Regály, Zs., K. Kadam, D. Tarczay-Nehéz: Planetary nurseries: Vortices formed at smooth viscosity transition, *MNRAS*, **521**, 396-410, doi, 2023.

Reiss, M.A., K. Muglach, R. Mullinix, M.M. Kuznetsova, C. Wiegand, M. Temmer, C.N. Arge, S. Dasso, S.F. Fung, J.J. Gonzalez-Aviles, S. Gonzi, L. Jian, P. MacNeice, C. Möstl, M. Owens, B. Perri, R.F. Pinto, L. Lastätter, P. Riley, E. Samara, ISWAT H1-01 Team: Unifying the validation of ambient solar wind models, *Adv. Space Res.*, **72**, 5275–5286, doi, 2023.

Rensen, F., Y. Miguel, M. Zilinskas, A. Louca, P. Woitke, Ch. Helling, O. Herbort: The deep atmospheric composition of Jupiter from thermochemical calculations based on Galileo and Juno data, *Remote Sens.*, **15**, 841, doi, 2023.

Roberts, O.W., Y. Narita, R. Nakamura, Z. Vörös: Spectral break of the density power spectrum in solar wind turbulence, *Astron. Astrophys.*, **677**, L16, doi, 2023.

Roberts, O.W., Z. Vörös, K. Torkar, J. Stawarz, R. Bandyopadhyay, D.J. Gershman, Y. Narita, R. Kieokaew, B. Lavraud, K. Klein, Y. Yang, R. Nakamura, A. Chasapis, W.H. Matthaeus: Estimation of the error in the calculation of the pressure-strain term: Application in the terrestrial magnetosphere, *J. Geophys. Res. Space Phys.*, **128**, e2023JA031565, doi, 2023.

Rocha, W.R.M., P. Woitke, S. Pilling, W.-F. Thi, J.K. Jørgensen, L.E. Kristensen, G. Perotti, I. Kamp: Simulation of CH_3OH ice UV photolysis under laboratory conditions, *Astron. Astrophys.*, **673**, A70, doi, 2023.

Rodgers-Lee, D., P.B. Rimmer, A.A. Vidotto, A.J. Louca, A.M. Taylor, A.L. Mesquita, Y. Miguel, O. Venot, Ch. Helling, P. Barth, E. Lacy: The energetic particle environment of a GJ 436 b-like planet, *MNRAS*, **521**, 5880–5891, doi, 2023.

Rojas Mata, S., G. Stenberg Wieser, Y. Futaana, T.-L. Zhang: Proton plasma asymmetries between Venus' quasi-perpendicular and quasi-parallel magnetosheaths, *J. Geophys. Res. Space Phys.*, **128**, e2022JA031149, doi, 2023.

Rumenskikh, M.S.; M.L. Khodachenko, I.F. Shaikhislamov, I.B. Miroshnichenko, A.G. Berezutsky, A.V. Shepelin, N.K. Dwivedi: Mysterious non-detection of He I (2^3S) transit absorption of GJ 436b, *MNRAS*, **526**, 4120–4129, doi, 2023.

Rustamkulov, Z., D.K. Sing, S. Mukherjee, E.M. May, J. Kirk, E. Schlawin, M.R. Line, C. Piaulet, A.L. Carter, N.E. Batalha, J.M. Goyal, M. López-Morales, J.D. Lothringer, R.J. MacDonald, S.E. Moran, K.B. Stevenson, H.R. Wakeford, N. Espinoza, J.L. Bean, N.M. Batalha, B. Benneke, Z.K. Berta-Thompson, I.J.M. Crossfield, P. Gao, L. Kreidberg, D.K. Powell, P.E. Cubillos, N.P. Gibson, J. Leconte, K. Molaverdikhani, N.K. Nikolov, V. Parmentier, P. Roy, J. Taylor, J.D. Turner, P.J. Wheatley, K. Aggarwal, E. Ahrer, M.K. Alam, L. Alderson, N.H. Allen, A. Banerjee, S. Barat, D. Barrado, J.K. Barstow, T.J. Bell, J. Blecic, J. Brande, S. Casewell, Q. Changeat, K.L. Chubb, N. Crouzet, T. Daylan, L. Decin, J. Désert, T. Mikal-Evans, A.D. Feinstein, L. Flagg, J.J. Fortney, J. Harrington, K. Heng, Y. Hong, R. Hu, N. Iro, T. Kataria, E.M.-R. Kempton, J. Krick, M. Lendl, J. Lillo-Box, A. Louca, J. Lustig-Yaeger, L. Mancini, M. Mansfield, N.J. Mayne, Y. Miguel, G. Morello, K. Ohno, E. Palle, D.J.M. Petit dit de la Roche, B.V. Rackham, M. Radica, L. Ramos-Rosado, S. Redfield, L.K. Rogers, E.L. Shkolnik, J. Southworth, J. Teske, P. Tremblin, G.S. Tucker, O. Venot, W.C. Waalkes, L. Welbanks, X. Zhang, S. Zieba: Early release science of the exoplanet WASP-39b with JWST NIRSpec PRISM, *Nature*, **614**, 659-663, doi, 2023.

Sainsbury-Martinez, F., P. Tremblin, A.D. Schneider, L. Carone, I. Baraffe, G. Chabrier, Ch. Helling, L. Decin, U.G. Jørgensen: Evidence of radius inflation in radiative GCM models of WASP-76b due to the advection of potential temperature, *MNRAS*, **524**, 1316-1325, doi, 2023.

Salvador, A., G. Avice, D. Breuer, C. Gillmann, H. Lammer, E. Marcq, S.N. Raymond, H. Sakuraba, M. Scherf, M.J. Way: Magma ocean, water, and the early atmosphere of Venus, *Space Sci. Rev.*, **219**, 51, doi, 2023.

Samra, D., Ch. Helling, K.L. Chubb, M. Min, L. Carone, A.D. Schneider: Clouds form on the hot Saturn JWST ERO target WASP-96b, *Astron. Astrophys.*, **669**, A142, doi, 2023.

Sánchez-Cano, B., O. Witasse, E.W. Knutsen, D. Meggi, S. Viet, M. Lester, R.F. Wimmer-Schweingruber, M. Pinto, R. Moissl, J. Benkhoff, H. Opgenoorth, U. Auster, J. de Brujine, P. Collins, G. De Marchi, D. Fischer, Y. Futaana, J. Godfrey, D. Heyner, M. Holmstrom, A. Johnstone, S. Joyce, D. Lakey, S. Martinez, D. Milligan, E. Montagnon, D. Müller, S.A. Livi, T. Prusti, J. Raines, I. Richter, D. Schmid, P. Schmitz, H. Svedhem, M.G.G.T. Taylor, E. Tremolizzo, D. Titov, C. Wilson, S. Wood, J. Zender: Solar energetic particle events detected in the housekeeping data of the European Space Agency's spacecraft flotilla in the solar system, *Space Weather*, **21**, e2023SW003540, doi, 2023.

Sartori, L.F., C. Lovis, J.-B. Delisle, M. Lendl, G. Cugno, A. Boehle, F. Dannert, A. Krenn, J.L. Gubler, S.P. Quanz: L 363-38 b: A planet newly discovered with ESPRESSO orbiting a nearby M dwarf star, *Astron. Astrophys.*, **670**, A42, doi, 2023.

Schmid, D., Y. Narita: Magnetohydrodynamic shocks revisited: Magnetically constraining the upstream solar wind condition, *Astrophys. J.*, **955**, 58, doi, 2023.

Sebastian, D., M.I. Swayne, P.F.L. Maxted, A.H.M.J. Triaud, S.G. Sousa, G. Olofsson, M. Beck, N. Billot, S. Hoyer, S. Gill, N. Heidari, D.V. Martin, C.M. Persson, M.R. Standing, Y. Alibert, R. Alonso, G. Anglada, J. Asquier, T. Bárczy, D. Barrado, S.C.C. Barros, M.P. Battley, W. Baumjohann, T. Beck, W. Benz, M. Bergomi, I. Boisse, X. Bonfils, A. Brandeker, C. Broeg, J. Cabrera, S. Charnoz, A. Collier Cameron, Sz. Csizmadia, M.B. Davies, M. Deleuil, L. Delrez, O.D.S. Demangeon, B.-O. Demory, G. Dransfield, D. Ehrenreich, A. Erikson, A. Fortier, L. Fossati, M. Fridlund, D. Gandolfi, M. Gillon, M. Güdel, J. Hasiba, G. Hébrard, K. Heng, K.G. Isaak, L.L. Kiss, E. Kopp, V. Kunovac, J. Laskar, A. Lecavelier des Etangs, M. Lendl, C. Lovis, D. Magrin, J. McCormac, N.J. Miller, V. Nascimbeni, R. Ottensamer, I. Pagano, E. Pallé, F.A. Pepe, G. Peter, G. Piotto, D. Pollacco, D. Queloz, R. Ragazzoni, N. Rando, H. Rauer, I. Ribas, S. Lalitha, A. Santerne, N.C. Santos, G. Scandariato, D. Ségransan, A.E. Simon, A.M.S. Smith, M. Steller, Gy.M. Szabó, N. Thomas, S. Udry, V. Van Grootel, N.A. Walton: The EBLM project - IX. Five fully convective M-dwarfs, precisely measured with CHEOPS and TESS light curves, *MNRAS*, **519**, 3546–3563, doi, 2023.

Signoles, C., M. Persson, Y. Futaana, S. Aizawa, N. André, S. Bergman, A. Fedorov, V. Lindwall, N. Martinez, C. Mazelle, S. Rojas Mata, A. Wolff, T.-L. Zhang: Influence of solar wind variations on the shapes of Venus' plasma boundaries based on Venus Express observations, *Astrophys. J.*, **954**, 95, doi, 2023.

Simon Wedlund, C., M. Volwerk, C. Mazelle, S. Rojas Mata, G. Stenberg Wieser, Y. Futaana, J. Halekas, D. Rojas-Castillo, C. Bertucci, J. Espley: Statistical distribution of mirror-mode-like structures in the magnetosheaths of unmagnetised planets - Part 1: Mars as observed by the MAVEN spacecraft, *Ann. Geophys.*, **41**, 225-251, doi, 2023.

Sindel, J.P., Ch. Helling, D. Gobrecht, K.L. Chubb, L. Decin: Infrared spectra of TiO_2 clusters for hot Jupiter atmospheres, *Astron. Astrophys.*, **680**, A65, doi, 2023.

Sreejith, A.G., K. France, L. Fossati, T.T. Koskinen, A. Egan, P. Wilson Cauley, P.E. Cubillos, S. Ambily, C. Huang, P. Lavvas, B.T. Fleming, J.-M. Desert, N. Nell, P. Petit, A. Vidotto: CUTE reveals escaping metals in the upper atmosphere of the ultrahot Jupiter WASP-189b, *Astrophys. J. Lett.*, **954**, L23, doi, 2023.

Sreejith, A.G., L. Fossati, P.E. Cubillos, S. Ambily, B. Fleming, K. France: The Colorado Ultraviolet Transit Experiment (CUTE) signal to noise calculator, *Astrophys. Space Sci.*, **368**, 31, doi, 2023.

Sreejith, A.G., L. Fossati, P.E. Cubillos, S. Ambily, K. France: Impact of Mg II interstellar medium absorption on near-ultraviolet exoplanet transit measurements, *MNRAS*, **519**, 2101-2118, doi, 2023.

Steinmeyer, M.-L., P. Woitke, A. Johansen: Sublimation of refractory minerals in the gas envelopes of accreting rocky planets, *Astron. Astrophys.*, **677**, A181, doi, 2023.

Su, Z., Y. Wang, T.-L. Zhang, Z. Wu, L. Cheng, Z. Zou, C. Shen, J. Guo, S. Xiao, G. Wang, Z. Pan, K. Liu, X. Hao, Y. Li, M. Chen, Y. Chi, M. Xu: Unusual Martian foreshock waves triggered by a solar wind stream interaction region, *Astrophys. J. Lett.*, **947**, L33, doi, 2023.

Sulis, S., M. Lendl, H.M. Cegla, L.F. Rodríguez Díaz, L. Bigot, V. Van Grootel, A. Bekkelien, A. Collier Cameron, P.F.L. Maxted, A.E. Simon, C. Lovis, G. Scandariato, G. Bruno, D. Nardiello, A. Bonfanti, M. Fridlund, C.M. Persson, S. Salmon, S.G. Sousa, T.G. Wilson, A. Krenn, S. Hoyer, A. Santerne, D. Ehrenreich, Y. Alibert, R. Alonso, G. Anglada, T. Bárczy, D. Barrado y. Navascues, S.C.C. Barros, W. Baumjohann, M. Beck, T. Beck, W. Benz, N. Billot, X. Bonfils, L. Borsato, A. Brandeker, C. Broeg, J. Cabrera, S. Charnoz, C. Corral van Damme, Sz. Csizmadia, M.B. Davies, M. Deleuil, A. Deline, L. Delrez, O.D.S. Demangeon, B.-O. Demory, A. Erikson, A. Fortier, L. Fossati, D. Gandolfi, M. Gillon, M. Güdel, K. Heng, K.G. Isaak, L.L. Kiss, J. Laskar, A. Lecavelier des Etangs, D. Magrin, M. Munari, V. Nascimbeni, G. Olofsson, R. Ottensamer, I. Pagano, E. Pallé, G. Peter, G. Piotto, D. Pollacco, D. Queloz, R. Ragazzoni, N. Rando, H. Rauer, I. Ribas, M. Rieder, N.C. Santos, D. Ségransan, A.M.S. Smith, M. Steinberger, M. Steller, Gy.M. Szabó, N. Thomas, S. Udry, N.A. Walton, D. Wolter: Connecting photometric and spectroscopic granulation signals with CHEOPS and ESPRESSO, *Astron. Astrophys.*, **670**, A24, doi, 2023.

Tabone, B., G. Bettoni, E.F. van Dishoeck, A.M. Arabhavi, S.L. Grant, D. Gasman, T. Henning, I. Kamp, M. Güdel, P.-O. Lagage, T.P. Ray, B. Vandenbussche, A. Abergel, O. Absil, I. Argyriou, D. Barrado, A. Boccaletti, J. Bouwman, A. Caratti o. Garatti, V. Geers, A.M. Glauser, K. Justannont, F. Lahuis, M. Mueller, C. Nehmé, G. Olofsson, E. Pantin, S. Scheithauer, C. Waelkens, L.B.F.M. Waters, J.H. Black, V. Christiaens, R. Guadarrama, M. Morales-Calderón, H. Jang, J. Kanwar, N. Pawellek, G. Perotti, A. Perrin, D. Rodgers-Lee, M. Samland, J. Schreiber, K.R. Schwarz, L. Colina, G. Östlin, G. Wright: A rich hydrocarbon chemistry and high C to O ratio in the inner disk around a very low-mass star, *Nat. Astron.*, **7**, 805-813, doi, 2023.

Taubner, S.-R., L.M.F. Baumann, M. Steiner, K. Pfeifer, B. Reischl, K. Korynt, T. Bauersachs, B. Mähnert, E.L. Clifford, J. Peckmann, B. Schuster, D. Birgel, S.K.-M.R. Rittmann: Lipidomics and comparative metabolite excretion analysis of methanogenic archaea reveal organism-specific adaptations to varying temperatures and substrate concentrations, *MSYSTEMS*, **8**, e01159-22, doi, 2023.

Teh, W.-L., T.K.M. Nakamura, S. Zenitani, T. Umeda, R. Nakamura: New aspects of energy conversion in magnetic island dynamics: Particle-in-cell simulation of multiple island coalescence and MMS observations, *Astrophys. J.*, **947**, 4, doi, 2023.

Tello Fallau, A., C. Goetz, C. Simon Wedlund, M. Volwerk, A. Moeslinger: Revisiting mirror modes in the plasma environment of comet 67P/Churyumov-Gerasimenko, *Ann. Geophys.*, **41**, 569-587, doi, 2023.

Teubenbacher, D., O.W. Roberts, R. Nakamura, Y. Narita, Z. Vörös, K. Torkar, P.-A. Lindqvist, R.E. Ergun: Density derivation using controlled spacecraft potential in Earth's magnetosheath and multi-scale fluctuation analysis, *J. Geophys. Res. Space Phys.*, **128**, e2022JA031041, doi, 2023.

Tong, Y., B. Zhou, L. Li, B. Cheng, Y. Zhang, W. Magnes, R. Lammegger, A. Pollinger, Y. Yang, Z. Zeren, X. Shen: In orbit calibration of the non-orthogonality of the two fluxgate sensors onboard CSES, *Earth Planets Space*, **75**, 21, doi, 2023.

Torkar, K., R. Nakamura, O.W. Roberts, H. Jeszenszky, P.-A. Lindqvist, Y. Khotyaintsev, B.L. Giles, A.C. Barrie: Active Spacecraft Potential Control in the MMS mission: Results from six years in orbit, *IEEE Trans. Plasma Sci.*, **51**, 2461-2467, doi, 2023.

Totorica, S.R., S. Zenitani, S. Matsukiyo, M. Machida, K. Sekiguchi, A. Bhattacharjee: Exact calculation of nonideal fields demonstrates their dominance of injection in relativistic reconnection, *Astrophys. J. Lett.*, **952**, L1, doi, 2023.

Trotta, D., O. Pezzi, D. Burgess, L. Preisser, X. Blanco-Cano, P. Kajdic, H. Hietala, T.S. Horbury, R. Vainio, N. Dresing, A. Retino, M.F. Marcucci, L. Sorriso-Valvo, S. Servidio, F. Valentini: Three-dimensional modelling of the shock-turbulence interaction, *MNRAS*, **525**, 1856-1866, doi, 2023.

Tsai, S.-M., E.K.H. Lee, D. Powell, P. Gao, X. Zhang, J. Moses, E. Hébrard, O. Venot, V. Parmentier, S. Jordan, R. Hu, M.K. Alam, L. Alderson, N.M. Batalha, J.L. Bean, B. Benneke, C.J. Bierson, R.P. Brady, L. Carone, A.L. Carter, K.L. Chubb, J. Inglis, J. Leconte, M. Line, M. López-Morales, Y. Miguel, K. Molaverdikhani, Z. Rustamkulov, D.K. Sing, K.B. Stevenson, H.R. Wakeford, J. Yang, K. Aggarwal, R. Baeyens, S. Barat, M. de Val-Borro, T. Daylan, J.J. Fortney, K. France, J.M. Goyal, D. Grant, J. Kirk, L. Kreidberg, A. Louca, S.E. Moran, S. Mukherjee, E. Nasedkin, K. Ohno, B.V. Rackham, S. Redfield, J. Taylor, P. Tremblin, C. Visscher, N.L. Wallack, L. Welbanks, A. Youngblood, E.-M. Ahrer, N.E. Batalha, P. Behr, Z.K. Berta-Thompson, J. Blecic, S.L. Casewell, I.J.M. Crossfield, N. Crouzet, P.E. Cubillos, L. Decin, J.-M. Désert, A.D. Feinstein, N.P. Gibson, J. Harrington, K. Heng, T. Henning, E.M.-R. Kempton, J. Krick, P.-O. Lagage, M. Lendl, J.D. Lothringer, M. Mansfield, N.J. Mayne, T. Mikal-Evans, E. Palle, E. Schlawin, O. Shorttle, P.J. Wheatley, S.N. Yurchenko: Photochemically produced SO_2 in the atmosphere of WASP-39b, *Nature*, **617**, 483–487, doi, 2023.

Turc, L., O.W. Roberts, D. Verscharen, A.P. Dimmock, P. Kajdič, M. Palmroth, Y. Pfau-Kempf, A. Johlander, M. Dubart, E.K.J. Kilpua, J. Soucek, K. Takahashi, N.

Takahashi, M. Battarbee, U. Ganse: Transmission of foreshock waves through Earth's bow shock, *Nat. Phys.*, **19**, 78–86, doi, 2023.

Tuson, A., D. Queloz, H.P. Osborn, T.G. Wilson, M.J. Hooton, M. Beck, M. Lendl, G. Olofsson, A. Fortier, A. Bonfanti, A. Brandeker, L.A. Buchhave, A. Collier Cameron, D.R. Ciardi, K.A. Collins, D. Gandolfi, Z. Garai, S. Giacalone, J. Gomes da Silva, S.B. Howell, J.A. Patel, C.M. Persson, L.M. Serrano, S.G. Sousa, S. Ulmer-Moll, A. Vanderburg, C. Ziegler, Y. Alibert, R. Alonso, G. Anglada, T. Braczy, D. Barrado Navascues, S.C.C. Barros, W. Baumjohann, T. Beck, W. Benz, N. Billot, X. Bonfils, L. Borsato, C. Broeg, J. Cabrera, S. Charnoz, D.M. Conti, Sz. Csizmadia, P.E. Cubillos, M.B. Davies, M. Deleuil, L. Delrez, O.D.S. Demangeon, B.-O. Demory, D. Dragomir, C.D. Dressing, D. Ehrenreich, A. Erikson, Z. Essack, J. Farinato, L. Fossati, M. Fridlund, E. Furlan, H. Gill, M. Gillon, C.L. Gnilka, E. Gonzales, M. Güdel, M.N. Günther, S. Hoyer, K.G. Isaak, J.M. Jenkins, L.L. Kiss, J. Laskar, D.W. Latham, N. Law, A. Lecavelier des Etangs, G. Lo Curto, C. Lovis, R. Luque, D. Magrin, A.W. Mann, P.F.L. Maxted, M. Mayor, S. McDermott, M. Mecina, C. Mordasini, A. Mortier, V. Nascimbeni, R. Ottensamer, I. Pagano, E. Pallé, G. Peter, G. Piotto, D. Pollacco, T. Pritchard, R. Ragazzoni, N. Rando, F. Ratti, H. Rauer, I. Ribas, G.R. Ricker, M. Rieder, N.C. Santos, A.B. Savel, G. Scandariato, R.P. Schwarz, S. Seager, D. Ségransan, A. Shporer, A.E. Simon, A.M.S. Smith, M. Steller, C. Stockdale, Gy.M. Szabó, N. Thomas, G. Torres, R. Tronsgaard, S. Udry, B. Ulmer, V. Van Grootel, R. Vanderspek, J. Venturini, N.A. Walton, J.N. Winn, B. Wohler: TESS and CHEOPS discover two warm sub-Neptunes transiting the bright K-dwarf HD 15906, *MNRAS*, **523**, 3090–3118, doi, 2023.

Ulmer-Moll, S., H.P. Osborn, A. Tuson, J.A. Egger, M. Lendl, P. Maxted, A. Bekkelien, A.E. Simon, G. Olofsson, V. Adibekyan, Y. Alibert, A. Bonfanti, F. Bouchy, A. Brandeker, M. Fridlund, D. Gandolfi, C. Mordasini, C.M. Persson, S. Salmon, L.M. Serrano, S.G. Sousa, T.G. Wilson, M. Rieder, J. Hasiba, J. Asquier, D. Sicilia, I. Walter, R. Alonso, G. Anglada, D. Barrado y. Navascues, S.C.C. Barros, W. Baumjohann, M. Beck, T. Beck, W. Benz, N. Billot, X. Bonfils, L. Borsato, C. Broeg, T. Bárczy, J. Cabrera, S. Charnoz, M. Cointepas, A. Collier Cameron, Sz. Csizmadia, P.E. Cubillos, M.B. Davies, M. Deleuil, A. Deline, L. Delrez, O.D.S. Demangeon, B.-O. Demory, X. Dumusque, D. Ehrenreich, N.L. Eisner, A. Erikson, A. Fortier, L. Fossati, M. Gillon, N. Grieves, M. Güdel, J. Hagelberg, R. Helled, S. Hoyer, K.G. Isaak, L.L. Kiss, J. Laskar, A. Lecavelier des Etangs, C. Lovis, D. Magrin, V. Nascimbeni, J. Otegi, R. Ottensammer, I. Pagano, E. Pallé, G. Peter, G. Piotto, D. Pollacco, A. Psaridi, D. Queloz, R. Ragazzoni, N. Rando, H. Rauer, I. Ribas, N.C. Santos, G. Scandariato, A.M.S. Smith, M. Steller, G.M. Szabó, D. Ségransan, N. Thomas, S. Udry, V. Van Grootel, J. Venturini, N.A. Walton: TOI-5678 b: A 48-day transiting Neptune-mass planet characterized with CHEOPS and HARPS, *Astron. Astrophys.*, **674**, A43, doi, 2023.

Verbeke, C., M.L. Mays, C. Kay, P. Riley, E. Palmerio, M. Dumbovic, M. Mierla, C. Scolini, M. Temmer, E. Paouris, L.A. Balmaceda, H. Cremades, J. Hinterreiter: Quantifying errors in 3D CME parameters derived from synthetic data using white-light reconstruction techniques, *Adv. Space Res.*, **72**, 5243–5262, doi, 2023.

Volwerk, M., C. Simon Wedlund, D. Mautner, S. Rojas Mata, G. Stenberg Wieser, Y. Futaana, C. Mazelle, D. Rojas-Castillo, C. Bertucci, M. Delva: Statistical distribution of mirror-mode-like structures in the magnetosheaths of unmagnetized planets - Part 2: Venus as observed by the Venus Express spacecraft, *Ann. Geophys.*, **41**, 389-408, doi, 2023.

Volwerk, M., T. Karlsson, D. Heyner, C. Goetz, C. Simon Wedlund, F. Plaschke, D. Schmid, D. Fischer, J. Mieth, I. Richter, R. Nakamura, Y. Narita, W. Magnes, U. Auster, A. Matsuoka, W. Baumjohann, K.-H. Glassmeier: Magnetic holes between Earth and Mercury: BepiColombo cruise phase, *Astron. Astrophys.*, **677**, A2, doi, 2023.

Vörös, Z., O.W. Roberts, E. Yordanova, L. Sorriso-Valvo, R. Nakamura, Y. Narita, D. Schmid, F. Plaschke, Á. Kis: How to improve our understanding of solar wind-magnetosphere interactions on the basis of the statistical evaluation of the energy budget in the magnetosheath?, *Front. Astron. Space Sci.*, **10**, 1163139, doi, 2023.

Wang, G., J. Shi, K. Torkar, Z. Wang, X. Wang, Z. Cheng, S. Shang: Statistical study on plasma velocities in the bottom-side ionosphere over low latitude Hainan station: Digisonde measurement, *Radio Sci.*, **58**, e2022RS007635, doi, 2023.

Wang, J., X. Shen, Y. Yang, Z. Zeren, B. Zhou, W. Magnes, A. De Santis, J. Huang, C. Yao, Z. Li, Y. Zheng, S. Zhao, H. Lu, Q. Wang, W. Chu, F. Guo, A. Pollinger, R. Lammegger: A global lithospheric magnetic field model between ± 65° latitude derived from CSES satellite scalar data, *Phys. Earth Planet. Inter*, **340**, 107036, doi, 2023.

Wang, Y.M., T.-L. Zhang, G.Q. Wang, S.D. Xiao, Z.X. Zou, L. Cheng, Z.H. Pan, K. Liu, X.J. Hao, Y.R. Li, M.M. Chen, Z.B. Zhang, W. Yan, Z.P. Su, Z.Y. Wu, C.L. Shen, Y.T. Chi, M.J. Xu, J.N. Guo, Y. Du: The Mars orbiter magnetometer of Tianwen-1: In-flight performance and first science results, *Earth Planet. Phys.*, **7**, 216-228, doi, 2023.

Way, M.J., C. Ostberg, B.J. Foley, C. Gillmann, D. Höning, H. Lammer, J. O'Rourke, M. Persson, A.-C. Plesa, A. Salvador, M. Scherf, M. Weller: Synergies between Venus & exoplanetary observations. Venus and its extrasolar siblings, *Space Sci. Rev.*, **219**, 13, doi, 2023.

Wu, S., S. Ye, G. Fischer, J. Wang, W.S. Kurth, Z. Yao, R. Guo, J.D. Menietti, M. Long, Y. Xu: Phase locking among Saturn radio emissions revealed by Cassini observations, *Astron. Astrophys.*, **680**, A7, doi, 2023.

Xu, Q., L. Xie, Z. Rong, X. Xu, Y. Wei, L. Li, T.-L. Zhang: The magnetic field clock angle departure in the Venusian magnetosheath and its response to IMF rotation, *Astron. Astrophys.*, **677**, A142, doi, 2023.

Yang, Y., Z. Zhima, X. Shen, B. Zhou, J. Wang, W. Magnes, A. Pollinger, H. Lu, F. Guo, R. Lammegger, N. Zhou, Y. Miao, Q. Tan, W. Li: An improved in-flight calibration scheme for CSES magnetic field data, *Remote Sens.*, **15**, 4578, doi, 2023.

Yao, S.T., J.H. Li, X.-Z. Zhou, Q.Q. Shi, Q.-G. Zong, H. Zhang, W.Y. Li, M. Hamrin, M. Volwerk, T. Pitkänen, F. Yang: Ion-vortex magnetic hole with reversed field direction in Earth's magnetosheath, *J. Geophys. Res. Space Phys.*, **128**, e2023JA031749, doi, 2023.

Yu, B., Y. Chi, M. Owens, C.J. Scott, C. Shen, X. Xue, L. Barnard, T.-L. Zhang, D. Heyner, H.-U. Auster, I. Richter, J. Guo, B. Sánchez-Cano, Z. Pan, Z. Zou, Z. Su, Z. Wu, G. Wang, S. Xiao, K. Liu, X. Hao, Y. Li, M. Chen, X. Dou, M. Lockwood: Tianwen-1 and MAVEN observations of the response of Mars to an interplanetary coronal mass ejection, *Astrophys. J.*, **953**, 105, doi, 2023.

Zaitsev, V.V., V.E. Shaposhnikov, M.L. Khodachenko, M.S. Rumenskikh: On the efficiency of radio emissions at the double plasma frequency in the magnetosphere of exoplanet HD189733 b, *Geomagn. Aeron.*, **63**, 892-898, doi, 2023.

Zenitani, S., S. Nakano: Loading loss-cone distributions in particle simulations, *J. Geophys. Res. Space Phys.*, **128**, e2023JA031983, doi, 2023.

Zhang, L.Q., C. Wang, W. Baumjohann, R.S. Wang, J.Y. Wang, J.L. Burch, Yu.V. Khotyaintsev: First observation of fluid-like eddy-dominant bursty bulk flow turbulence in the Earth's tail plasma sheet, *Sci. Rep.*, **13**, 19201, doi, 2023.

Zou, Z.X., Y.M. Wang, T.-L. Zhang, G.Q. Wang, S.D. Xiao, Z.H. Pan, Z.B. Zhang, W. Yan, Y. Du, Y.T. Chi, L. Cheng, Z.Y. Wu, X.J. Hao, Y.R. Li, K. Liu, M.M. Chen, Z.P. Su, C.L. Shen, M.J. Xu, J.N. Guo: In-flight calibration of the magnetometer on the Mars orbiter of Tianwen-1, *Sci. China Technol. Sci.*, **66**, 2396–2405, doi, 2023.

BOOKS

Louis, C.K., C.M. Jackman, G. Fischer, A.H. Sulaiman, P. Zucca (Eds.): Planetary, Solar and Heliospheric Radio Emissions IX, Dublin Institute for Advanced Studies, Trinity College Dublin, Dublin, 2023.

Vidotto, A.A., L. Fossati, J.S. Vink (Eds.): Winds of Stars and Exoplanets. Proceedings IAU Symposium No. 370, Cambridge University Press, Cambridge, UK, 290 pages, 2023.

PROCEEDINGS & BOOK CHAPTERS

Aivar, L., A. Águeda, M. Ploner, A. Kloth, N. Håkansson, L. Heinzl, C. Heese, T. Flohrer, M.A. Steindorfer, G. Kirchner, N.M. Trummer: SLR - Evolution towards active sensor networking for debris observation including the update of the Izaña-1 station. In: *Proceedings of the 2nd NEO and Debris Detection Conference, Darmstadt*, Eds. Flohrer, T., R. Moissl, F. Schmitz, ESA Space Debris Office, Darmstadt, 9 p., 2023.

Bach-Moeller, N.: Wie erforschen wir Exoplaneten?. In: *Atmosphären. Kunst, Klima- und Weltraumforschung. Ausstellung - Mobiler Pavillon*, Steiermarkschau, Herberstein - Wien, 2 pp., 2023.

Barth, P.: Wie können wir Blitze auf Exoplaneten beobachten?. In: *Atmosphären. Kunst, Klima- und Weltraumforschung. Ausstellung - Mobiler Pavillon*, Steiermarkschau, Herberstein - Wien, 2 pp., 2023.

Boudjada, M.Y., S. Sawas, P.H.M. Galopeau, H. Lammer, W. Voller: Statistical analysis of Solar Type III radio bursts observed by RPWS experiment in 2004-2017 during the Solar cycles 23-24. In: *Proceedings 2023 Kleinheubach Conference*, Ed. U.R.S.I. Landesausschuss in Deutschland e.V., IEEE, Miltenberg, 4 p., 2023.

Dachwald, B., S. Ulamec, J. Kowalski, M.S. Boxberg, F. Baader, J. Biele, N. Kömle: Ice melting probes. In: *Handbook of Space Resources*, Eds. Badescu, V., K. Zacny, Y. Bar-Cohen, Springer, Cham, 955-996, doi, 2023.

Fischer, G., U. Taubenschuss, D. Pisa, L. Lamy, S. Wu, S.-Y. Ye, C.M. Jackman, E. O'Dwyer: A particular form of Saturn kilometric radiation at the low end of its spectrum. In: *Planetary, Solar and Heliospheric Radio Emissions IX*, Eds. Louis, C.K., C.M. Jackman, G. Fischer, A.H. Sulaiman, P. Zucca, Dublin Institute for Advanced Studies, Trinity College Dublin, Dublin, 103099, doi, 2023.

Fossati, L.: Wie verändert sich die Atmosphäre, wenn alles Leben auf der Erde ausstirbt?. In: *Atmosphären. Kunst, Klima- und Weltraumforschung. Ausstellung - Mobiler Pavillon*, Steiermarkschau, Herberstein - Wien, 2 pp., 2023.

Grießmeier, J.-M., N.V. Erkaev, C. Weber, H. Lammer, V.A. Ivanov, P. Odert: On the required mass for an exoplanet to emit radio waves. In: *Planetary, Solar and Heliospheric Radio Emissions IX*, Eds. Louis, C.K., C.M. Jackman, G. Fischer, A.H. Sulaiman, P. Zucca, Dublin Institute for Advanced Studies, Trinity College Dublin, Dublin, 103090, doi, 2023.

Helling, Ch.: Exoplaneten - Vorstellbare Welten jenseits unseres Sonnensystems. In: *Atmosphären. Kunst, Klima- und Weltraumforschung. Ausstellung - Mobiler Pavillon*, Steiermarkschau, Herberstein - Wien, 50-51, 2023.

Kubyshkina, D.: The origin of planetary winds. In: *Winds of Stars and Exoplanets. Proceedings IAU Symposium No. 370*, Eds. Vidotto, A.A., L. Fossati, J.S. Vink, Cambridge University Press, Cambridge, UK, 103-121, doi, 2023.

Lecoq Molinos, H.: Ist die Erde einzigartig?. In: *Atmosphären. Kunst, Klima- und Weltraumforschung. Ausstellung - Mobiler Pavillon*, Steiermarkschau, Herberstein - Wien, 2 pp., 2023.

Narita, Y.: Magnetic helicity measurements in the solar wind. In: *Helicities in Geophysics, Astrophysics and Beyond*, Eds. Kuzanyan, K., N. Yokoi, M.K. Georgoulis, R. Stepanov, Wiley, Weinheim, 105-116, doi, 2023.

Padilla Gutierrez, E., T. Soares, M.A. Steindorfer, S. Schneider: Satellite laser ranging for attitude determination and D4R to enable ADR of future space debris. In: *Proceedings of the 2nd NEO and Debris Detection Conference, Darmstadt*, Eds. Flohrer, T., R. Moissl, F. Schmitz, ESA Space Debris Office, Darmstadt, 5 p., 2023.

Samra, D.: Wie ist das Wetter auf anderen Planeten?. In: *Atmosphären. Kunst, Klima- und Weltraumforschung. Ausstellung - Mobiler Pavillon*, Steiermarkschau, Herberstein - Wien, 2 pp., 2023.

Sindel, J.-P.: Sind Tag und Nacht Orte oder Zeiten?. In: *Atmosphären. Kunst, Klima- und Weltraumforschung. Ausstellung - Mobiler Pavillon*, Steiermarkschau, Herberstein - Wien, 2 pp., 2023.

Steindorfer, M.A., F. Koidl, P. Wang, S. Schneider, C. Jonglez, M.F. Barschke, T. Soares, E. Padilla, A. Cipriano: A tool for simulating SLR residuals - Placement of backup retroreflectors for future satellite missions. In: *Proceedings of the 22nd International Workshop on Laser Ranging*, ILRS, Greenbelt, Maryland, S04-T01; 6 pp., 2023.

Steindorfer, M.A., P. Wang, F. Koidl, S. Schneider, N.M. Trummer, G. Kirchner: Multiple techniques at Graz SLR station for the characterization of space debris. In: *Proceedings of the 2nd NEO and Debris Detection Conference, Darmstadt*, Eds. Flohrer, T., R. Moissl, F. Schmitz, ESA Space Debris Office, Darmstadt, 4 p., 2023.

Taubenschuss, U., G. Fischer, D. Pisa, O. Santolík, J. Soucek: Classification of the spectral fine structure in auroral kilometric radiation. In: *Planetary, Solar and Heliospheric Radio Emissions IX*, Eds. Louis, C.K., C.M. Jackman, G. Fischer, A.H. Sulaiman, P. Zucca, Dublin Institute for Advanced Studies, Trinity College Dublin, Dublin, 103089, doi, 2023.

Taubner, R.-S.: Wo sollen wir nach Leben suchen? Was hoffen wir zu finden?. In: *Atmosphären. Kunst, Klima- und Weltraumforschung. Ausstellung - Mobiler Pavillon*, Steiermarkschau, Herberstein - Wien, 2 pp., 2023.

Trummer, N.M., M.A. Steindorfer, F. Koidl, P. Wang, G. Kirchner, A. Kloth, J. Munder, J. Steinborn, T. Flohrer, A. di Mira, C. Heese: Modular setup of SLR laser and detection packages. In: *Proceedings of the 22nd International Workshop on Laser Ranging*, ILRS, Greenbelt, Maryland, S08-P07, 5 pp., 2023.

Vananti, A., D. Kucharski, M.A. Steindorfer, R. Kanzler, P. Kärräng, D. Cerutti-Maori, J. Rosebrock, T. Schildknecht: Multi-sensor space object tracking for tumbling motion characterization. In: *Proceedings of the 2nd NEO and Debris Detection Conference, Darmstadt*, Eds. Flohrer, T., R. Moissl, F. Schmitz, ESA Space Debris Office, Darmstadt, 8 p., 2023.

Vidotto, A.A., S. Carolan, G. Hazra, C. Villarreal D'Angelo, D. Kubyshkina: Double tail structure in escaping atmospheres of magnetised close-in planets. In: *Winds of Stars and Exoplanets. Proceedings IAU Symposium No. 370*, Eds. Vidotto, A.A., L. Fossati, J.S. Vink, Cambridge University Press, Cambridge, UK, 103-121, doi, 2023.

Wang, P., M.A. Steindorfer, F. Koidl, G. Kirchner: Day- and night-time SLR at MHz repetition rate in Graz. In: *Proceedings of the 22nd International Workshop on Laser Ranging*, ILRS, Greenbelt, Maryland, S08-T03; 9 pp., 2023.

PERSONNEL

Agú, Martín A., Dipl.-Ing.
Aickara Gopinathan, Sreejith, Dr.
Bach-Møller, Nanna, MSc
Balduin, Thorsten, MSc
Bangera, Nidhi R., MSc
Berghofer, Gerhard, Ing.
Besser, Bruno P., Dr.
Betzler Alexander-Pieter, Dipl.-Ing.
Blasl, Kevin-Alexander, MSc
Bonfanti, Andrea, Dr.
Boudjada, Mohammed Y., Dr.
Campos Estrada, Beatriz, MSc
Carone, Ludmila, Dr.
Delva, Magda, Dr.
Eichelberger, Hans U., Dr.
Fabian, Peter
Fauland, Daniel, Ing.
Fischer, David, Dr.
Flock, Barbara, Mag.
Fossati, Luca, Doz.
Fremuth, Gerhard, Dipl.-Ing.
Gabalier, Franz, BSc
Giner, Franz, Dipl.-Ing.
Giono, Gabriel, Dr.
Graf, Christian, Ing.
Gratzer, Alexander J.
Grill, Claudia
Hasiba, Johann, Dipl.-Ing.
Helling, Christiane, Prof. Dr.
Höck, Eduard, Dipl.-Ing.
Hofmann, Karl, Dipl.-Ing.
Hosner, Martin, MSc
Hradecky, Doris
Jernej, Irmgard, Ing.
Jeszenszky, Harald, Dipl.-Ing.
Kadam, Kundan V., Dr.
Kargl, Günter, Dr.
Käufer, Till F., MSc
Khodachenko, Maxim L., Dr.
Kiefer, Sven, MSc
Kim, Hyangpyo, Dr.
Koidl, Franz, Ing.
Krenn, Andreas F., MSc
Kubyshkina, Daria, Dr.
Kürbisch, Christoph, Ing.
Laky, Gunter, Dipl.-Ing.
Lammer, Helmut, Doz.
Lecoq Molinos, Helena, MSc
Leichtfried, Mario, Ing.
Lentz, Constant M. F., Dipl.-Ing.
Lentz, Maurice
Lewis, David A., MSc
Macher, Wolfgang, Dr.
Magnes, Werner, Dr.
Muck, Cosima
Nakamura, Rumi, Doz.
Narita, Yasuhito, Doz.
Neukirchner, Sonja, Ing.
Nischelwitzer-Fennes, Ute, Ing.
Ottacher, Harald, Dipl.-Ing.
Panov, Evgeny, Dr.
Pitterle, Martin
Preisser Renteria, Luis F., Dr.
Reza, Amit, Dr.
Roberts, Owen W., Dr.
Samra, Dominic B. S., Dr.
Scherr, Alexandra, Mag.
Scherzer Maximilian, MSc
Schmid, Daniel, Dr.
Schneider, Sebastian, BSc
Settino, Adriana, Dr.
Simon Wedlund, Cyril Laurent, Dr.
Stachel, Manfred, Dipl.-Ing.
Steinberger, Michael, Dipl.-Ing.
Steindorfer, Michael, Dr.
Steinhöfler, Raphael
Steller, Manfred B., Dr.
Stieninger, Reinhard, Ing.
Suslina, Elena, MSc
Taubner, Ruth-Sophie, Dr.
Teubenbacher, Daniel, Dipl.-Ing.
Tonfat Seclen, Jorge L., Dr.
Trummer, Nadine M., MSc
Tschachler, Elvira, Mag.
Valavanoglou, Aris, Dipl.-Ing.
van Terwisga, Sierk, Dr.
Varsani, Ali, Dr.
Voller, Wolfgang G., Mag.
Volwerk, Martin, Dr.
Vörös, Zoltan, Dr.
Wallner, Robert, Ing.
Wang, Peiyuan, MSc
Weichbold, Fabian, BSc
Wilfinger, Josef, BSc
Woitke, Peter, Dr.
Zenitani, Seiji, Dr.
Zhang, Tie-Long, Prof.
Zivithal, Stephan, BSc

As of 31 December 2023

IMPRINT

PUBLISHER

Prof. Dr. Christiane Helling, Director
Institut für Weltraumforschung (IWF)
Österreichische Akademie der Wissenschaften (OeAW)
Schmiedlstraße 6, 8042 Graz, Austria
www.oeaw.ac.at/iwf
X: @IWF_oeaw

EDITORS

Bruno Besser, Alexandra Scherr, Martin Volwerk

DESIGN

Alexandra Scherr
pr.iwf@oeaw.ac.at

PRINT

Servicebetrieb ÖH-Uni Graz GmbH

All rights reserved
© 2023 by OeAW